The Pennsylvania State University

The Graduate School

CALIBRATION AND VALIDATION OF A ROTORCRAFT DESIGN AND ANALYSIS TOOL FOR ELECTRIC POWERED MULTIROTOR CONFIGURATIONS

A Thesis in

Aerospace Engineering

by

Evan T. Topper

Submitted in Partial Fulfillment

of the Requirements

for the Degree of

Master of Science

May 2022

The thesis of Evan T. Topper was reviewed and approved by the following:

Joseph F. Horn
Professor of Aerospace Engineering
Thesis Advisor

Jacob W. Langelaan
Professor of Aerospace Engineering
Director of Graduate Programs

Edward C. Smith
Professor of Aerospace Engineering
Director – Penn State Rotorcraft Center

Amy R. Pritchett
Professor of Aerospace Engineering
Department Head

Abstract

The software known as NASA Design and Analysis of Rotorcraft (NDARC) had been thoroughly tested and validated for use in sizing and low-fidelity performance analysis of large-scale traditional rotorcraft and fixed-wing aircraft. As small-scale (less than 10lbs), multirotor unmanned aerial vehicles (UAVs) have increased in popularity and use, the need for a low-fidelity design tool that can provide rapid and accurate results has increased so that designers can improve their designs. This thesis demonstrates that NDARC can serve as this design tool and details a process to tune the model. NDARC was tuned to match wind tunnel data for two different quadrotor UAVs, the DJI Phantom and the SUI Endurance. Through this process, important parameters for tuning the model were identified along with potential design improvements, including rotor-to-rotor interference effects and relocating the center of gravity to generate equal thrust on the front and rear rotors in forward flight, respectively. Using the knowledge gained from tuning the UAVs, the process was then applied to a piloted multirotor passenger urban air mobility (UAM) aircraft featuring four lift rotors, a pusher propeller, wings, and tails. Because there is no public data available to validate NDARC against for the selected aircraft, a high fidelity model, the Distributed Electric Propulsion Simulation (DEPSim), was used to generate data that could be compared directly with the NDARC model. Again, it was proven that NDARC can serve as a viable low-fidelity design tool for these larger, novel rotorcraft by demonstrating good matching with DEPSim. Areas for design improvement were also identified. Primarily, it was seen that increasing the solidity of the lift rotors and moving the location of the horizontal tail could provide marked improvement as aerodynamic interference effects relating to the rotors are influential on the performance of the aircraft.

Table of Contents

List of Figures

List of Tables

List of Symbols

Variables

C_D	Coefficient of Drag
C_{D0}	Zero-lift Drag Coefficient
C_{Dfit}	Drag Coefficient for Fixtures and Fittings
C_{Drb}	Drag Coefficient for Rotor-body Interference
C_L	Coefficient of Lift
$C_{L\alpha}$	Lift Curve Slope
C_M	Pitch Moment Coefficient
C_{M0}	Zero-lift Pitch Moment Coefficient
$C_{M\alpha}$	Pitch Curve Slope
D	Drag Force
ΔSL	Change in Center of Gravity Location Along Stationline
K_d	Coefficient for Angle of Attack Variation at Low Angles
L	Lift Force
ℓ_{fus}	Fuselage Length
M	Pitch Moment
Ω	Rotor Speed
q	Dynamic Pressure
S_{wet}	Wetted Area
X_d	Drag Variation Exponent (linear, quadratic)
α	Angle of Attack
α_e	Effective Angle of Attack

θ	Pitch
κ	Induced power factor or correction factor
μ	Advance Ratio
σ	Solidity
Ω	Rotor Rotational Rate

Acronyms

AIDEN	An Integrated Design Environment for NDARC
BL	Buttline (positive right)
CD&A	Concept Design and Assessment
CDI	Continuum Dynamics Inc.
CFD	Computational Fluid Dynamics
CG	Center of Gravity
CHARM	Comprehensive Hierarchical Aeromechanics Rotorcraft Model (CFD Program)
DEPSim	Distributed Electric Propulsion Simulation
DJI	Da-Jiang Innovations
DOF	Degrees of Freedom
eVTOL	Electronic Vertical Takeoff and Landing
FM	Figure of Merit
GUI	Graphical User Interface
HS-eVTOL	High Speed Electronic Vertical Takeoff and Landing
NASA	National Aeronautics and Space Administration
NDARC	NASA Design and Analysis of Rotorcraft
SL	Stationline (positive aft)

SUI	Straight Up Imaging
TDD	Technology Development Directorate
UAM	Urban Air Mobility
UAS	Unmanned Aerial System
UAV	Unmanned Aerial Vehicle
VLRCOE	Vertical Lift Research Center of Excellence
VTOL	Vertical Takeoff and Landing
WL	Waterline (positive up)

Acknowledgements

Firstly, I would like to acknowledge my family and loved ones for supporting my ambitions despite the distance and complications due to the pandemic that occurred and continues to have an impact on daily life for many people. Without that support for these last couple of years, this would have been a much more challenging endeavor. They have kept me grounded and provided me with plenty of help during what could have been extremely stressful times. I can only hope to find ways to properly repay them for their love and support in the future.

I would also like to thank my advisor Dr. Horn. Despite being busy with numerous other projects, teaching, and a personal life, he was always able to make sure he provided me the help I needed when I needed it. He has served as an invaluable source of knowledge and expertise with not only calculations, but software, theory, and critical thinking for rotorcraft design. I would like to specifically thank him for providing me the opportunity to work on such an interesting project through the Vertical Lift Research Center of Excellence (VLRCOE). Additionally, my other professors from my courses have provided me with fantastic classes and taught me far more than I anticipated while demonstrating an incredible passion for the work that they do. The efforts from Dr. Horn and my other professors have been paramount to my success.

Lastly, I need to acknowledge Mark Scott, Robert Scott, Jeff Sinsay, and Gerardo Nunez from the Army Development Directorate. Each of the aforementioned individuals have provided me with a wealth of advice and assistance with the project and NDARC/AIDEN. Not only that, but are also the group responsible for creating this project and allowing me to take advantage of a great opportunity for learning and pursuing my passions.

This research was partially funded by the Government under Agreement No. W911W6-17-2-0003. The U.S. Government is authorized to reproduce and distribute reprints for

Government purposes notwithstanding any copyright notation thereon. The views and conclusions contained in this document are those of the authors and should not be interpreted as representing the official policies, either expressed or implied, of the Aviation Development Directorate or the U.S Government.

Chapter 1: Introduction

1.1 Motivation

Multirotor vehicles of various sizes and weights are becoming increasingly popular within the aerospace industry for a multitude of reasons ranging from package delivery with small, lightweight unmanned aircraft vehicles/unmanned aircraft systems (UAV/UAS) to passenger transportation with piloted vehicles weighing thousands of pounds. Furthermore, these multirotor vehicles are designed to be electric-powered vertical takeoff and landing (eVTOL) aircraft with the ability to maneuver around buildings in populated areas to satisfy urban air mobility (UAM) based missions. The NASA designed software "NASA Design and Analysis of Rotorcraft" (NDARC) is a design software originally made for large-scale, traditional rotorcraft like single rotor helicopters, but has since been updated to work for tandem rotor helicopters, coaxial helicopters, tilt-wing and tilt-rotor rotorcraft, and even fixed-wing aircraft. Using NDARC to model small-scale quadcopter UAVs and larger multirotor configurations has been largely unexplored and using the software to confirm rotor-to-rotor interactions is something that could greatly benefit the community going forward.

In addition to electric vehicles that operate using multiple rotors for both hover and forward flight, new concept vehicles that use one set of multiple edgewise rotors for hover and low speed, and a separate set of one or more axial flow rotors (propellers) for forward flight have recently become more popular. These novel concepts are known as "lift+cruise" configurations that present a number of challenges given unique designs with multiple rotors, varying lift surfaces. The aerodynamics are especially complex in transition flight. While there are a number of lift+cruise concepts being studied in the industry, there is still much more to learn about these unique concepts in terms of accurate modeling and design. Because of the popularity of quadrotors for UAV

purposes, large-scale quadrotors have been studied and in a multitude of ways, which are discussed in the next section, that could and should be done with lift+cruise models too as their popularity increases.

The Alia vehicle designed by BETA Technologies has gained a lot of attention from both the United States military and private companies as evidenced by military air worthiness approval from the United State Air Force and multiple orders from UPS and BLADE. Given the heightened interest in the BETA Alia, it was deemed both relevant and valuable to determine how well NDARC can model the transition flight range between using the lift rotors in hover and switching to the propulsive rotor with wing lift in cruise. In addition, it was decided that using NDARC to determine what design changes could be made to further improve such a lift+cruise concept would be useful to the industry as well.

1.2 Background

For this thesis, there are two primary sections that detail the objectives of this project. Within the first section, two small quadcopter UAVs are modelled. In the second section, the research turned toward modelling a piloted multi-passenger multicopter used for UAM missions. In both sections, the main program used was NDARC. In Ref. [1], the creator of NDARC, Wayne Johnson, details the uses of the program, how it works, how it calculates various parameters, and what it can do. Then, in Ref. [2], Johnson goes on to demonstrate the purpose of NDARC by modelling multiple large-scale rotorcrafts of differing designs and configurations that are currently operational. By modelling a single main-rotor and tail-rotor helicopter (UH-60A), a tandem helicopter (CH-47D), a coaxial lift-offset helicopter (XH-59A), and a tiltrotor aircraft (XV-15) that have ample flight test data available, Johnson was able to validate NDARC as a reliable code for conceptual design of more traditional, large-scale rotorcraft. In the following years, more work

would be done to validate the effectiveness of NDARC as a viable conceptual design tool for fixed-wing aircraft as well, but it needed both validation and calibration for both small-scale multirotor UAVs and multirotor UAM vehicles.

1.2.1 Multirotor UAVs

Previous work has been done to confirm whether or not NDARC can accurately model key flight parameters and characteristics for small multirotor vehicles. One of the first major steps to allow this work to be done was accomplished in Ref. [3] where researchers at NASA Ames Research Center tested and compiled the hover data, forward flight data, and rotor data for a number of quadcopter UAVs and one octocopter UAV. The empirical data collected in Ref. [3] using multiple commercially available models and a full-scale 7'- by 10' wind tunnel was paramount for confirming the validity of the results generated by NDARC and tuning the model within NDARC. Then, in Ref. [4-5], the wind tunnel and hover data from Ref. [3] was used to both confirm the validity of using NDARC to design and evaluate small UAS vehicles and to conduct a comprehensive analysis of the two rotor blades used on the two models studied in this thesis. More specifically, the SUI Endurance was studied in depth by Russell et al. in Ref. [4] which provided reference points for the work presented in this thesis.

In depth studies on seventy-nine different multicopter rotor blades of varying sizes and material properties were conducted by Brandt and Selig in Ref. [6] at the University of Illinois which provides UAV designers with a valuable database of propellers and relevant data, something that existed for full-scale aircraft but was not previously available for small-scale UAVs. This also provided empirical evidence that the propeller selection for the design of the UAV has a significant influence on the aircraft's performance. Furthermore, using this data and study, Nowicki conducted a more in-depth analysis of the rotor blades used by the DJI Phantom and the SUI

endurance in Ref. [7] which provided important parameters for each blade that were then input into NDARC for more accurate modelling. In 2018, Diaz and Yoon performed high-fidelity CFD simulations for three UAVs, two of which were the DJI Phantom and the SUI Endurance and the third was an UAM concept, in Ref. [8]. Furthermore, in their study, they explored various configurations for each of the quadcopters and compared the high-fidelity CFD generated results to provide valuable information regarding rotor-to-rotor interactions and other interactional aerodynamics. Lastly, in Ref. [9], Govindarajan and Sridharan used a different conceptual design tool known as HYDRA to size various configurations for UAV package delivery and to evaluate a quadcopter design against the other configurations. This work led to the conclusion that the other non-quadcopter configurations offered various improvements based on their design, but presented unique challenges for manufacturing and from a control standpoint.

1.2.2 Multirotor UAM Vehicles

In Ref. [10], Mark Scott discusses and investigates the feasibility of multiple eVTOL aircraft configurations with respect to urban air mobility missions from a military perspective. More specifically, he discusses the typical mission requirements and obstacles a UAM-like configuration might encounter for a military mission and how the different eVTOL aircraft configurations might struggle to conquer these issues. His discussion on the typical UAM mission prompted valid questioning and interest in investigating how well some of the more novel and unique eVTOL concepts can navigate the transition region from hover to cruise. Lift+cruise concepts typically feature a predominant lifting surface in the form of a wing as well as tails in addition to multiple rotors that provide the necessary lift to hover like traditional single main rotor and tandem rotor configurations. Through the use of the rotors and the wing, a strong understanding of how the aircraft will perform in hover, cruise, and high-speed forward flight can be determined fairly easily.

The transition from hover to forward flight is the challenging segment of the flight envelope to accurately model given the interactions of one rotor to another and even the interactions between the rotors, wings, and empennage.

Johnson et al. utilized NDARC to size concept VTOL air taxi operations in Ref. [11]. They opted to create and test a single-passenger quadrotor with electric propulsion, a six-passenger side-by-side rotorcraft with turboshaft hybrid propulsion, and a fifteen-passenger tiltwing aircraft with turboelectric propulsion. This study did not, however, conceptualize and test a lift+cruise aircraft. The decision to model three different designs was to test a diverse range of aircraft attributes consisting of: number of passengers, un-refueled range, market, aircraft type, and propulsion system. From their work, they concluded that design methods and comprehensive data bases detailing the electrical subsystems for unconventional aircraft propulsion systems would be needed to have greater confidence in NDARC results for these eVTOL aircraft. Additionally, they concluded that the reliability of design tools, such as NDARC, would depend on correlation of generated results with measured data for the aircraft types and that the correlation, or lack thereof, would identify the need for the development of new or improved analysis methods. This is part of the motivation for this thesis.

Ref. [12] explored a new conceptual design method for a single-main-rotor and a lift-augmented eVTOL aircraft which was used in turn to determine the feasible design space for electric powered helicopters. Through the work of Cole et al. in the aforementioned reference, they found that the most efficient configuration for an eVTOL aircraft transitions from the single-main-rotor helicopter to the lift-augmented compound helicopter by a function of cruise distance and hover time. This supports the idea that a lift+cruise concept, such as the BETA Alia, would serve

well for a longer cruise distance and shorter hover time as it has multiple rotors. The work done by the researchers in Ref. [12] was dependent upon the work done in Ref. [13].

In Ref. [13], which expanded upon the research conducted by Johnson et al. in Ref. [11], Silva et al. models and investigates six different six-passenger aircrafts. The six aircrafts are comprised of: two quadrotor VTOL concept aircraft (one battery powered and the other a turboshaft-powered mechanical drive), two side-by-side helicopters (one battery powered and the other a turboshaft-powered mechanical drive), and two lift+cruise VTOL aircraft (one fully electric and the other turboelectric). The relevant model here is the lift+cruise VTOL aircraft which features a conventional tail and eight lift rotors, where the front four are mounted underneath the boom, the back four are mounted above the boom, and the innermost four lift rotors are cambered outward (shown in Figure 1.1).

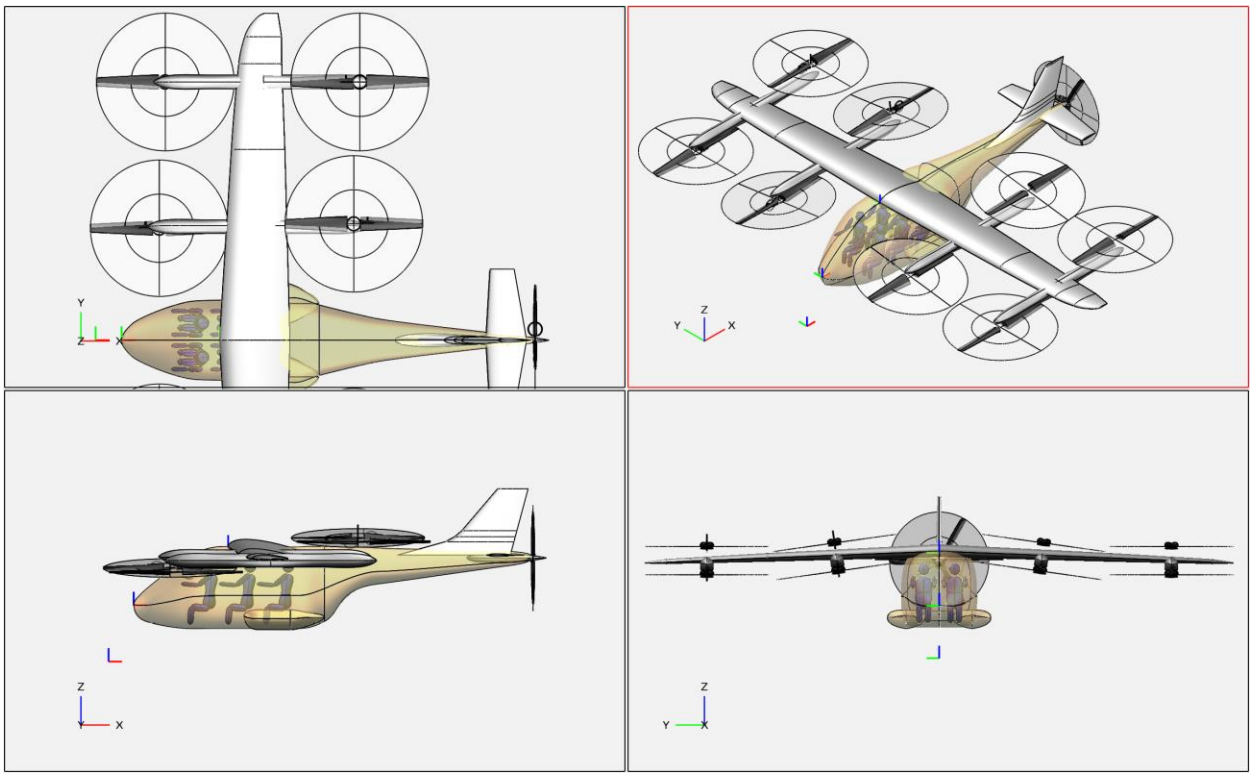

Figure 1.1 Concept Lift+Cruise VTOL Aircraft from Silva et al. Ref. [13].

Although it differs in design when compared to the BETA Alia, the researchers were still able to present relevant advantages and observations that pertain to all lift+cruise designs. Of these observations, the most pertinent ones are that the front lift rotors heavily influence the performance of the rear rotors and the wing in transition due to the lack of cyclic pitch control which requires the entire aircraft to pitch forward, a prescribed body pitch schedule is likely required in transition, the lift rotors can approach high blade loading values near stall when edgewise speed increases, and that the lift+cruise configuration actually produces a high FM.

To better understand the work done in Ref. [11] and Ref. [13], Patterson et.al compiled various data to develop and propose a specific UAM mission in Ref. [14] that would allow other researchers, like those in Ref. [13], to quantify the discovered tradeoffs and performance markets. To do so, Patterson et al. canvassed twenty-eight different cities within the U.S. and to account for common obstacles that would affect UAM based missions, including geography, weather, city infrastructure, and population patterns. This information combined with data related to what they found to be typical proposed flight ranges and passenger numbers for UAM missions and UAM vehicles allowed them to generate three missions to judge future aircraft. A long-range, small-payload mission, a short-range, large-payload mission, and a mission combining the most straining characteristics of both aforementioned missions were proposed by Patterson et al. These missions were then used by Silva et al. to evaluate the eVTOL aircraft designed in Ref. [13].

In 2020, more work was done to evaluate the handling qualities of rotors controlled using either variable blade pitch and constant rotor speed or variable rotor speed and constant blade pitch on eVTOL quadrotor concepts intended for UAM missions. This work was done by C. Malpica and S. Withrow-Maser in Ref. [15]. In their study, they used NASA reference concept aircraft that consisted of a single-passenger, 50 nautical mile range and a six-passenger quadrotor designs

which inspired their final candidate configurations. Malpica and Withrow-Maser chose to also use two- and four-passenger quadrotor configurations that would utilize electric motors for propulsion, similar to the BETA Alia without a pusher propeller. The general aircraft configuration is shown below in Figure 1.2.

Figure 1.2 NASA Reference Concept Quadrotor Aircraft from Ref. [15].

Through their work, they found that the variable pitch-controlled demonstrated the ability to "easily" meet Level 1 handling qualities and control system specifications for all four of the varying quadrotor sizes, which was significantly different compared to the capabilities of the variable speed-controlled quadrotor vehicles. While the variable speed-controlled quadrotor models struggled to stabilize for the required closed-loop performance given the current technology, the study concluded that NDARC served as a viable tool for determining flight control systems for quadrotor designs with electric propulsion and that even large variations in vehicle design parameters caused minimal variation in handling qualities metrics. The previous work was continued in Ref. [16] by Withrow-Maser et al. By reducing the restrictions and increasing the variation of power constraints for the passenger-sized quadcopter design, the vehicle was able to stabilize in the roll axis within reasonable response times from pilot input which was not previously possible in Ref. [15]. Furthermore, the motor optimization used with the quadcopter was extended to use with a hexacopter and octocopter configuration which in turn demonstrated improved response to pilot inputs as more rotors were added. The six-passenger quadcopter was then tested

using high-fidelity CFD tools to evaluate the interactions between rotors in both forward flight and hover. This was done by Diaz and Yoon in Ref. [17]. Using CFD, they were able to confirm power required to fly in forward flight decreases as the rotor-to-rotor interactions decrease due to increased vertical separation from the front rotors to the rear rotors.

Lastly, in Ref. [18], researchers from Boeing's Aurora Flight Sciences division conducted wind tunnel testing for a full-scale, eVTOL, UAM multirotor sized rotor that featured fixed-pitch, variable rotor speed control and a rigid rotor. The focus of the study was to investigate the vibratory loads of such a rotor. From their work, they concluded that the fixed-pitch rotors on UAM designed aircraft, such as the lift+cruise concepts, will encounter large vibratory loads in edgewise flight and such loads should be anticipated early in the design process. Additionally, the resonant response can cause the vibratory loads to reach failure points and the use of a wide range of rotor speeds, as well as two bladed rotors, can create difficulties in avoiding a violent response. They proposed introducing collective pitch variation, adding more rotor blades, and/or adding flapping or teetering hinges to eVTOL aircraft that feature lift rotors in edgewise flight.

1.3 Objectives

The objective of this thesis is to demonstrate that NDARC can serve as a viable option for optimizing and synthesizing small, multirotor UAS vehicles as well as providing valuable low fidelity simulations for even larger multirotor eVTOL vehicles intended for UAM missions of transporting cargo and/or passengers. This paper is primarily split into two major sections, both of which share an additional collective objective to understand what inputs allow the NDARC models to reflect interaction effects between aircraft components. The first section focuses on the modelling, in terms of geometry and key aerodynamic parameters for aircraft performance for key rotorcraft comoponents, of smaller vehicles roughly 10lbs or less in gross weight. Particularly, a

large focus was placed on the rotor-to-rotor interactions given the interference from front rotors to aft rotors for multirotor vehicles and the impact these interactions can have on rotor performance. Previously, NDARC documentation only provided suggestions for large-scale rotor craft (single main rotor with tail rotor, tandem rotors, coaxial rotors, etc.), but no values were suggested for quadrotors and other multirotor configurations exceeding two rotors. This thesis addresses this.

The second primary section of this thesis focuses on the modelling of the much larger lift+cruise concept vehicles in NDARC. Generating accurate data for the transition region of a lift+cruise eVTOL concept vehicle is something that is quite challenging given the geometry and design of the vehicle, but would provide valuable insight for both NDARC and the design process of the selected lift+cruise model and future lift+cruise models. The objective of the second section is to confirm that NDARC serves as a viable, low-fidelity software for rapidly designing and testing these complicated lift+cruise concepts by comparing to data generated via a higher fidelity software due to the lack of public data and actual physical flight test data. Using the data generated by NDARC, the next objective is to provide recommendations and conclusions for the selected lift+cruise model.

1.4 Software Used

The primary software tool used for this study was version 1.14 of NDARC. NDARC served as a sizing and analysis tool for the rotorcraft discussed in this thesis and is discussed in greater detail in Ref. [1], Ref. [2], and Ref. [19]. The changes made to the inputs in NDARC are done using a GUI known as AIDEN, Ref. [20]. Vehicles are built in NDARC using a modular architecture in which each component of the aircraft (i.e. wings, rotors, engines, batteries, fuselage, landing gear, etc.) is created using various parameters relevant to each component. This method of building the aircraft based upon general models provided by NASA enables people to test

relatively untraditional aircraft designs with ease. Additionally, a previous version of NDARC, version 1.13, introduced the critical feature of being able to model stopped rotors, which was necessary for the modelling of the BETA Alia. Once an aircraft is built, users can then create specific conditions to explore the performance of the aircraft across its flight envelope. Users can also create larger missions that simulate what the aircraft could and would actually see when used, spanning from any combination of takeoff, to hover, to forward flight, to descent, and eventually landing. The software is very useful because it allows for the user to rapidly generate results while also being able to quickly change and alter the design. based upon its multitude of components. Once results were generated using NDARC, MATLAB was then used to parse and plot the data.

Because so many of the new eVTOL and UAM related concept vehicles feature unique designs with multiple rotors and varying propulsion systems, it should be noted that NDARC does have some challenges for modelling these new vehicles, as noted in Ref. [21]. In their study, Vegh et al. concluded that, due to the lack of "true" data from flight tests performed with previous designs, calibrating empirical correlations from NDARC is impossible without using high-fidelity analysis or testing. It was found that the semi-empirical model used by NDARC does not capture the effect of spanwise loading on the wing, thus NDARC tends to generate more optimistic aerodynamic assumptions and create a more aerodynamic configuration based upon its optimization. Additionally, this optimistic approach by NDARC also leads to smaller batteries that struggle at high disk loading.

Due to a lack of empirical data, including flight test data or wind tunnel data, for the BETA Alia, a second program named DEPSim (Ref. [22] and Ref. [23]) was used to generate higher-fidelity results and analysis of flight dynamics ad aeromechanics to compare to the results generated by NDARC and, in turn, validate NDARC as a valid and reliable tool for these lif+cruise

concept vehicles. DEPSim is collaborative project that involved both Pennsylvania State University, who provided the flight simulation code PSUDEPSim, and Continuum Dynamics Inc, who provided their aeromechanics code known as CHARM. PSUDEPSim was developed in Mathworks Simulink and is capable of working as a stand-alone, low-fidelity flight simulator. The program uses a non-linear, 6-DOF Newtonian dynamics for the rigid body dynamics model while the rotors use a rigid blade flapping dynamics model, three-state Pitt-Peter inflow, and look-up tables for the airfoils. By itself, PSUDEPSim is primarily used to trim the aircraft, initialize the simulation, and for performing the initial control design. This program was then combined with CHARM to overcome the lack of complex wake dynamics and interactional effects in PSUDEPSim. CHARM utilizes a higher fidelity aeromechanics model for the rotors and lifting surfaces that features a full-span, constant vorticity contour, free-vortex wake model and a vortex lattice lifting surface blade model. These features allow users of CHARM to model wake interactions from rotor-to-rotor, rotor-to-lifting surface, and so on. The ability to model these interactions is critical for an aircraft like the BETA Alia. The high-fidelity wake modeling of CHARM combined with the low-fidelity flight simulation of PSUDEPSim creates a medium-fidelity program (DEPSim) that can validate the results from NDARC.

Chapter 2: Small-Scale UAS Modelling

2.1 Introduction

Since its initial release, NDARC has been confirmed to be an accurate and useful tool throughout the industry for many large-scale aircraft, Ref. [2]. NDARC has been able to provide valuable information relating to sizing, power, aerodynamics, controls, and vehicle dynamics as a quick-edit, low-fidelity tool for aircraft ranging from full-scale helicopters to fixed wing aircraft. Since then, however, it has yet to be confirmed as a reliable tool for the same when it comes to small, multirotor UAVs. Using the wind tunnel data collected in Ref. [3] that includes resultant forces, moments, and electrical power data for the full vehicle and individual rotor as well as forces and moments for the bare airframe of five different commercially available UAV models, validating NDARC for this purpose becomes possible.

Of the five aircraft tested, four were quadcopter configurations and one was an octocopter configuration. The octocopter was neglected for this study due to its notably different geometry, number of rotors, and use of ducted rotors. From the remaining four quadcopters used in Ref. [3], the DJI Phantom and Straight Up Imaging (SUI) Endurance were selected for modelling and comparison. These quadcopters can be seen in Figure 2.1. The selection of the vehicles was based upon their relatively similar geometry, but difference in sizing and weight. The DJI Phantom has similar geometric proportions and a similar gross weight when compared to the other two unselected quadcopters which left the SUI Endurance as the other option so that two vehicles of varying gross weights and dimensions could be compared. The SUI Endurance is also slightly different in the sense that its design is meant to be more aerodynamic, as seen in the more streamlined body, and serve as a UAV that is more catered to forward flight and faster speeds when compared to the DJI Phantom and its symmetric X-shaped airframe.

(a)

(b)

Figure 2.1 Small multirotor UAVs: (a) DJI Phantom 4 Pro+ V2.0 (downloaded from https://store.dji.com) (b) SUI Endurance (downloaded from https://www.suasnews.com).

2.2 DJI Phantom

As mentioned previously, the DJI Phantom is both the lighter and smaller UAS of the two aircraft selected for this study. Because of this smaller size, it features smaller rotors. Furthermore, the DJI Phantom has a fairly bulky fuselage (compared to the more streamlined look of the Endurance) that resembles a nearly symmetrical "X" shape. Based upon this geometry, one can surmise that this particular aircraft is better suited for hover or low speed flight in multiple directions when compared to other multirotor UAVs. The main physical characteristics of the DJI Phantom are displayed in Table 2.1.

Physical Characteristic	Value
Weight	2.8 lbs
Length (incl. rotors)	19.2"
Length (rotor-to-rotor)	9.8"
Width (incl. rotors)	19.3"
Width (rotor-to-rotor)	9.9"
Rotor Diameter	9.4"

Table 2.1 Physical characteristics of DJI Phantom.

The initial DJI Phantom model used in NDARC was provided by the CD&A group of the U.S. Army TDD. Once a small, multirotor UAV is "built" within NDARC using as many dimensions and technical specifications as possible from documentation to accurately model the geometry of the vehicle, other physical characteristics, electrical components, etc., and further adjustments will need to be made to match flight performance results from NDARC to empirical data. Particularly, it is important to match the results for lift, drag, pitching moment, and power required with the greatest emphasis on lift, drag, and power required as these results are key for

validating the model with respect to rotor performance and pitch moment is subjective to many other inputs (component weights, geometry, etc.). The best way to match this data, is to manipulate parameters found in the fuselage, aircraft, and rotor components whose values are not well known. These changes will be detailed below.

2.2.1 Airframe Calibration

Typically, when running performance conditions for tasks in NDARC, the desire is for the vehicle to be trimmed, but this is not necessary when matching wind tunnel data where the vehicle is not in free flight so there is no need to balance forces and moments. Instead, the controls and attitude of the aircraft are specified in the wind tunnel test. To ensure that NDARC does not trim the vehicle, the trim solution/aircraft trim state (*STATE_trim*) should be set to "none" in the appropriate performance conditions where users defines the conditions for the atmosphere, the aircraft, and what the aircraft will be doing (i.e. hover, forward flight, climb, performance sweeps, etc.). Once NDARC is set to run in "wind tunnel mode" (i.e. no trim solution), a baseline set of force, moment, and power values for the NDARC model can be made and compared to the empirical wind tunnel results.

After a baseline is made by running the model in its original state as delivered by the Army TDD and compared to the test data, there will likely be differences in the lift, drag, pitching moment, and power required results. To begin tuning the NDARC model to match the test data, the forces attributed to each of the rotors are removed to isolate the forces generated by the fuselage of the vehicle. The lift of the fuselage is most likely linear with respect to increasing angle of attack and the NDARC model should match this. To do this, it is recommended that the lift model be set to a fixed value determined by L/q (*SET_lift* = 1). Furthermore, this means the lift slope for the fuselage ($d(L/q)/d\alpha$ (variable), *dLoQda* (NDARC mnemonic)) will need to be input and this value

for the DJI Phantom. The value was derived using the airframe wind tunnel data and this value provided a relatively good match for the fuselage lift as shown in Figure 2.2. These inputs are found in the fuselage component of NDARC and the effects of these values can be seen below in the equations used by NDARC, Ref. [1], to calculate the lift coefficient (1) and the lift force (2) when the effective angle of attack is less than or equal to the maximum angle of attack. The maximum lift coefficient is defined in equation (3) In these equations, the effective angle of attack (α_e) is defined as the difference between the fuselage angle of attack and the angle of zero lift.

$$C_L = C_{L\alpha}\alpha_e \tag{1}$$

$$L = qS_{wet}C_L \tag{2}$$

$$C_L = C_{L\alpha}\alpha_{\max}\sin\alpha_e\left(\frac{\frac{\pi}{2}-|\alpha_e|}{\frac{\pi}{2}-|\alpha_{max}|}\right) \tag{3}$$

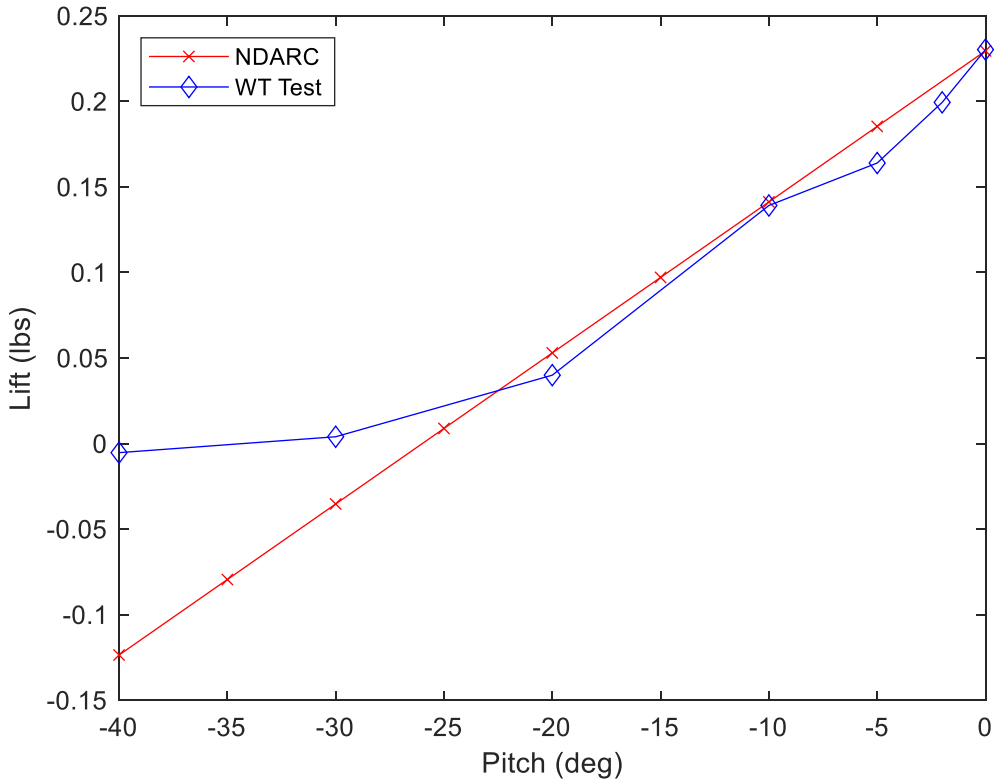

Figure 2.2 Comparison of the bare airframe lift at 40 fps airspeed from wind tunnel testing in Ref. [3] and NDARC for the DJI Phantom.

The same general process was done for the drag of the fuselage and again, the pertinent inputs are located in the fuselage component. The drag model for forward flight (*SET_drag*) was also be set to a fixed input like the lift. From here, the area (*D/q*, *DoQ*) and drag coefficient (C_D, *CD*) for the fuselage component are determined using the wind tunnel data. Based upon the equation used for the drag coefficient in NDARC for when the angle of attack is lower than the transition angle (4) and the drag force (5), it is seen that as any of these of these inputs increase, the drag of the fuselage will also increase. For drag, it is important to note that the effective angle of attack (α_e) is the difference between angle of attack of the aircraft and angle of attack for minimum drag.

$$C_D = C_{D0}(1 + K_d|\alpha_e|^{X_d}) \tag{4}$$

$$D = qS_{wet}\left(C_D + C_{Dfit} + \sum C_{Drb}\right) + q\left((D/q)_{pay} + (D/q)_{cont}\right) \quad (5)$$

Still within the fuselage component in NDARC, the drag correction factor (K_d, *Kdrag*) greatly influences the drag results for the airframe and should be tuned as well. Given the geometry of the DJI Phantom, the drag of the airframe is essentially constant across the pitch attitudes tested in Ref. [1] and this was replicated in NDARC by setting K_d to 0. The comparison of the drag results from NDARC and the wind tunnel are shown in Figure 2.3.

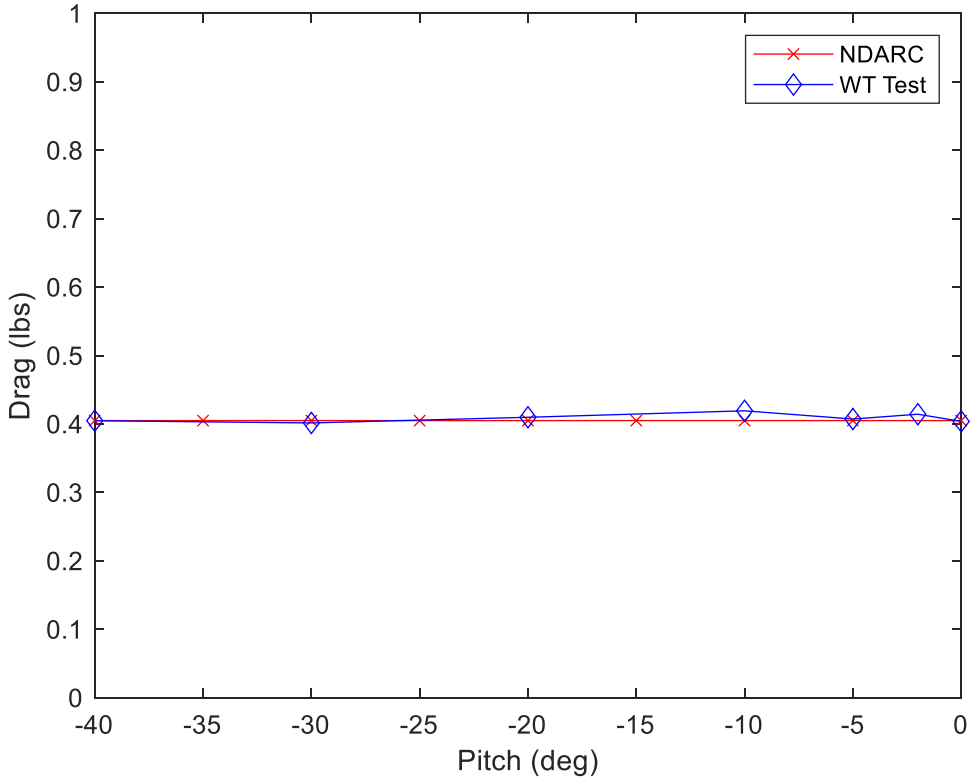

Figure 2.3 Comparison of the bare airframe drag at 40 fps airspeed from wind tunnel testing in Ref. [3] and NDARC for the DJI Phantom.

Lastly, in the fuselage component for the bare airframe results, the pitching moment was tuned as well by setting the moment model to a fixed input (*SET_moment*) like the lift and drag models mentioned previously. In addition to this, it was necessary to input the pitch moment at

zero lift ($(M/q)_0$, *MoQ0*) based upon an average taken from the wind tunnel results and it is recommended that the slope for the moment (*d(M/q)/dα*, *dMoQda*) be set to zero and keep the moment for the fuselage constant. The following equations for the pitch moment coefficient (6) and pitch moment (7) used by NDARC demonstrate that the coefficient and thus the moment, will increase as these inputs are increased. Like the lift equations, the effective angle of attack (α_e) is defined as the difference between the fuselage angle of attack and the angle of zero lift.

$$C_M = C_{M0} + C_{M\alpha}\alpha_e \tag{6}$$

$$M = qS_{wet}\ell_{fus}C_M \tag{7}$$

The decision and recommendation to remove any slope input and keep the pitch moment constant was made because the DJI Phantom features a quadratic shape for its pitch moment, shown in Figure 2.4, which was not possible to replicate in NDARC. Therefore, the best solution for modeling the pitching moment of the DJI Phantom was to focus on average the pitching moment from the wind tunnel data from a range of pitch attitudes that likely contains the trim pitch angle.

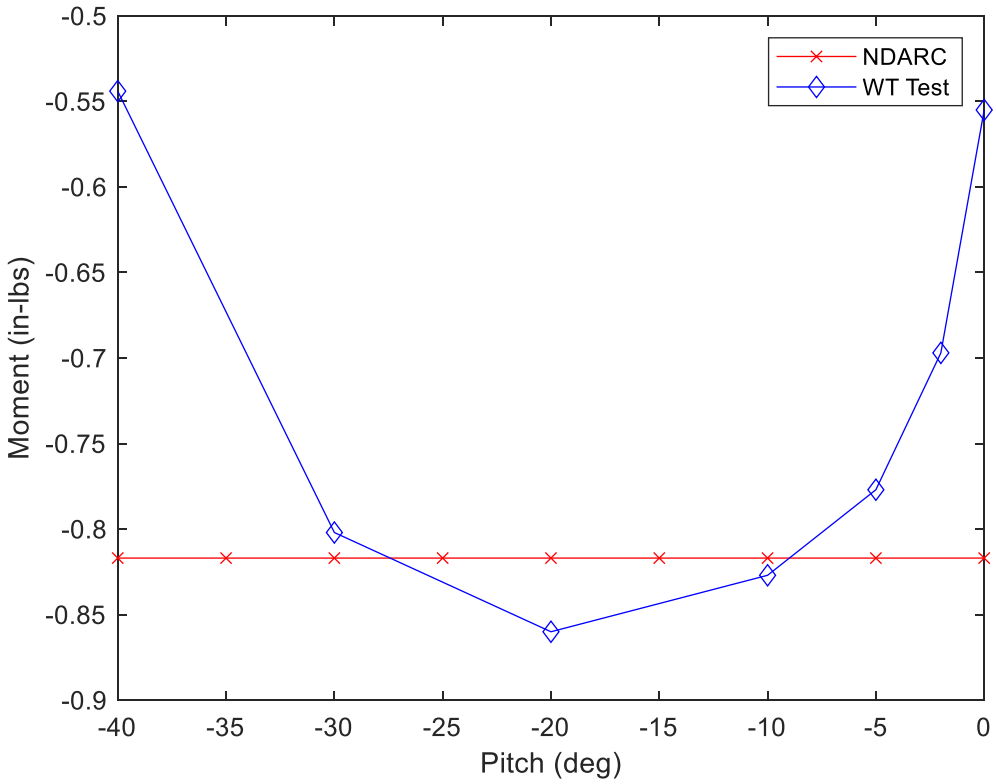

Figure 2.4 Comparison of the bare airframe pitch moment at 40 fps airspeed from wind tunnel testing in Ref. [3] and NDARC for the DJI Phantom.

Using these inputs and the data from Ref. [3] to tune the NDARC inputs provided a satisfactory level of correlation between the wind tunnel data and the NDARC results given the limitations of NDARC. It should also be noted that the forces and moments of the fuselage are relatively small in comparison to that of the rotors, and thus the discrepancies are not expected to have a notable effect on performance. The design of the DJI Phantom itself also presents challenges, but the emphasis was to match lift, drag, and pitch moment near trim attitudes.

2.2.2 Full Vehicle Calibration

Once the airframe results from NDARC were tuned to match the wind tunnel results, the forces and power results related to the rotors were added in to complete the DJI Phantom model. Of course, this will require a number of inputs found in the rotor components to be manipulated in

order to make the total results from NDARC match the wind tunnel results again. Therefore, all of the following inputs will be for the rotor components. Before immediately attempting to model the complete DJI Phantom model (airframe and rotors) in forward flight, the model was tested in hover to ensure that the model could accurately model this flight mode. To do this, the total lift, which is almost entirely generated by the four rotors, and the power required results from NDARC were directly compared to data collected in Ref. [3]. To see the comparison in hover, refer to Figure 2.5 and Figure 2.6.

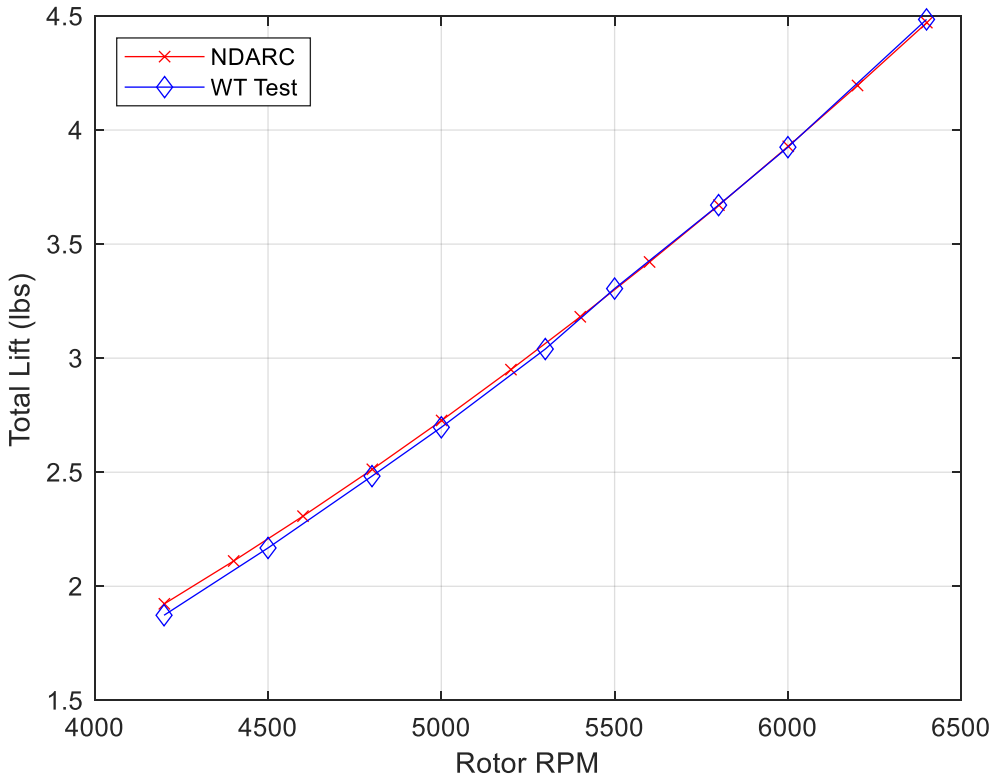

Figure 2.5 Total lift of the DJI Phantom in hover.

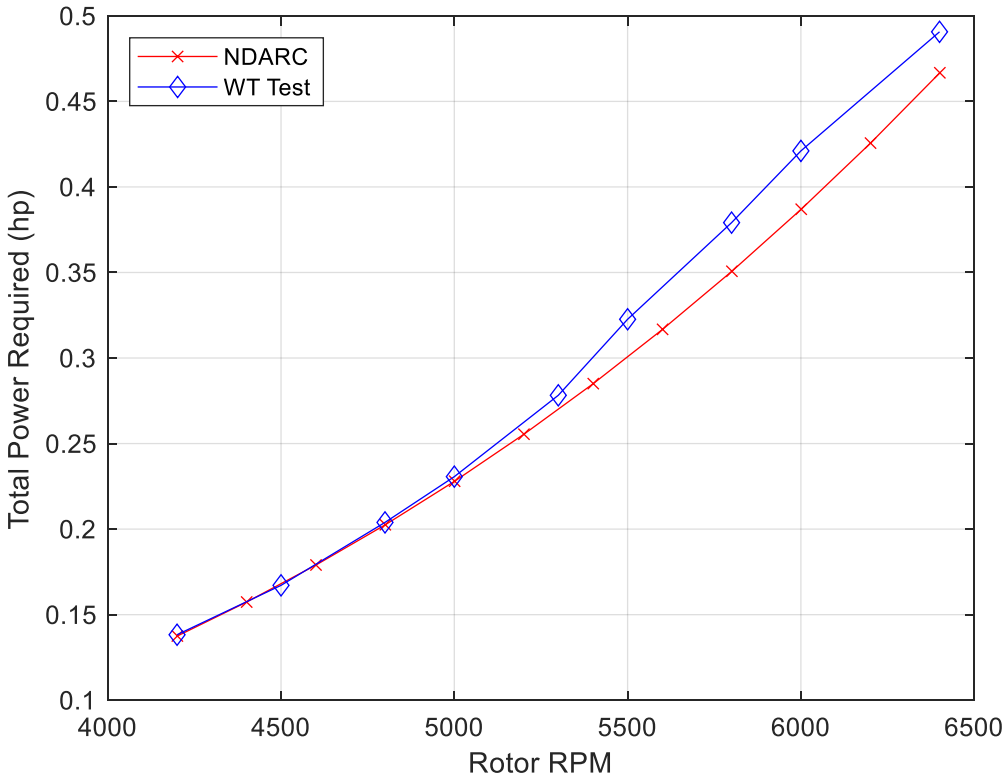

Figure 2.6 Power required of the DJI Phantom in hover.

It is important to note that before tuning any of the other inputs, there was no need to include in-plane forces so "*MODEL_Ftpp*" and "*MODEL_Fpro*" were neglected, but it is critical to include flapping effects in the model as this accounts for large H forces on the rotor in forward flight. To include flapping, *KIND_control* should be set to 4 in NDARC, which sets the model to the no-feathering plane control command. In this mode, the blade cyclic pitch values are set to 0, and the collective pitch is constant. The rotors can then flap according to the flap frequency and lock number properties of the rotor as defined by the NDARC inputs (*flapfreq*, *gamma*).

Beginning again with the calibration of the lift forces, $\kappa_{f\,twin}$ (*Kf_twin*) can be adjusted to move the lift results up or down with an increasing or decreasing value, respectively. It is important to note that manipulations to this value also impact the pitch moment results, which will be discussed later. $K_{f\,twin}$ (*Kf_twin*) is defined in Ref. [24] as the ideal induced velocity correction

factor for forward flight, which is only used for configurations with multiple rotors, and because of its impact on the pitch moment, it was set to 1. Next, moving to the drag again, this is greatly impacted by two inputs. Increasing the values for the blade profile drag coefficient for the propeller, d_{0prop} (*d0_prop*), and the profile drag coefficient for the helicopter rotor, d_{0hel} (*d0_hel*), will directly increase the drag forces on the rotor blades, affecting the drag of the as well as the profile power required. Because of this, it requires some tuning for both variables and some acceptance for a certain amount of error.

The biggest challenge was tuning the pitching moment for the model across various pitch moments with respect to rotor RPM. Thus far, using the aforementioned $\kappa_{f\,twin}$ (*Kf_twin*) and the multirotor thrust factor for forward flight, x_f (*xf_multi*), had proven to be the best way to tune the pitching moment for one or more of the pitch angles at a given airspeed while providing good slopes for the rest of the pitch angles.

These correction factors are applied to the induced velocities used in computing thrust and induced power of each of the rotors, which usually experience advance ratios in the 0.1 to 0.25 range for the Phantom and the Edurance. In forward flight, the induced velocity of an isolated rotor is well-approximated using Glauert's approximation of momentum theory:

$$v_i = \frac{\kappa T}{2\rho A V} \tag{8}$$

where κ is an induced velocity correction factor. The multiple rotor interference model NDARC uses a modification of this:

$$v_i = \kappa_{twin}\left(\frac{x_1 T_1}{2\rho A V} + \frac{x_2 T_2}{2\rho A V} + \cdots \frac{x_n T_n}{2\rho A V}\right) \tag{9}$$

where the correction factors x_1, x_2, etc. … model the influence of each rotor on the induced velocity of the specific rotor being computed. Each rotor model will have a different set of x_i values to

model the effect of each rotor on its own inflow. A rotor's theoretical value for x_i corresponding to itself, is 1.0. In forward flight, it is expected there will be non-zero values of x_i for rotors forward of the rotor being modelled. Similar correction values can also be applied in hover, so there are x_h and x_f values corresponding to hover and forward flight. The value is blended between hover and forward flight as shown in equation 10.

$$x = \frac{x_f \mu^2 + x_h C \lambda_h^2}{\mu^2 + C \lambda_h^2} \tag{10}$$

It should, however, be noted that this inflow model would not be valid below advance ratios below 0.1. To achieve this level of accuracy, x_f required tuning in two different ways. In NDARC, x_f is set up as a vector with the same number of values as there are rotors (i.e. a 1x4 for a 4 rotor UAV). Initially, all values within each rotor component will be set to zero, but the value that lines up with the desired rotor will be assigned a tuned value that matches the rest of the rotors (i.e. (1., 0, 0, 0) for rotor 1, (0, 1., 0, 0) for rotor 2, etc.). The other value for this input that needs to be tuned is the interference value for the aft rotor from the forward rotor directly in front of it.

The other feature that must be considered when tuning the pitch moment of the Phantom is the vertical distance of the rotor to the CG of the aircraft. This was initially set to a distance of 2.39 inches, but was reduced to a fourth of that distance (0.59 inches) to provide better results as it is difficult to determine this dimension without a tangible model. By manipulating both of these values for the thrust factor and the vertical distance of the rotor to the CG, a fair amount of pitch moment accuracy can be achieved, particularly at lower magnitude pitch attitudes.

The power required for the DJI Phantom remained largely unaffected throughout the process of tuning the lift, drag, and pitch moment and was quite accurate from the beginning with the model provided by the CD&A group. To see how the changes to the different inputs in the

rotor components affected the lift, drag, pitch moment, and power required and how the final results compared to the wind tunnel data, refer to Figures 2.7-2.10.

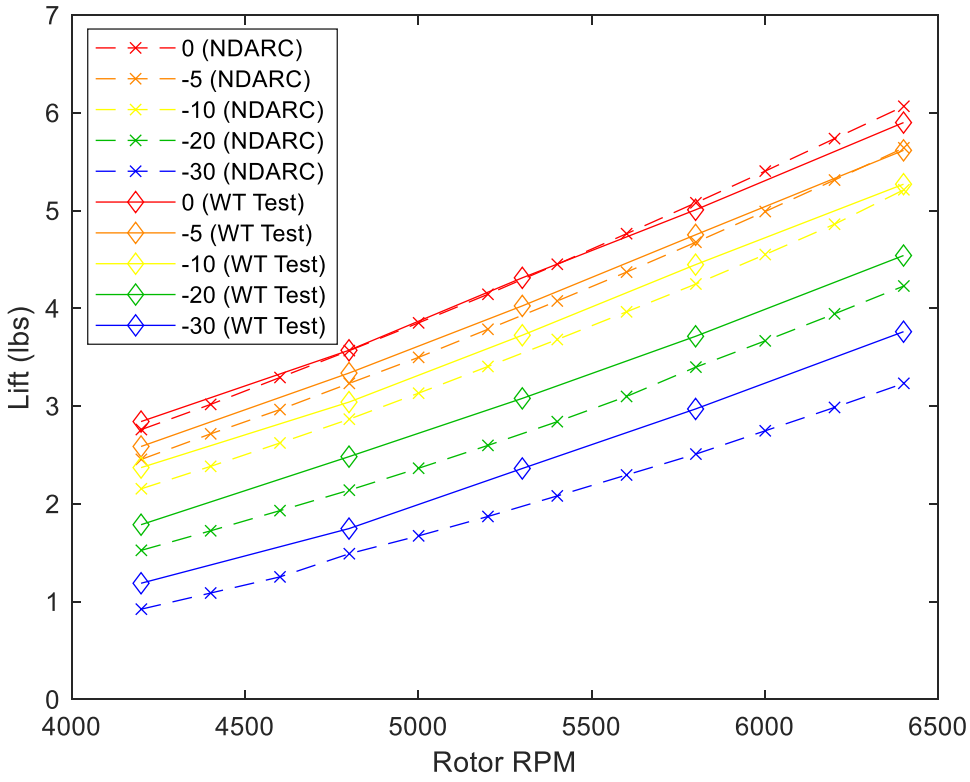

(a)

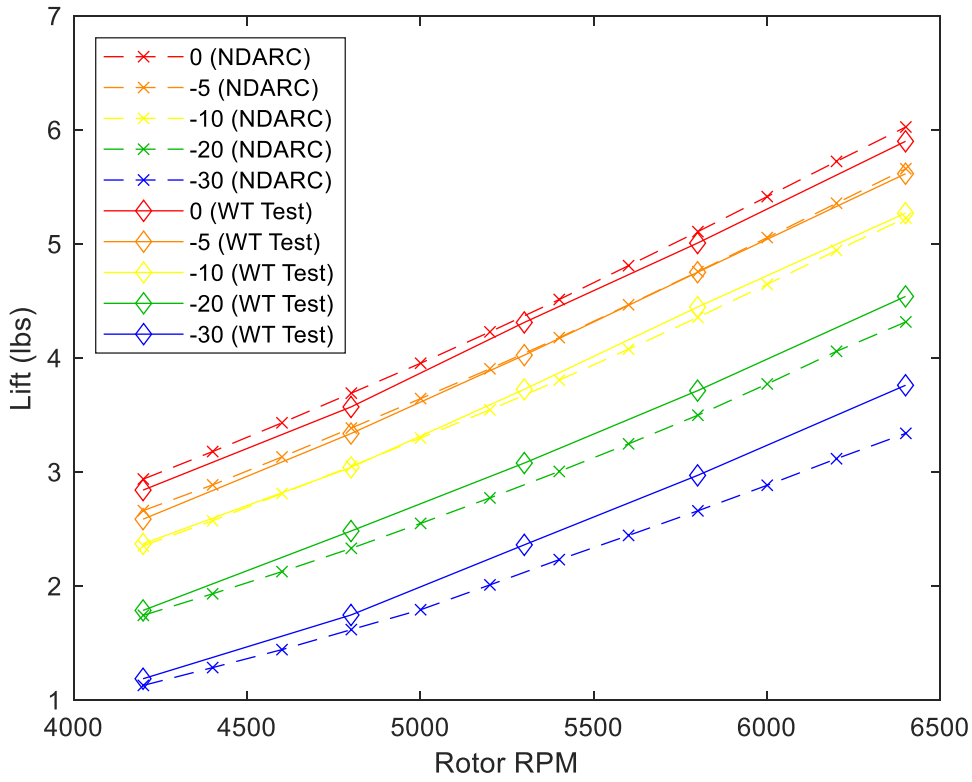

(b)

Figure 2.7 Lift of the complete aircraft at 40 fps airspeed across multiple pitch attitudes before (a) and after (b) including blade flapping and rotor-to-rotor interference effects, or decreasing vertical rotor distance to CG.

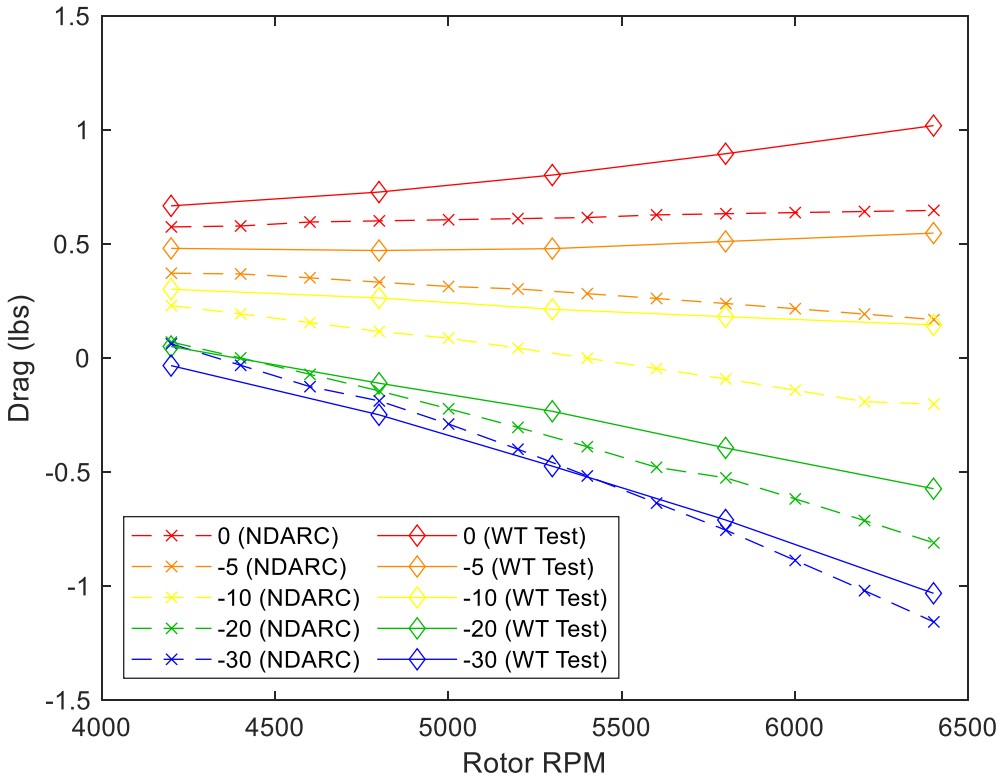
1.5
1
0.5
0
-0.5
-1
-1.5
Drag (lbs)
4000
4500
5000
5500
6000
6500
Rotor RPM
0 (NDARC)
-5 (NDARC)
-10 (NDARC)
-20 (NDARC)
-30 (NDARC)
0 (WT Test)
-5 (WT Test)
-10 (WT Test)
-20 (WT Test)
-30 (WT Test)

(a)

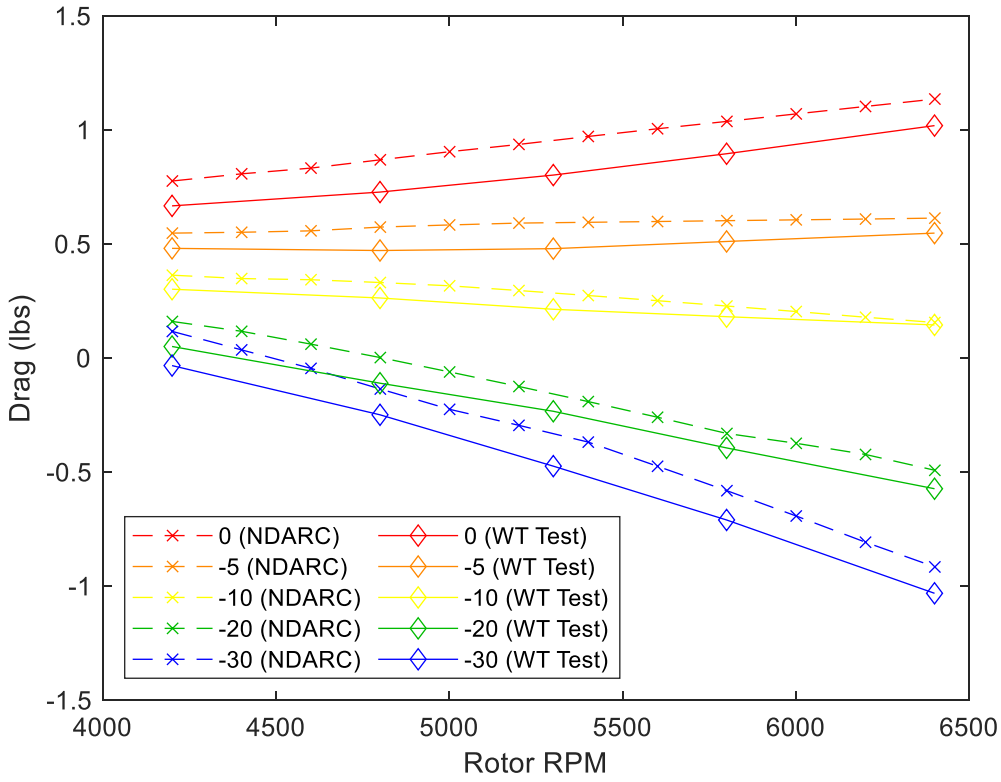

(b)

Figure 2.8 Drag of the complete aircraft at 40 fps airspeed across multiple pitch attitudes before (a) and after (b) including blade flapping and rotor-to-rotor interference effects, or decreasing vertical rotor distance to CG.

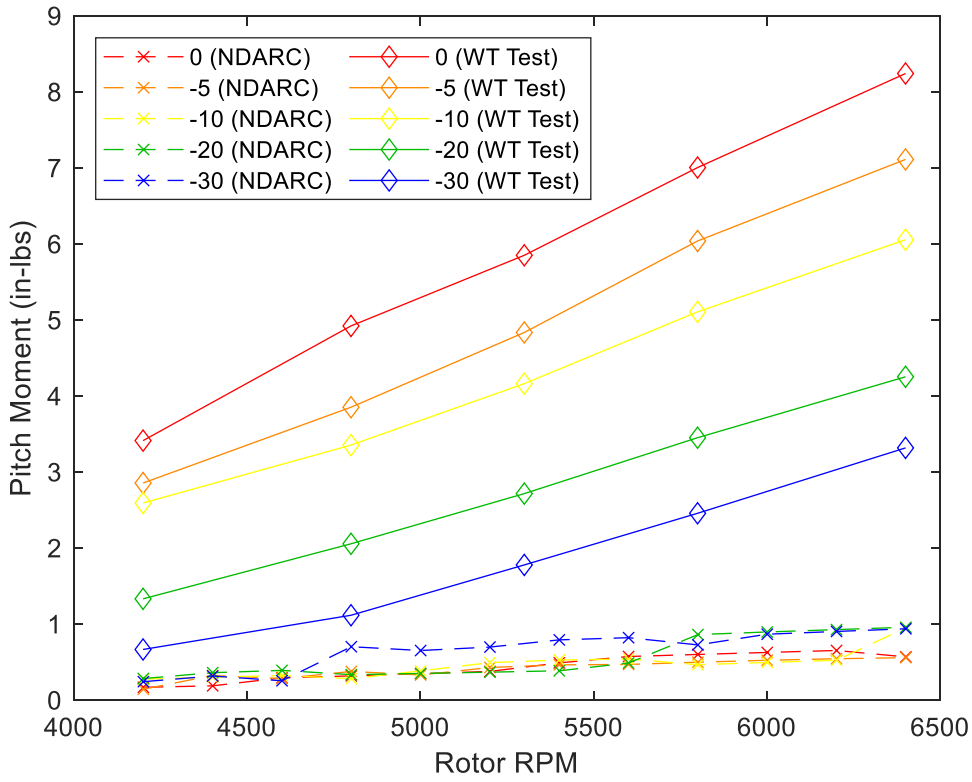
0 (NDARC)
-5 (NDARC)
-10 (NDARC)
-20 (NDARC)
-30 (NDARC)
0 (WT Test)
-5 (WT Test)
-10 (WT Test)
-20 (WT Test)
-30 (WT Test)
Pitch Moment (in-lbs)
Rotor RPM
0
1
2
3
4
5
6
7
8
9
4000
4500
5000
5500
6000
6500

(a)

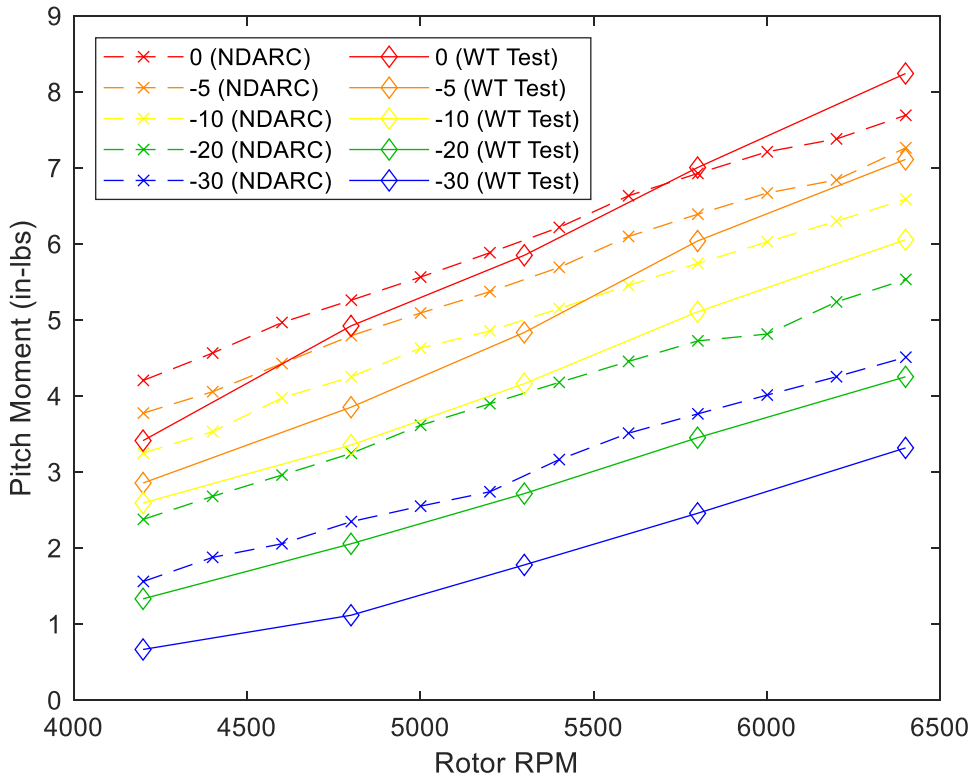

(b)

Figure 2.9 Pitching moment of the complete aircraft at 40 fps airspeed across multiple pitch attitudes before (a) and after (b) including blade flapping and rotor-to-rotor interference effects, or decreasing vertical rotor distance to CG.

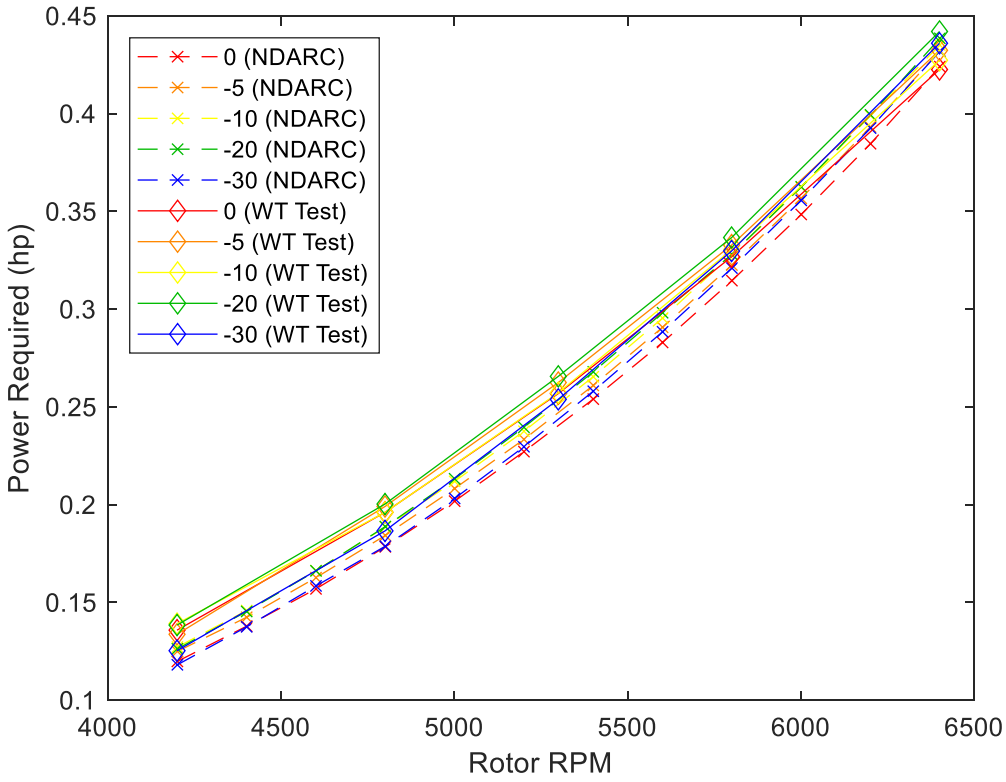
0.45
0.4
0.35
0.3
0.25
0.2
0.15
0.1
Power Required (hp)
4000
4500
5000
5500
6000
6500
Rotor RPM
0 (NDARC)
-5 (NDARC)
-10 (NDARC)
-20 (NDARC)
-30 (NDARC)
0 (WT Test)
-5 (WT Test)
-10 (WT Test)
-20 (WT Test)
-30 (WT Test)

(a)

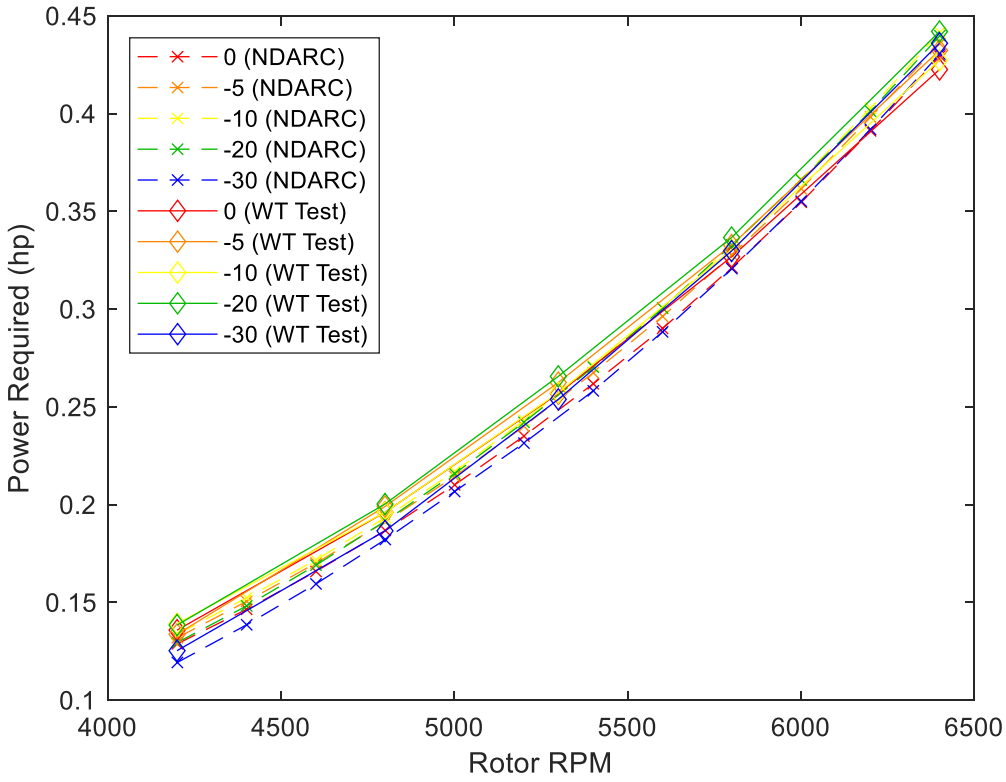

(b)

Figure 2.10 Power required for the complete aircraft at 40 fps airspeed across multiple pitch attitudes before (a) and after (b) including blade flapping and rotor-to-rotor interference effects, or decreasing vertical rotor distance to CG.

To see a full step-by-step summary of the NDARC inputs that were manipulated and tuned for the DJI Phantom, refer to the Appendix.

2.2.3 Center of Gravity Shifting

In an effort to confirm the power required results of the DJI Phantom, the center of gravity of the NDARC model was shifted differing distances in the longitudinal direction (varying the station line, positive aft) at both 20 fps and 40 fps. The model was then trimmed instead of analyzed in wind tunnel mode. It is important to note that because the model is being trimmed, *STATE_trim* must be set to appropriate string in the condition quant (“symm”). The initial guess

for the input in NDARC, ΔSL_{cg} (*dSLcg*, applied in the condition component), was found by trimming the Phantom at each airspeed with the condition that each rotor had equivalent RPMs. These trimmed values were then used to determine how far forward the CG of the Phantom needed to moved to generate equivalent RPMs for all four rotors. Additionally, using the calculated RPM and pitch attitude values required for trim, the power required in trim with a shifted CG for each of the four Phantom rotors was able to be calculated using the data from Ref. [3] and two-dimensional interpolation, the results of which can be seen in Table 2.2.

Parameter	Value at 20fps	Value at 40fps
θ	-8.70°	-17.3°
Ω	4790 RPM	4760 RPM
ΔSL	-0.85”	-0.88”
$P_{req,FL}$	0.0495 hp	0.0520 hp
$P_{req,FR}$	0.0455 hp	0.0474 hp
$P_{req,RL}$	0.0503 hp	0.0472 hp
$P_{req,RR}$	0.0483 hp	0.0484 hp

Table 2.2 Values of trimmed parameters at different airspeeds for DJI Phantom.

Using the suggested distance based upon the wind tunnel data to shift the CG in NDARC worked well for the DJI Phantom at 20fps, but did not work well at 40 fps when comparing the results generated by NDARC to the wind tunnel data, specifically the rotor speed, body pitch of the Phantom, or the power required for each rotor. From here, the CG stationline (*dSLcg*) input in NDARC was hand tuned for each airspeed until the Phantom achieved equivalent rotor speeds for all four rotors. This resulted in a final CG stationline shift of 0.882” and 1.44” in NDARC for the 20fps and 40 fps airspeeds, respectively. The results for rotor speed, aircraft pitch attitude, and

power required for each rotor can be seen in Figures 2.11-2.13. In each of the three figures, the black vertical lines serve as the marker for both 20fps and 40 fps, while the red circle and red "X" markers indicate the values derived from the wind tunnel data at 20fps and 40fps, respectively. The goal was to have the matching lines intercept each other at the 20fps and 40fps and because the NDARC model trims the left and right sides of the aircraft symmetrically, only one front rotor line and one rear rotor line is necessary for plotting.

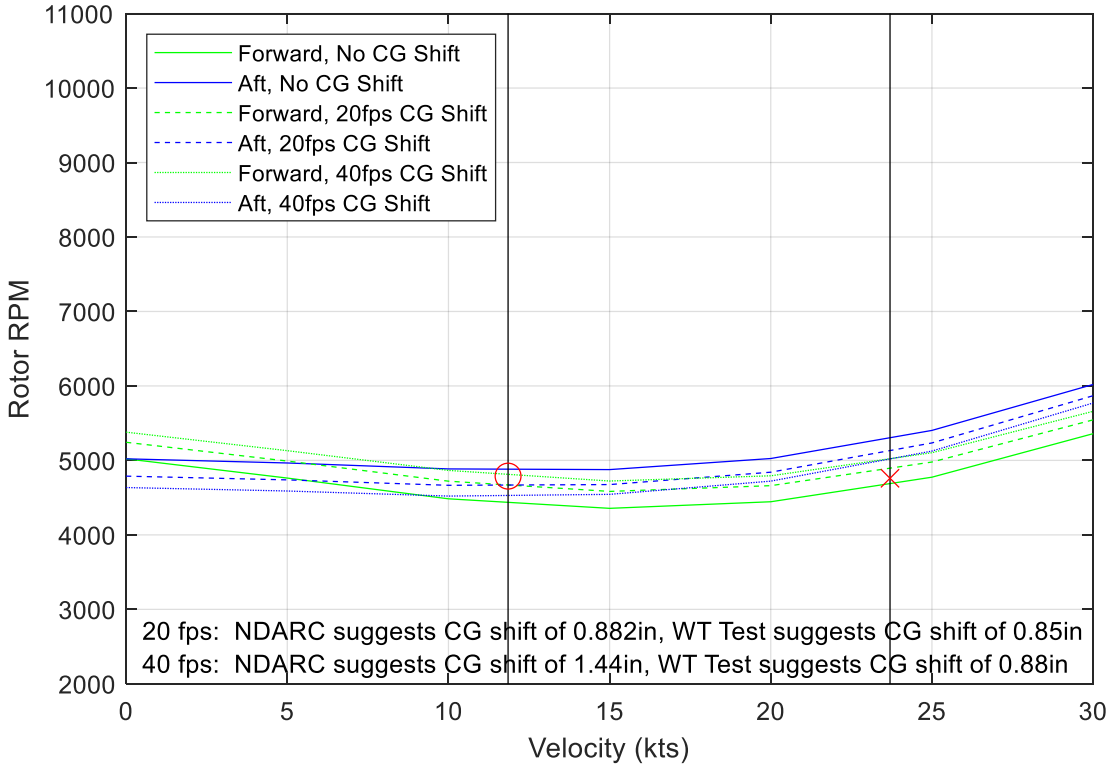

Figure 2.11 Matching DJI Phantom rotor RPM using the suggested shift in aircraft CG as defined by NDARC and wind tunnel data.

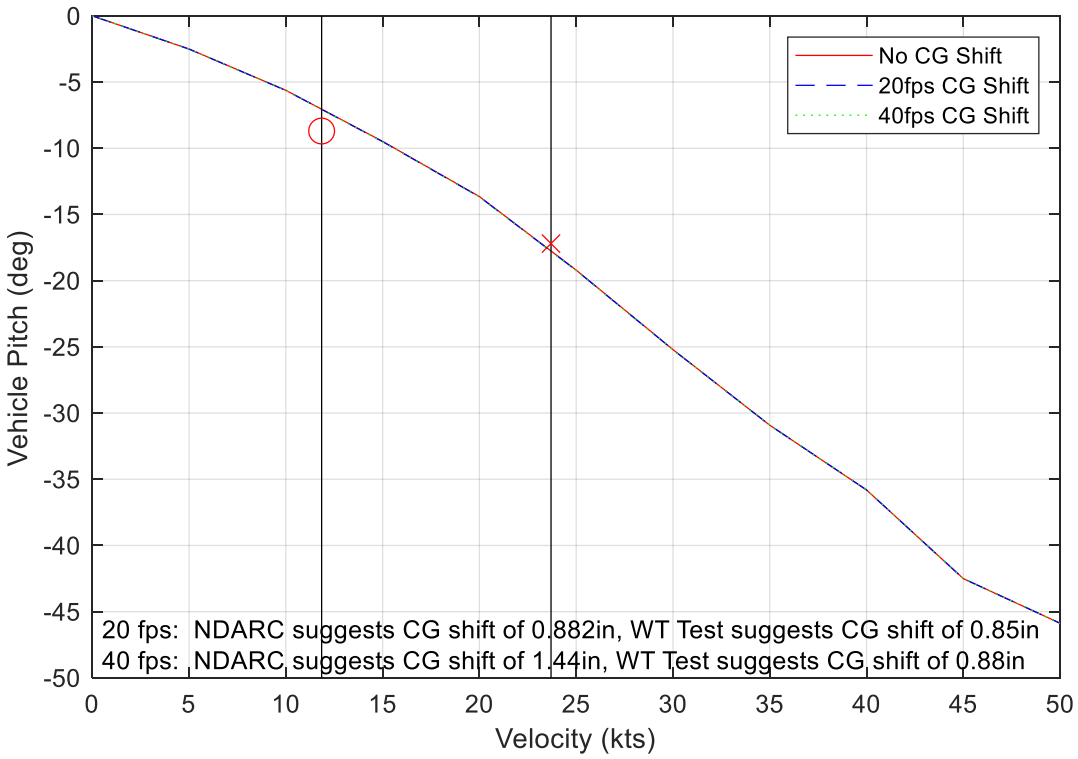

Figure 2.12 Matching DJI Phantom pitch attitude using the suggested shift in aircraft CG as defined by NDARC and wind tunnel data.

It can be seen in the above figure that the trimmed pitch attitude of the Phantom does not change in NDARC despite the shifting the center of gravity, and this is because pitch attitude is driven by the need to balance drag forces with the forward component of thrust, which is unaffected by the location of the center of gravity.

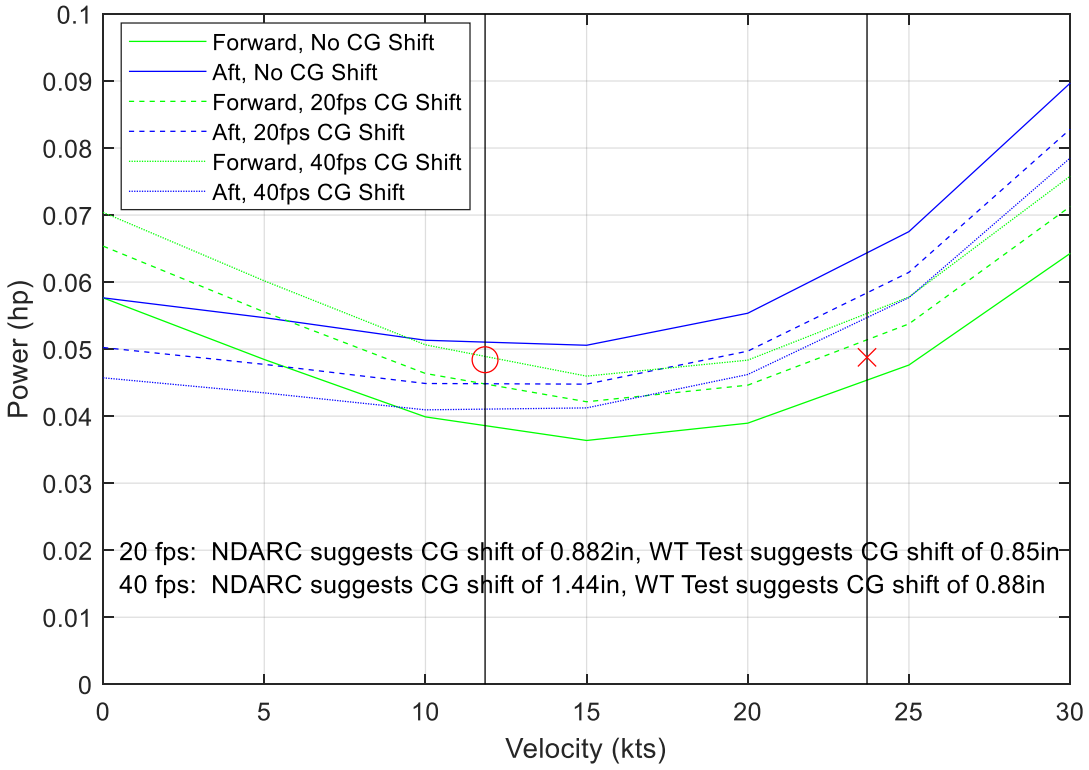

Figure 2.13 Matching power required for each DJI Phantom rotor using the suggested shift in aircraft CG as defined by NDARC and wind tunnel data.

2.3 SUI Endurance

To further validate the method of tuning and calibrating a small, multirotor UAV detailed in the previous section, the same method was applied to a different model. The second model used to validate the work done with the DJI Phantom 3, was the Straight Up Imaging (SUI) Endurance. The SUI Endurance has a weight roughly double that of the DJI Phantom, a rotor-to-rotor span that is also roughly double that of the Phantom, and a larger rotor diameter. These increased dimensions allow the method to be validated across two vehicles with relatively different gross weights. Additionally, the SUI endurance features a much more streamlined fuselage (center body) when compared to the DJI Phantom which presents different aerodynamic results that need to be captured and verified within NDARC. Furthermore, these two models were selected based upon

amount of wind tunnel testing data made available by NASA as both models were tested at the same conditions.

Physical Characteristic	Value
Weight	6 lbs
Length (incl. rotors)	35.1”
Length (rotor-to-rotor)	20.1”
Width (incl. rotors)	35.1”
Width (rotor-to-rotor)	20.1”
Rotor Diameter	15”

Table 2.3 Physical characteristics of SUI Endurance.

Because of the obvious differences in sizes, it was paramount to adjust the geometry of the vehicle accordingly within NDARC so that the dimensional ratios represented the SUI Endurance rather than the DJI Phantom. Furthermore, this includes changing the necessary parameters for the rotor, specifically the radius, solidity, and lock number, which was calculated in Ref. [7]. Furthermore, it is important to ensure that the weights of the vehicle in NDARC are changed to match the gross weight of the SUI Endurance.

From here, it was decided to focus on running the SUI Endurance in hover conditions and forward flight conditions at 20fps and 40fps so the results could be directly compared to that of the DJI Phantom. For reference, both the Endurance and the Phantom experience hover tip speeds in the range of 170fps to 185 fps. The 40fps condition received the most focus, but trim was calculated for both forward flight conditions using 2-D interpolation solver programmed in MATLAB and the data collected from the wind tunnel tests. Using this solver, it was determined that trim was achieved at -4.4° pitch attitude and 3427 RPM when flying at 20fps and when flying

at 40fps, trim was achieved at -10.7° pitch attitude and 3456 RPM. These calculated values serve as valuable reference points for checking and comparing the results for NDARC to the empirical data.

2.3.1 Airframe Calibration

Once again, to begin calibrating the model within NDARC, the empirical wind tunnel data for the bare airframe (no rotors) was used to determine certain important parameters that are then input in NDARC for the "*airframe*" and "*fuselage*" components. Beginning with the lift of the airframe in forward flight (40fps), this was calibrated the same way as the DJI Phantom model using a calculated angle of attack for zero lift and lift slope. Using values determined by the wind tunnel data yielded largely similar numbers given the trend for the wind tunnel data was essentially linear and the lift model in the program was set to a fixed, linear trend. The comparison of the results from NDARC and the wind tunnel results are shown in Figure 2.14.

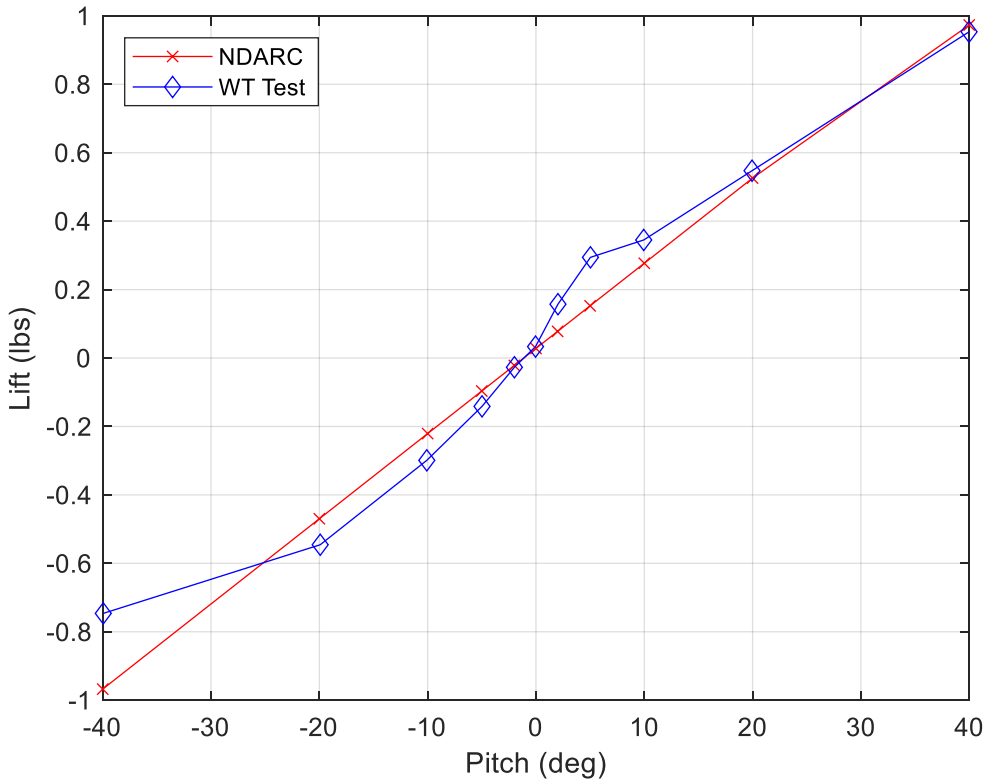

Figure 2.14 Comparison of the bare airframe lift at 40 fps airspeed from wind tunnel testing in Ref. [3] and NDARC for the SUI Endurance.

Previously, for the DJI Phantom, drag for the fuselage was predominantly determined by value in the aircraft component known as "*kDrag*" which is defined as the total aircraft drag while drag settings in the fuselage component were set to default values of 0. However, these settings did not work well for the SUI Endurance because of the more streamlined, aerodynamic shape of the model's fuselage which created a quadratic shape for drag when plotted against pitch angle, whereas the DJI Phantom airframe featured a much more constant drag force. Due to this, the drag from the aircraft component was essentially "turned off" by eliminating the *kDrag* value in the aircraft component and the drag for the fuselage component was "turned on". This allows one to input certain drag related parameters to properly fit the NDARC generated results with the wind tunnel results in an accurate manner. To do so, the default value for the drag model in the fuselage

was kept (*MODEL_drag* = 2, quadratic), as was the angle of attack for minimum drag (0°), and the fuselage K_d (*Kdrag*) value was found by fitting the resultant plot by hand. This method resulted in strong correlation between the NDARC generated results and empirical wind tunnel data, shown in Figure 2.15.

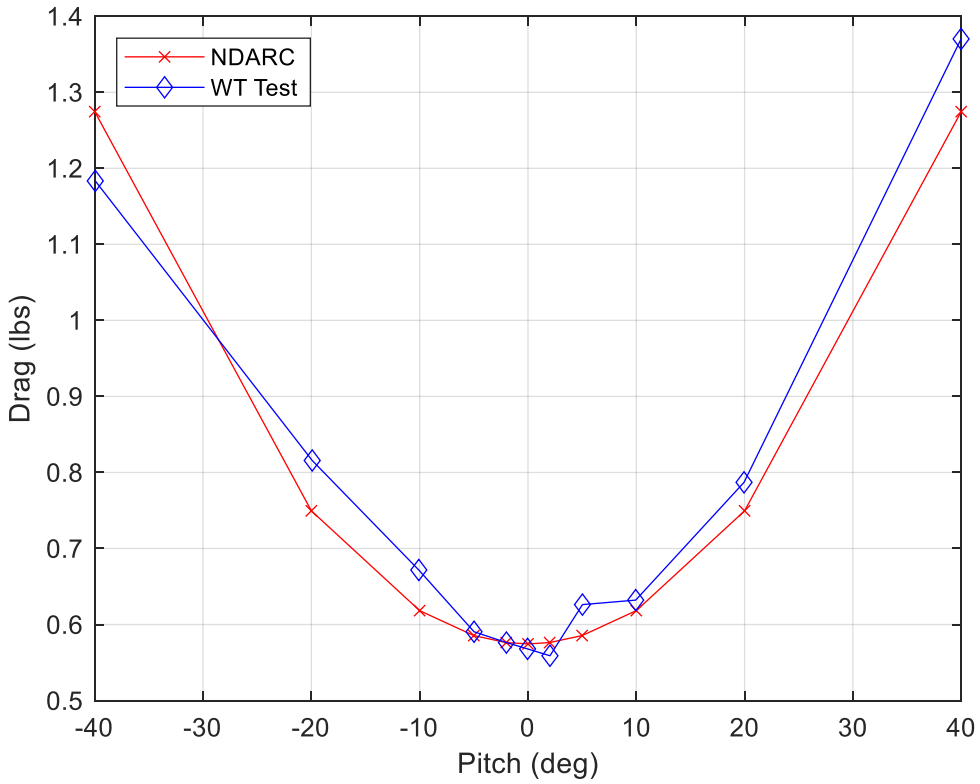

Figure 2.15 Comparison of the bare airframe drag at 40 fps airspeed from wind tunnel testing in Ref. [3] and NDARC for the SUI Endurance.

The calibration for the pitching moment of the bare SUI Endurance airframe was completed in a similar fashion to the method used for the bare airframe pitching moment of the DJI Phantom, despite the Phantom featuring a more quadratic shape for its pitching moment, and the lift for both UAVs. Using the wind tunnel data, key parameters for defining the pitching moment trends can be derived and input into NDARC. Like the lift for the fuselage, the moment model is set to a fixed trend dependent upon the moment at zero lift and the moment slope. It should be noted that while

the pitching moment for the airframe of the SUI endurance is not completely linear, nor is it constant, it was decided to focus on matching the NDARC results with the essentially constant values between pitch angles of -20° and 0° as this provided the best results across the sweep of tested pitch angles and this is also where trim takes place for this vehicle at both 20fps and 40 fps airspeed. As a result of this decision, the slope of the moment was set to 0 and the moment at zero angle of attack was set to match this section of data rather than using values that provided a better fit for the full data set from -40° to 40° pitch attitude, shown in Figure 2.16.

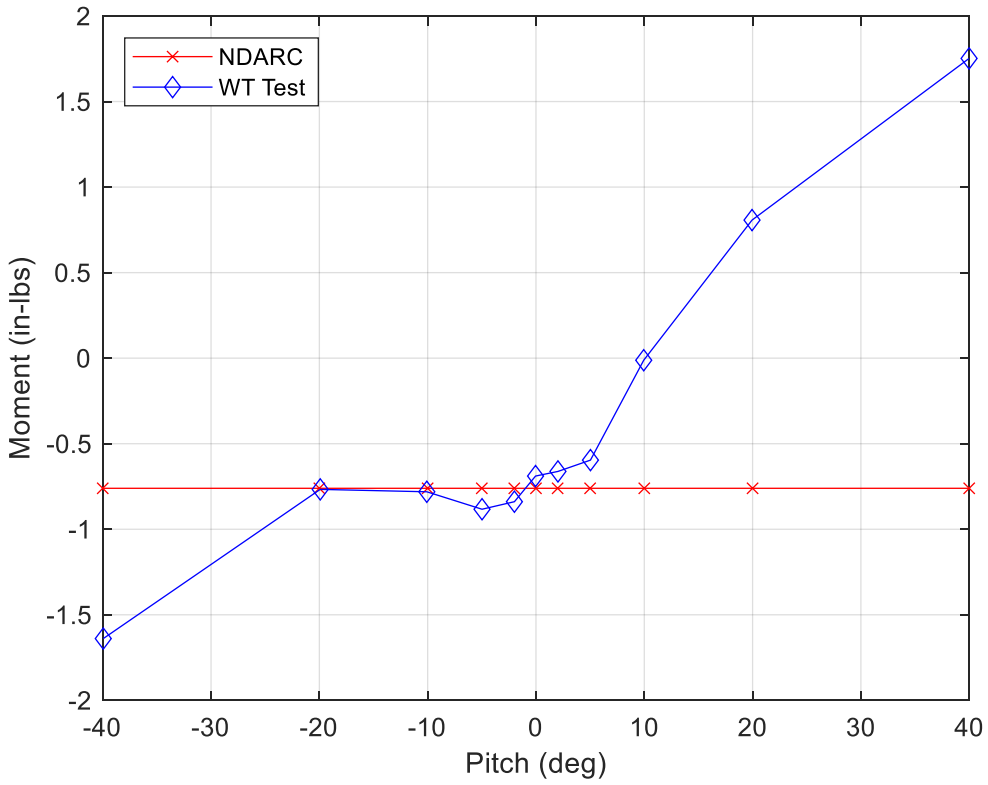

Figure 2.16 Comparison of the bare airframe pitching moment at 40 fps airspeed from wind tunnel testing in Ref. [3] and NDARC for the SUI Endurance.

2.3.2 Full Vehicle Calibration

After achieving accurate matching between the NDARC generated results and the empirical wind tunnel data for the bare airframe of the SUI Endurance, the rotor data was then

included in the NDARC results, with power on, to compare with the full vehicle data obtained from the wind tunnel tests. While the bare airframe was tested in forward flight conditions with an airspeed of 40fps, the full vehicle was initially tested in hover conditions to make sure that both the lift of the vehicle with rotors and the power required would match the hover data taken from the wind tunnel. When first plotting the NDARC results for total lift and vehicle power required against the wind tunnel data, it was obvious that NDARC was over predicting both values by a considerable margin. To rectify this issue, the collective pitch of the blade was decreased from 17°, from the DJI Phantom, to 13.25° which was initially tuned by hand, but was also found to match the average pitch of the Endurance blades (T-Motor 15x5 CF) across the radius of the blade based on the measurements taken in Ref. [3]. The DJI Phantom uses its own blade that differs from the blade used by the Endurance in many ways, including pitch. This change yielded much more accurate results for NDARC when compared to the data from the wind tunnel. Because these vehicles use fixed pitch blades, this change in collective pitch was critical for matching the data and the results. Additionally, if more tuning for power required is needed, then changes can be made to the induced power factor for hover conditions, κ_{hover} (*Ki_hover*).

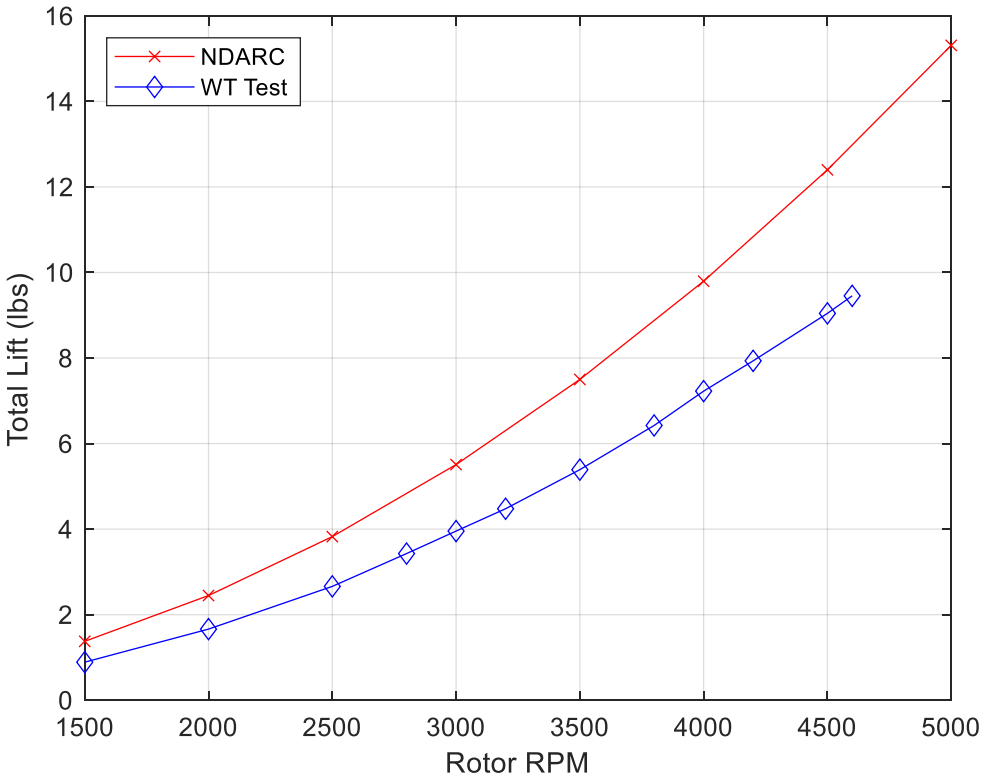
NDARC
WT Test
Total Lift (lbs)
Rotor RPM
0
2
4
6
8
10
12
14
16
1500
2000
2500
3000
3500
4000
4500
5000

(a)

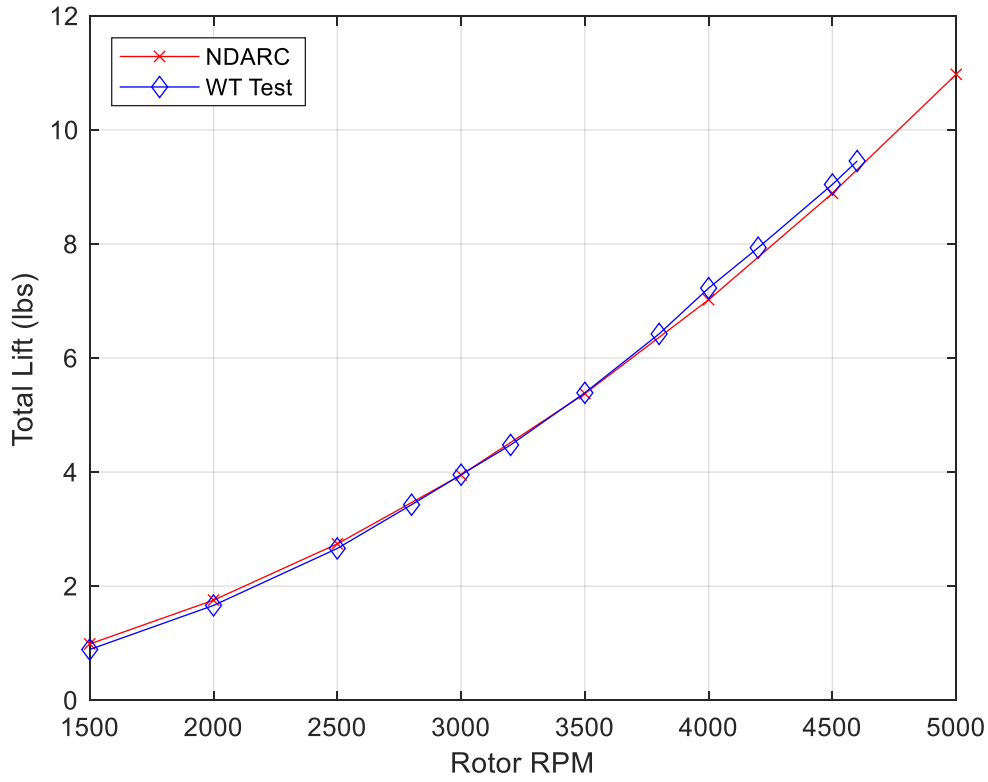

(b)

Figure 2.17 Total lift of the SUI Endurance in hover before (a) and after (b) decreasing the pitch of the rotor blades.

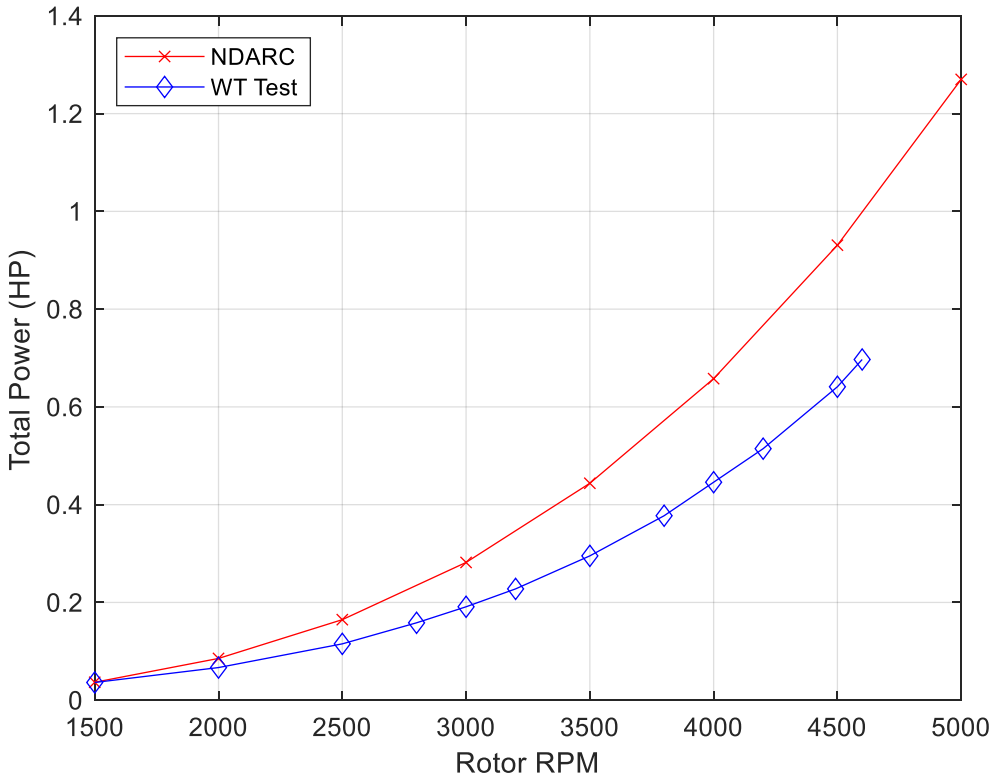
NDARC
WT Test
Total Power (HP)
Rotor RPM
0
0.2
0.4
0.6
0.8
1
1.2
1.4
1500
2000
2500
3000
3500
4000
4500
5000

(a)

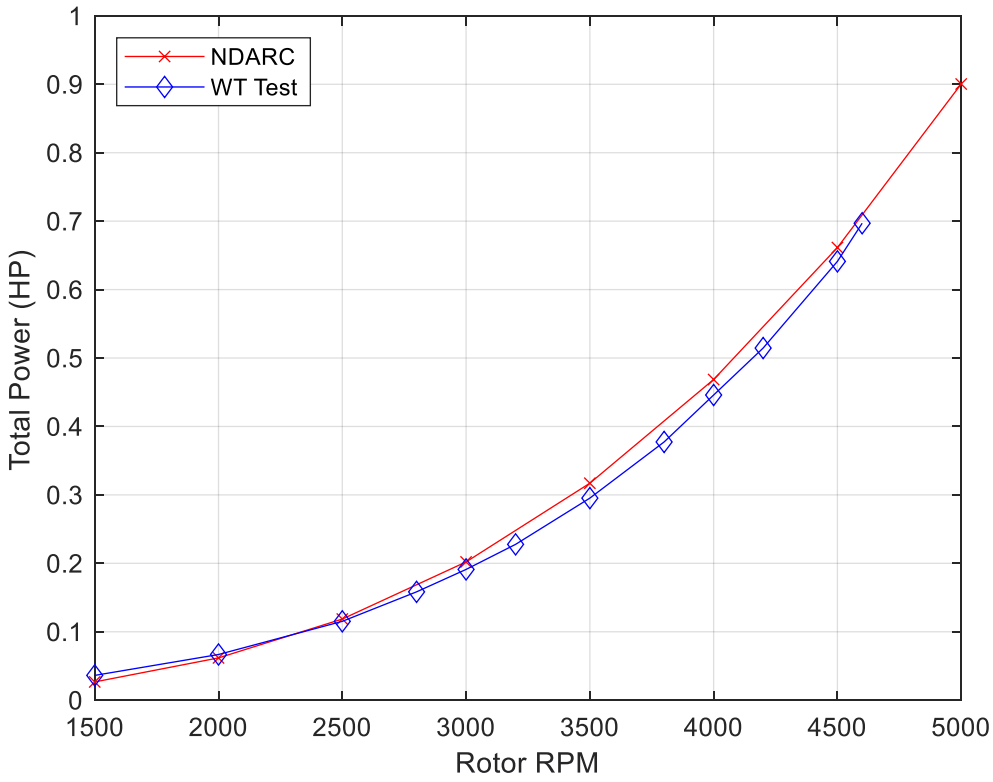

(b)

Figure 2.18 Power required for the SUI Endurance in hover before (a) and after (b) decreasing the pitch of the rotor blades.

A return to forward flight conditions was made once the hover results had adequate matching. Again, like, the process used with the DJI Phantom, much of the change in the results was created by changes to the interference factors related to the rotors. Changes to both the forward flight thrust factor for all rotors and the forward flight thrust factor for the front rotors to the aft rotors has influence on both the lift and the pitching moment of the vehicle. Given the similar geometry of the DJI Phantom and the SUI Endurance in terms of nearly square rotor-to-rotor placement and the ratio of the blade radius to the length of the vehicle, the forward flight thrust factor values used for the DJI Phantom yielded lift results in NDARC that were fairly accurate when compared to the full vehicle lift taken from the wind tunnel at 40fps airspeed. With minor

tweaks, the results in NDARC for both lift and pitch moment were improved. However, the greatest impact on aircraft pitching moment stems from the distance between the rotor and the vehicle's center of gravity. This distance was originally set to 0.500 in NDARC for both the DJI Phantom and the SUI Endurance which is a ratio based upon the rotor radius for each vehicle, therefore that distance was about 2.35 inches for the DJI Phantom and 3.75 inches for SUI Endurance. This led to a large over-prediction of the pitching moment for both vehicles and in turn, this geometric ratio was decreased from 0.500 for the SUI Endurance to 0.050 to provide better matching for the vehicle pitching moment, specifically at -10° pitch attitude and 40fps airspeed given that this was the closest angle to trim tested within the wind tunnel. Further improvement was made to both the vehicle drag, which was slightly over-predicted once rotors forces were added, and vehicle pitching moment across all tested pitch attitudes by slightly increasing the flap frequency of the rotors. The impact of these adjustments is shown in Figures 2.19-2.22.

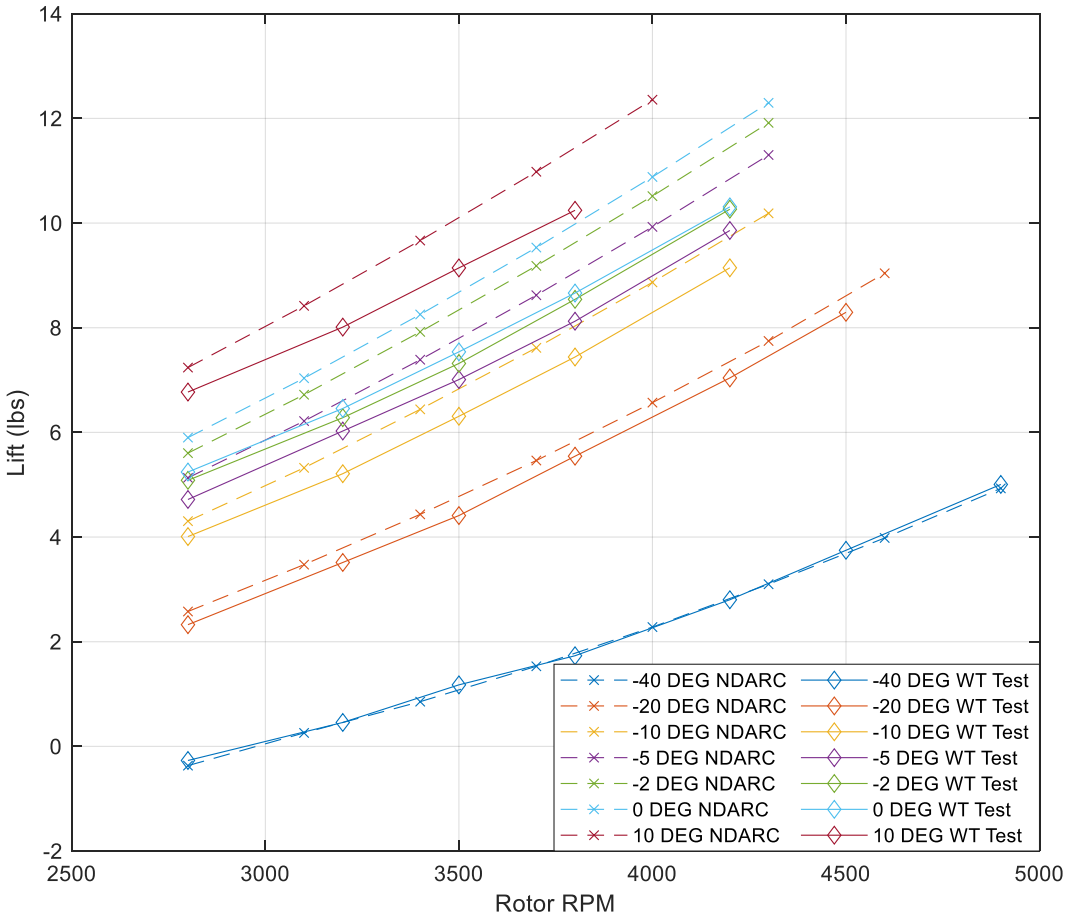
Lift (lbs)
Rotor RPM
14
12
10
8
6
4
2
0
-2
2500
3000
3500
4000
4500
5000
-40 DEG NDARC
-20 DEG NDARC
-10 DEG NDARC
-5 DEG NDARC
-2 DEG NDARC
0 DEG NDARC
10 DEG NDARC
-40 DEG WT Test
-20 DEG WT Test
-10 DEG WT Test
-5 DEG WT Test
-2 DEG WT Test
0 DEG WT Test
10 DEG WT Test

(a)

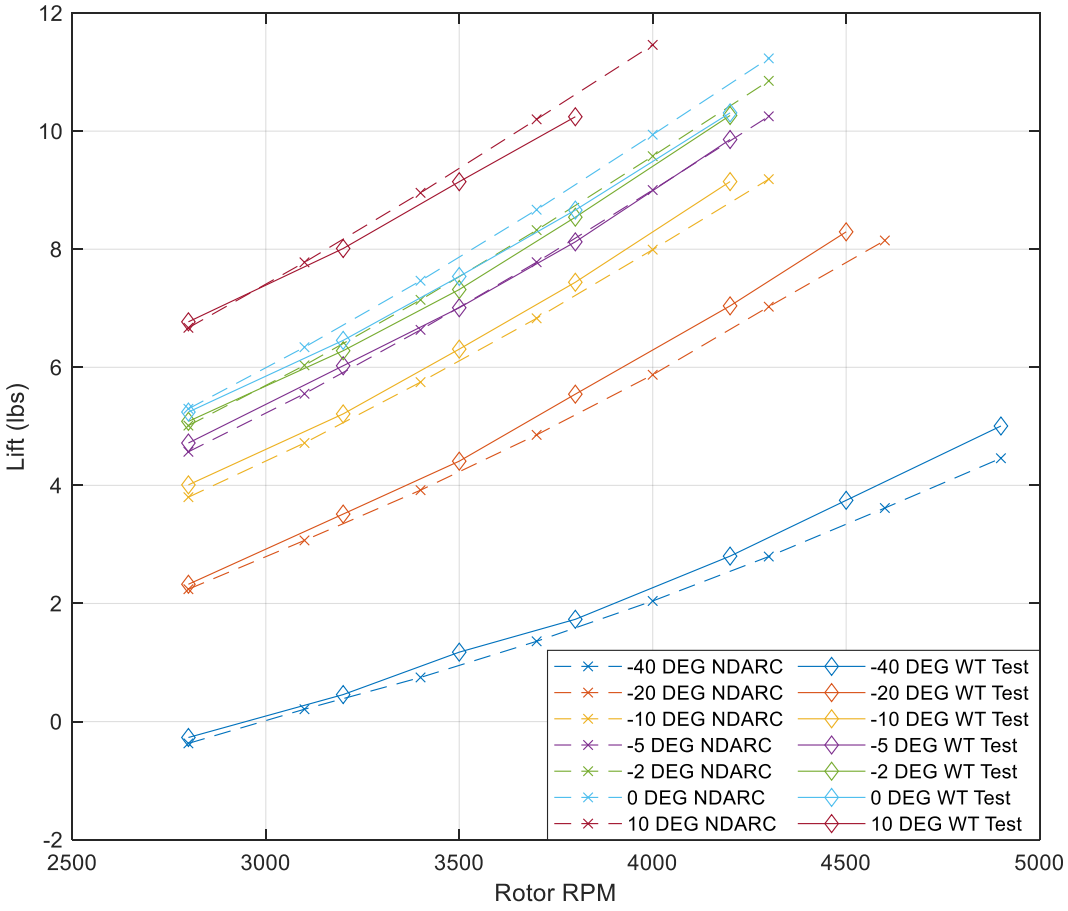

(b)

Figure 2.19 Lift of the complete aircraft at 40 fps airspeed across multiple pitch attitudes before (a) and after (b) changes were made to flap frequency, interference factors, and vertical rotor distance.

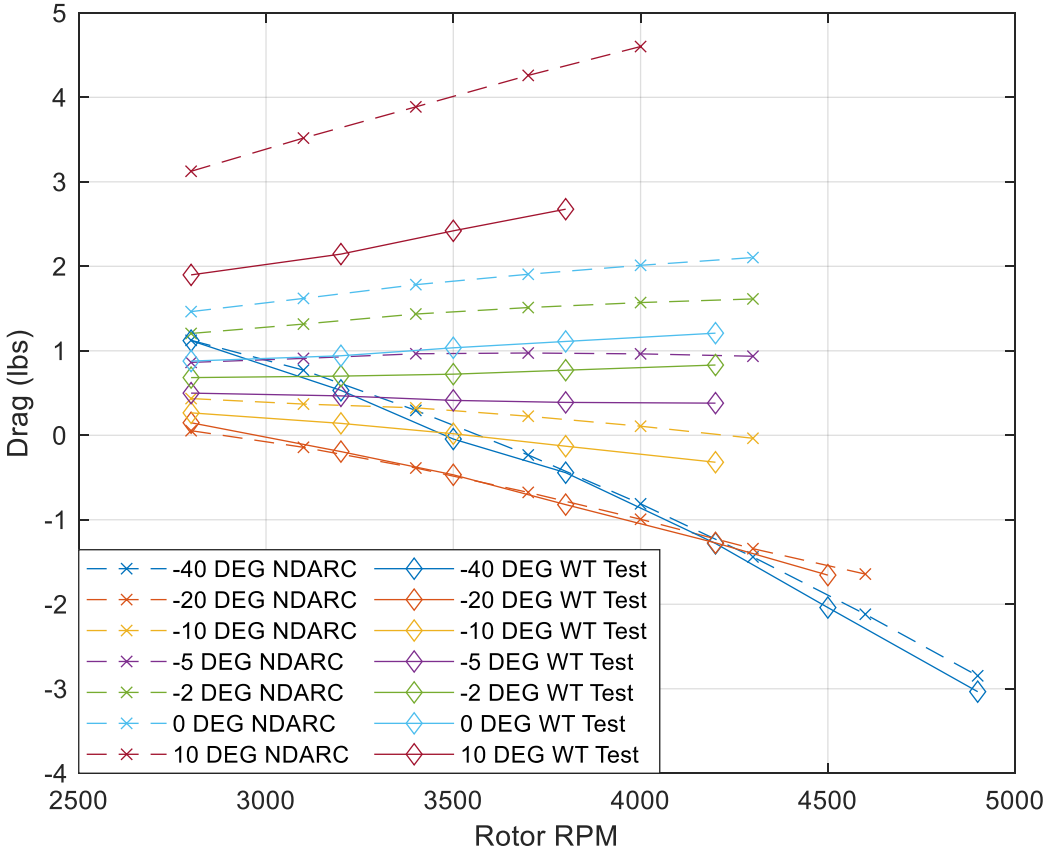
Drag (lbs)
Rotor RPM
5
4
3
2
1
0
-1
-2
-3
-4
2500
3000
3500
4000
4500
5000
-40 DEG NDARC
-20 DEG NDARC
-10 DEG NDARC
-5 DEG NDARC
-2 DEG NDARC
0 DEG NDARC
10 DEG NDARC
-40 DEG WT Test
-20 DEG WT Test
-10 DEG WT Test
-5 DEG WT Test
-2 DEG WT Test
0 DEG WT Test
10 DEG WT Test

(a)

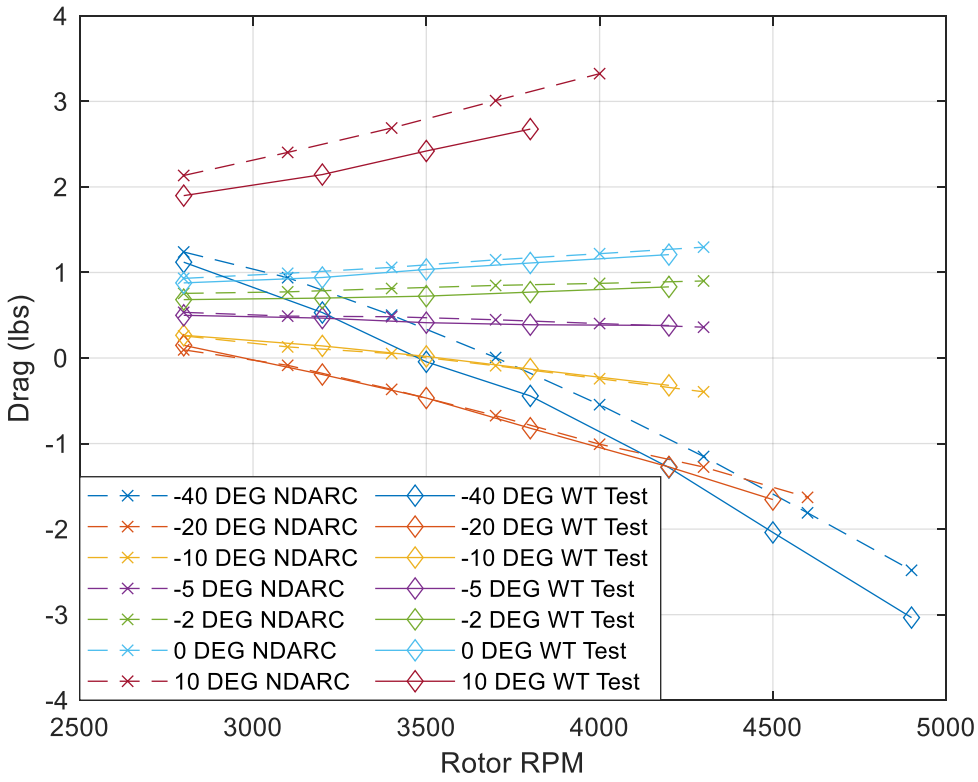

(b)

Figure 2.20 Drag of the complete aircraft at 40 fps airspeed across multiple pitch attitudes before (a) and after (b) changes were made to flap frequency, interference factors, and vertical rotor distance.

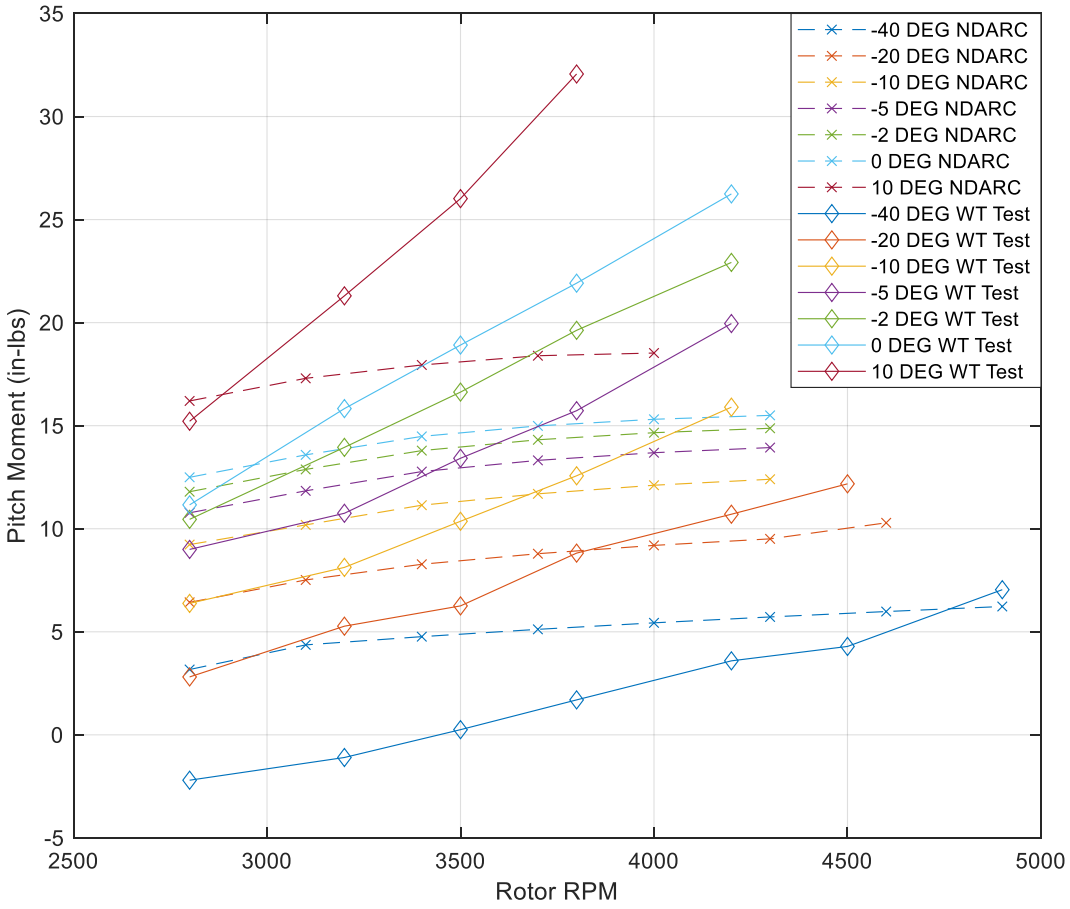
Pitch Moment (in-lbs)
Rotor RPM
35
30
25
20
15
10
5
0
-5
2500
3000
3500
4000
4500
5000
-40 DEG NDARC
-20 DEG NDARC
-10 DEG NDARC
-5 DEG NDARC
-2 DEG NDARC
0 DEG NDARC
10 DEG NDARC
-40 DEG WT Test
-20 DEG WT Test
-10 DEG WT Test
-5 DEG WT Test
-2 DEG WT Test
0 DEG WT Test
10 DEG WT Test

(a)

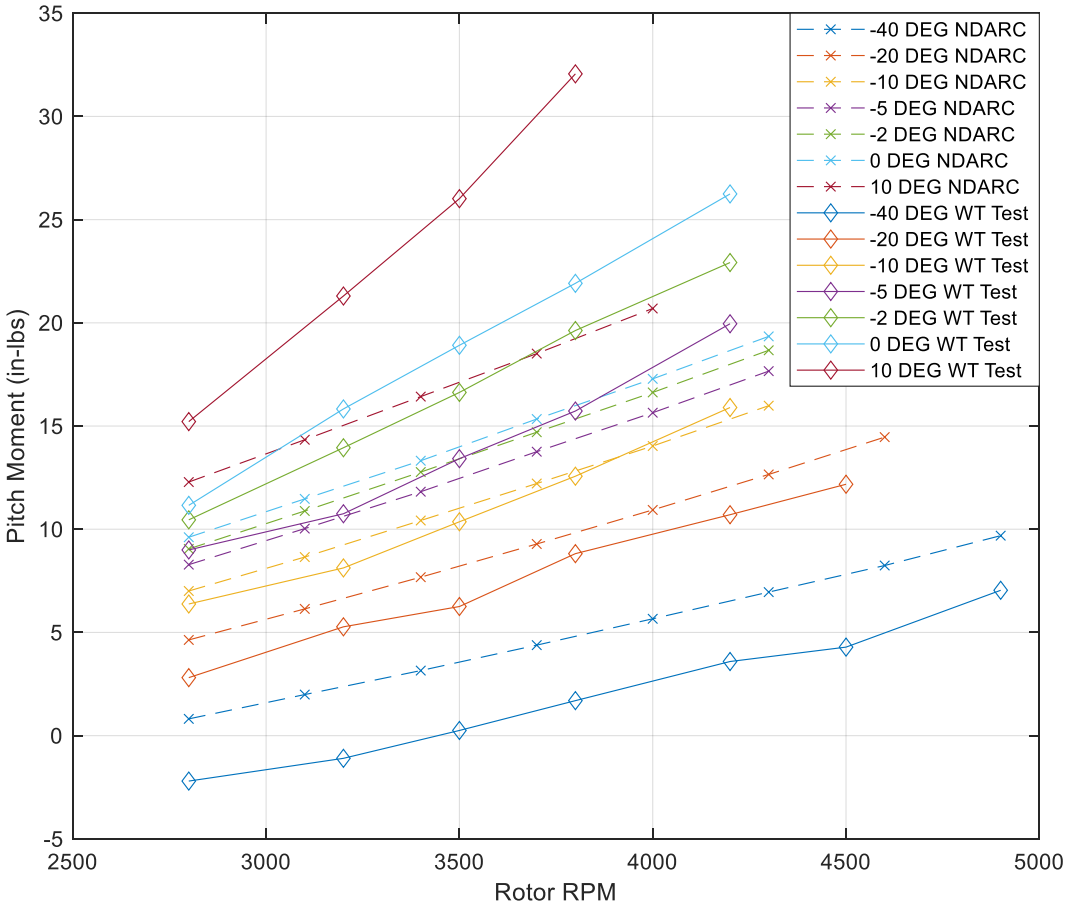

(b)

Figure 2.21 Pitching Moment of the complete aircraft across multiple pitch attitudes before (a) and after (b) changes were made to flap frequency, interference factors, and vertical rotor distance.

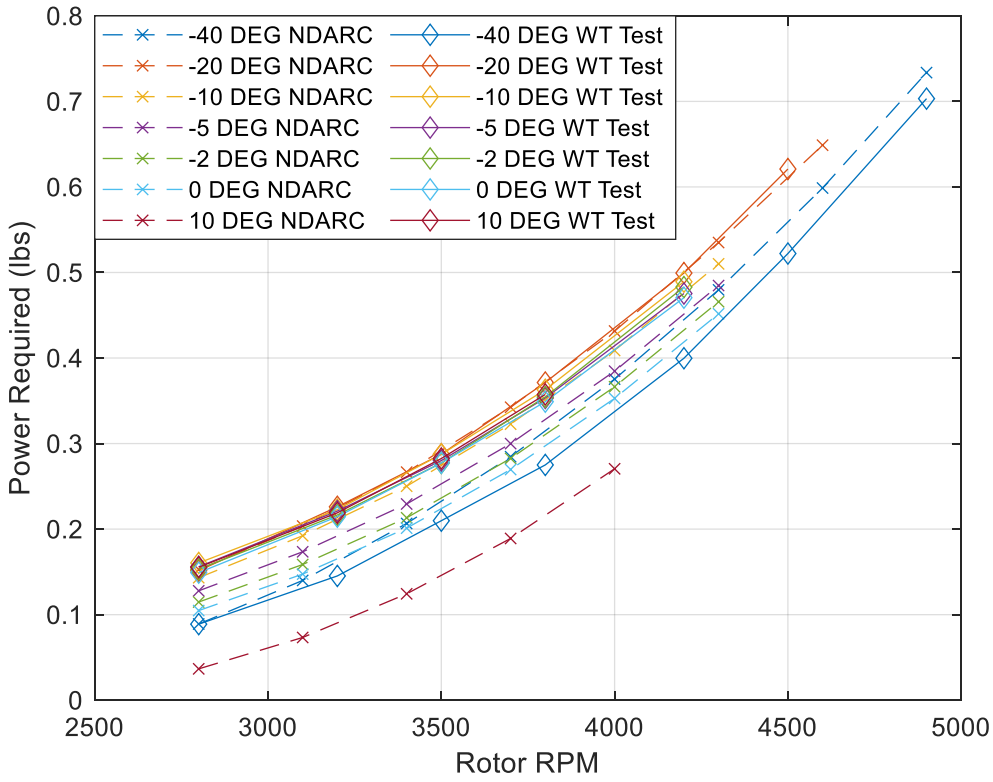
-40 DEG NDARC
-20 DEG NDARC
-10 DEG NDARC
-5 DEG NDARC
-2 DEG NDARC
0 DEG NDARC
10 DEG NDARC
-40 DEG WT Test
-20 DEG WT Test
-10 DEG WT Test
-5 DEG WT Test
-2 DEG WT Test
0 DEG WT Test
10 DEG WT Test
Power Required (lbs)
Rotor RPM
0
0.1
0.2
0.3
0.4
0.5
0.6
0.7
0.8
2500
3000
3500
4000
4500
5000

(a)

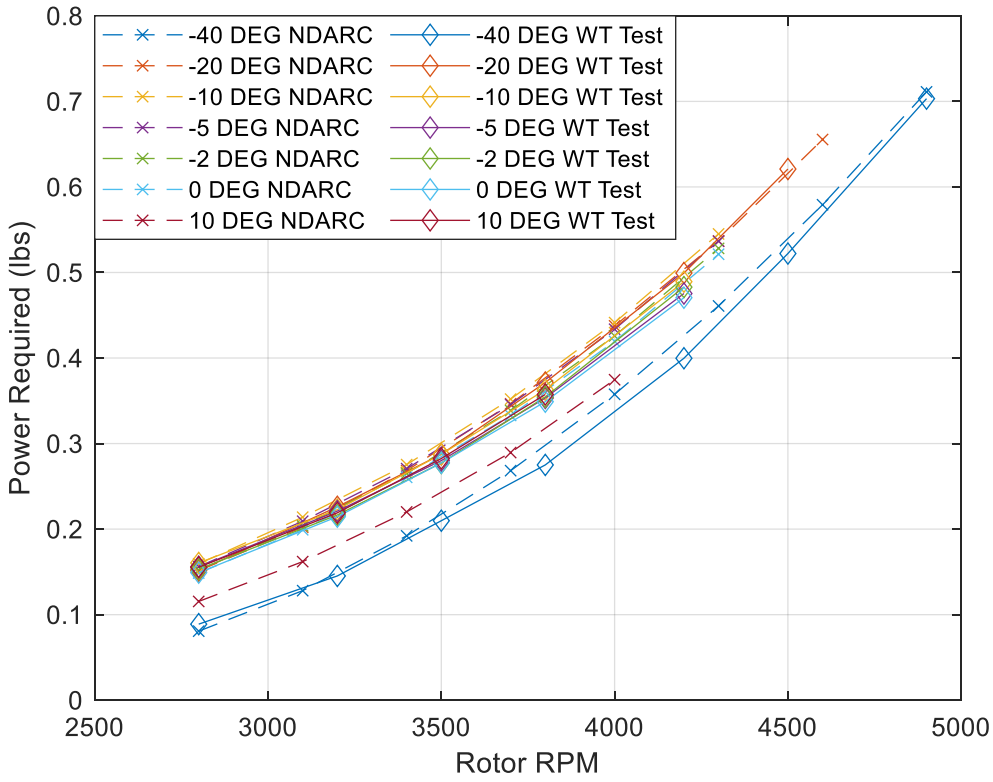

(b)

Figure 2.22 Power Required of the complete aircraft at 40 fps airspeed across multiple pitch attitudes before (a) and after (b) changes were made to flap frequency, interference factors, and vertical rotor distance.

To see a full step-by-step summary of the NDARC inputs that were manipulated and tuned for the SUI Endurance, refer to the Appendix.

2.3.3 Center of Gravity Shifting

The next step after confirming an adequate level of correlation between the NDARC results and the data from the wind tunnel was to determine if the two sets of results would yield the same or similar recommended distances for moving the stationline of the center of gravity of the SUI Endurance. Like the DJI Phantom, this process was used to verify the power required results. Using the trim values previously calculated in tandem with the geometry of the vehicle allows one to

calculate how far forward the center of gravity would need to be moved in order to maintain equivalent RPM and power required values on the fore and aft rotors during forward flight. Then, by determining where the RPM and power required for the fore and aft rotors intercept when plotted against airspeed with a shifted center of gravity that is adjusted using "*dSLcg*" in the condition component, the suggested center of gravity can be determined within NDARC. Determining this shifted center of gravity distance requires some trial and error if the value taken from the wind tunnel data does not yield similar results in NDARC. The values derived from the wind tunnel data are shown in Table 2.4 and the results from NDARC are shown with the wind tunnel values in Figures 2.23-2.25. Again, the black, vertical lines in these figures represent 20fps and 40 fps, while the red markers represent the results derived from the wind tunnel data.

Parameter	Value at 20fps	Value at 40fps
θ	-4.38°	-10.7°
Ω	3430 RPM	3460 RPM
ΔSL	-1.56"	-1.39"
$P_{req,FL}$	0.0673 hp	0.0703 hp
$P_{req,FR}$	0.0633 hp	0.0657 hp
$P_{req,RL}$	0.0640 hp	0.0664 hp
$P_{req,RR}$	0.0692 hp	0.0716 hp

Table 2.4 Values of trimmed parameters at different airspeeds for SUI Endurance.

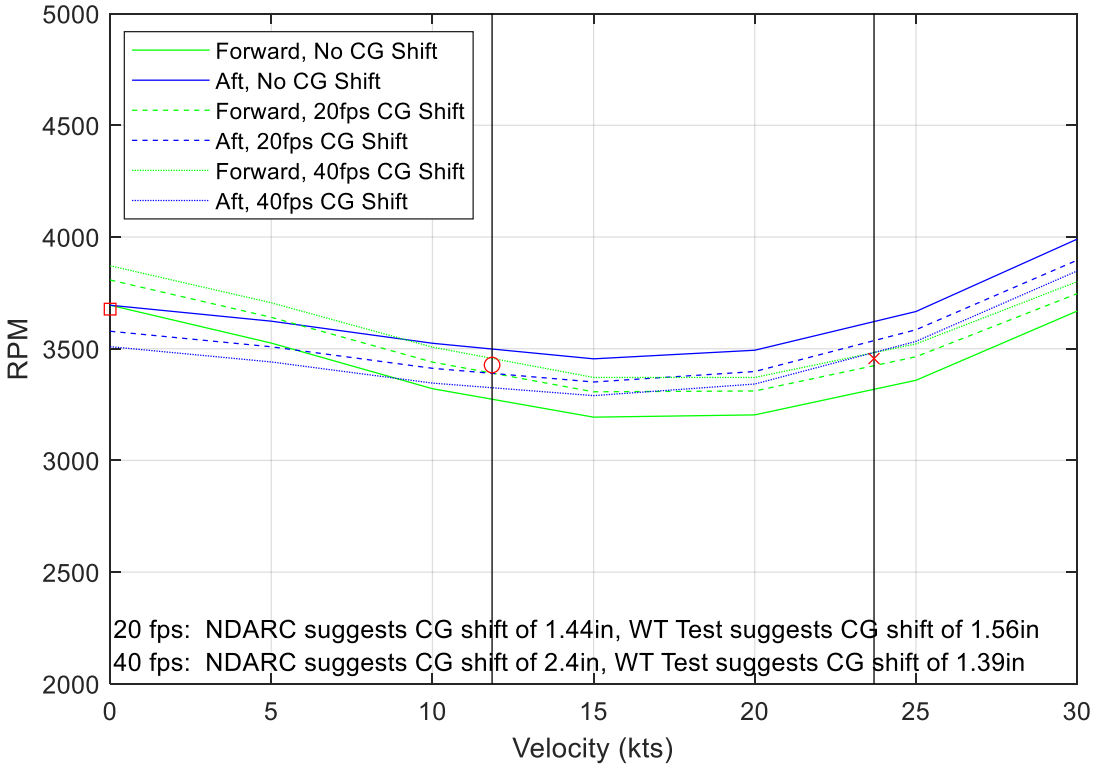

Figure 2.23 Matching SUI Endurance rotor RPM using the suggested shift in aircraft CG as defined by NDARC and wind tunnel data.

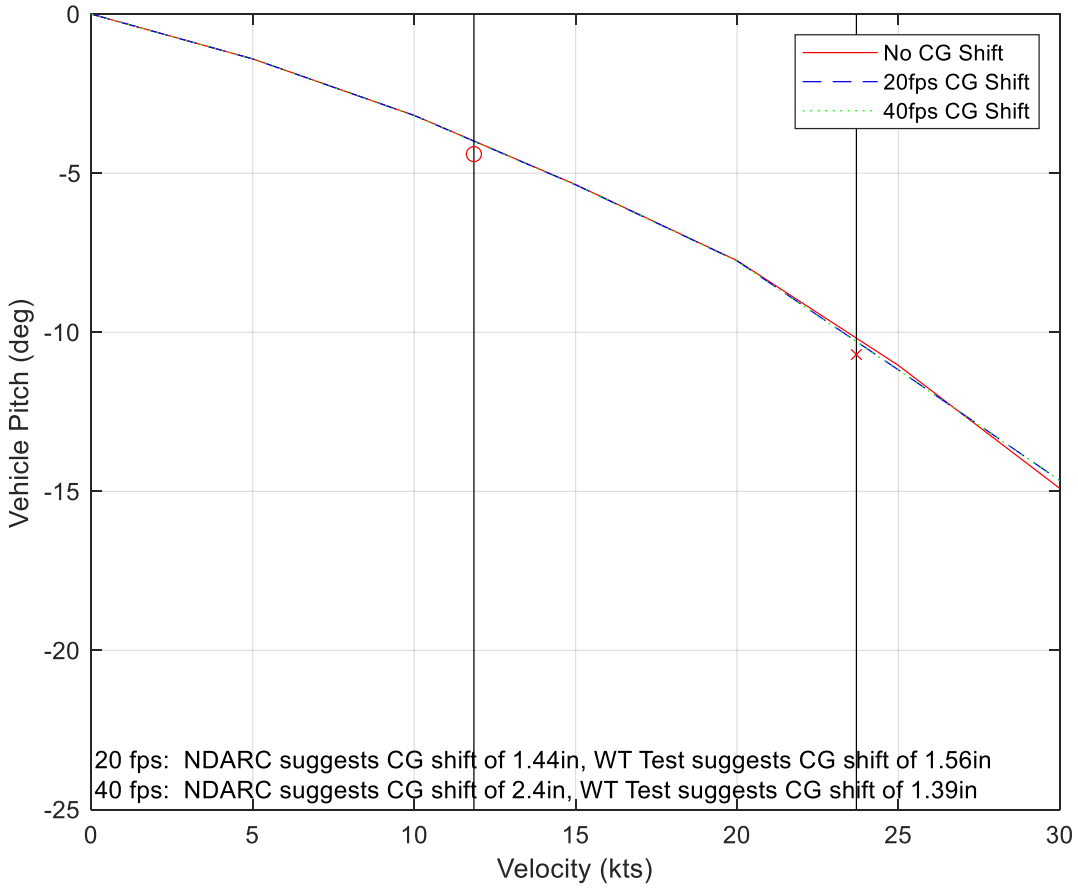

Figure 2.24 Matching SUI Endurance pitch attitude using the suggested shift in aircraft CG as defined by NDARC and wind tunnel data.

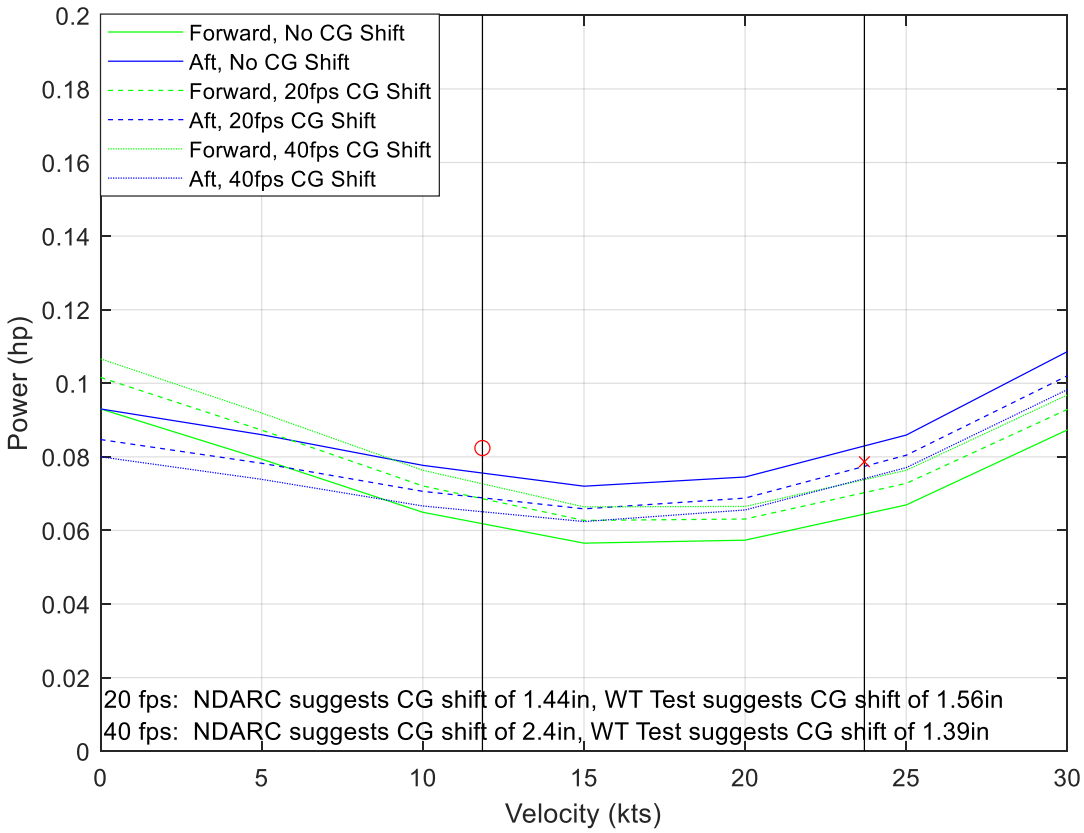

Figure 2.25 Matching power required for each SUI Endurance rotor using the suggested shift in aircraft CG as defined by NDARC and wind tunnel data.

It is clear that, despite the matching for rotor RPM and pitch attitude of the Endurance, the power required at 20fps could benefit from further tuning to better match the average taken from the wind tunnel data.

Chapter 3: Large-Scale DEP UAM Lift+Cruise Modelling

3.1 Introduction

As UAM becomes of greater interest to the larger aerospace community and, more specifically, to the government and United States military, there is an increasing need for reliable, validated design tools that can rapidly and accurately model new concept vehicles. While some high-speed VTOL (HS-VTOL), primarily the tilting thruster designs, have been heavily modeled or even flying for some time (i.e. the Bell Boeing V-22 Osprey, a tilt rotor vehicle), lift+cruise HS-eVTOL vehicles have not been as heavily modeled and tested using design tools. One specific lift+cruise vehicle that has gained increased interest from both the professional industry and the military is the BETA Alia, shown in Figure 3.1. BETA has received over 150 orders already for the Alia from United Therapeutics, BLADE, and UPS while also achieving airworthiness approval for a manned electric aircraft from the Agility Prime program of the United States Air Force. Furthermore, the BETA Alia has recently received funding and interest from Amazon's Climate Pledge Fund for zero-emission aircraft. Additionally, the Concept Design and Assessment (CD&A) Technology Area of the U.S. Army has deemed this particular vehicle of interest and therefore it has been selected for modeling in NDARC. It is important to note that this NDARC model is merely a configuration representative of the BETA Alia that was developed using limited publicly available data with engineering estimates of the aircraft properties. Many of the relevant aircraft properties are not known precisely, but the NDARC model is sufficiently representative of a viable UAM lift+cruise configuration to viably demonstrate the modeling capabilities of NDARC. While the model is not the exact BETA Alia, it will continue to be referred to as the Alia.

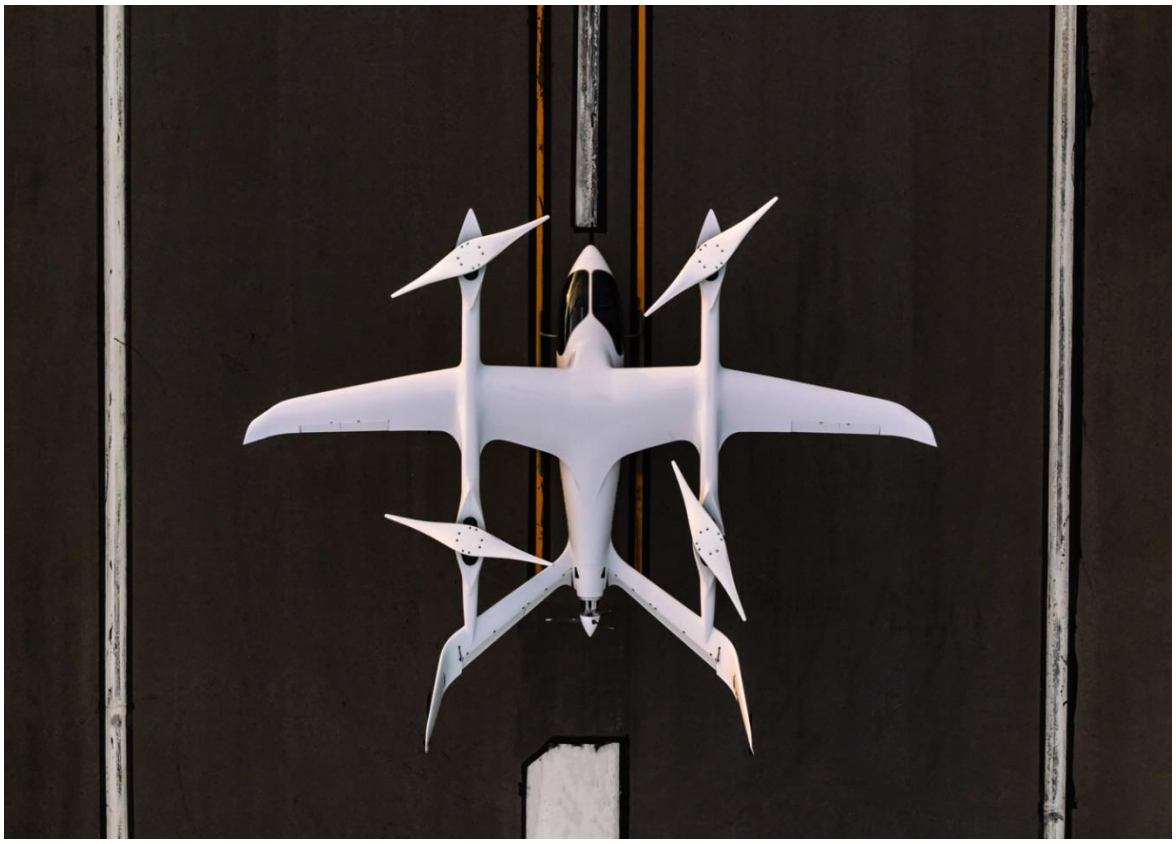

Figure 3.1 BETA Alia (downloaded from https://evtol.com).

The BETA Alia aircraft features four fixed-pitch lifting rotors for takeoff and hover, one variable-pitch pusher prop for forward flight, a wing with no flaps, and an unconventional tail meant to imitate the tail of an arctic tern as its major control features. For its power supply, the Alia has five battery packs that power the five electric motors designed and manufactured by BETA. Using this design, BETA has targeted a maximum range of 250 nautical miles with a cruising speed of 170 miles per hour. To public knowledge, BETA has extensively tested the Alia in forward flight, or "airplane mode," using only the pusher propeller. The flight tests, at the time of writing, have all been completed without any use of the four lift rotors and often times the aircraft does not have the lift rotors attached. It is also understood that there have been limited hover tests completed for the Alia that recently began to resume as of September 9th, 2021, Ref. [25]. Because of this, combined with the interest from the U.S. Army's Technology Development

Directorate (TDD), the BETA Alia was deemed a valuable aircraft to model within NDARC and attempt to gather data and information on the aircraft's three flight modes, "hover" or "helicopter" mode, "cruise" or "airplane" mode, and "transition" mode. Also, validating NDARC as a viable tool for modeling a lift+cruise aircraft can be accomplished by comparing the results against a higher fidelity program given the lack of empirical flight test data for the Alia. To do so, DEPSim was used and served as the higher fidelity model for the Alia. DEPSim serves as the higher fidelity model in this study because of its utilization of vortex lattice method for aerodynamics and free-vortex wake modelling to model the wakes of not only the rotors, but also the lifting surfaces as well as aerodynamic interactions between these components. Additionally, to reiterate previous statements about the limited public data, the high-fidelity model was developed using DEPSim to validate the NDARC model of the Alia, and used equivalent estimated aircraft properties as used in the NDARC model.

3.2 Model Setup

Like the DJI Phantom, the initial NDARC model used for the BETA Alia was provided by the CD&A group of the U.S. Army TDD. The original NDARC model was able to run trimmed cases for hover, when the Alia is only using the four lift rotors and the propeller is stopped, as well as trimmed cases for forward flight at cruising speeds, when the Alia has fully transitioned to wing-borne flight via the lift surfaces and propeller while the four lift rotors are stopped. Both the challenge and the objective were to then model the transition region between hover and cruise as accurately as possible, as this is the region where the lift rotors are used (as edgewise rotors) in conjunction with the propeller, wing, and tails until the Alia reaches an airspeed where the wing generates most, if not all, of the lift required to then turn off the lift rotors.

3.3 Model Trim

Typical aircraft have four control axes: roll, pitch, yaw, and thrust (longitudinal thrust for airplanes, vertical thrust for rotorcraft). Given the nature of the nature of the Alia's configuration with four lift rotors and one pusher propeller, it is possible for the aircraft to trim over a range of pitch attitudes in transition because of its ability to have both longitudinal and vertical thrust controls. In a trim solution is possible to prescribe pitch attitude, longitudinal thrust control, or vertical thrust control, while solving for the other two. For the Alia, the longitudinal control is the propeller pitch, while the vertical control is collective variation in the lift rotor RPM (the lift rotors are fixed pitch). It was quickly determined that for the Alia, it is best to prescribe pitch attitude through transitional flight. During transition the pitch should remain close to 0 (to prioritize pilot vision capabilities) and then transition to a pitch attitude suitable for cruise mode at the end of the transition corridor. During the transition all five rotors are running, while the RPM of the four lift rotors and the collective pitch of the propeller are trimmed out in NDARC to balance forces and moments. The transition trim solution is repeated with increasing airspeeds until the aircraft can fully taper off use of the lift rotors. The initial pitch schedule is referred to as "level at low speeds" where the pitch attitude is 0° until 30 knots where it steadily increases to 8° at 70 knots before reducing to 7° at 80 knots. These simulations and prescribed values were all determined using an atmosphere of 2000 feet altitude and 70 degrees Fahrenheit for ambient temperature. The prescribed pitch attitude for transition is shown in Figure 3.2 along with the trimmed pitch angles for cruise.

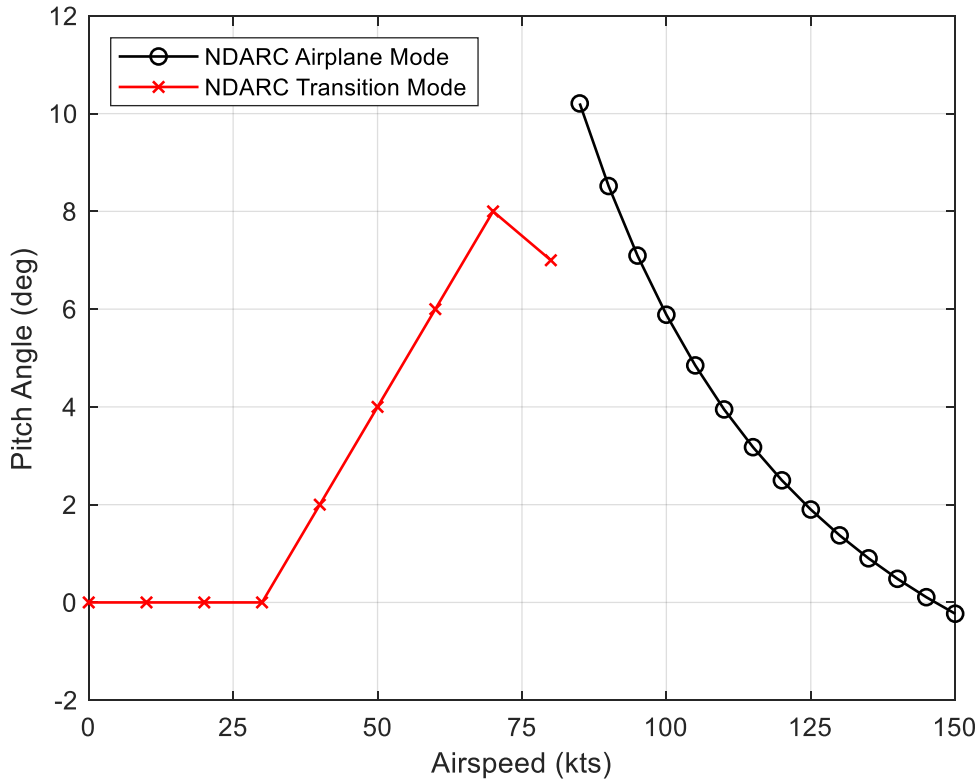

Figure 3.2 Pitch attitude of the BETA Alia at various speeds in NDARC.

This prescribed pitch schedule was found through trial and error in NDARC to surmise what the maximum pitch attitude would be at each airspeed in order to gradually approach the necessary airspeed and pitch required for cruising flight. Because the low airspeed threshold of airplane mode requires a higher angle of attack to maintain the necessary lift, it is necessary to increase pitch attitude with airspeed through transition mode. Using this pitch schedule and plotting it with the trimmed pitch of cruising flight demonstrates what kind of gap between both pitch and airspeed for the Alia must be overcome and how feasible it is. The power required through hover and transition for both pitch schedules as well as the power required for trimmed cruise were also plotted to provide both a baseline and a better understanding of this performance gap between flight modes. The power required results are shown in Figure 3.3.

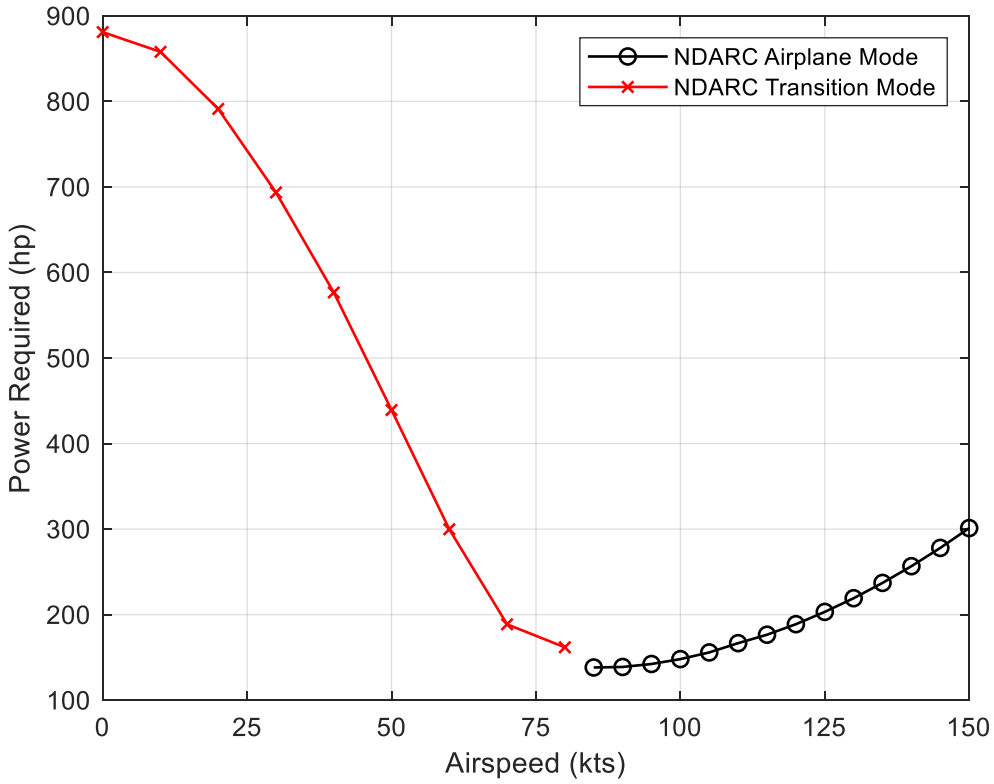

Figure 3.3 Total power required for the Alia from hover, through transition, and through cruise.

In addition, the total lift of the Alia was broken down to understand how much of the lift was being generated by the four lift rotors and how much lift was being generated by the wing and tails at the different airspeeds through transition. The breakdown is shown in Figure 3.4 and it illustrates how much more the Alia needs to taper off of the lift rotors to reach cruise where all lift is generated by the wing in forward flight.

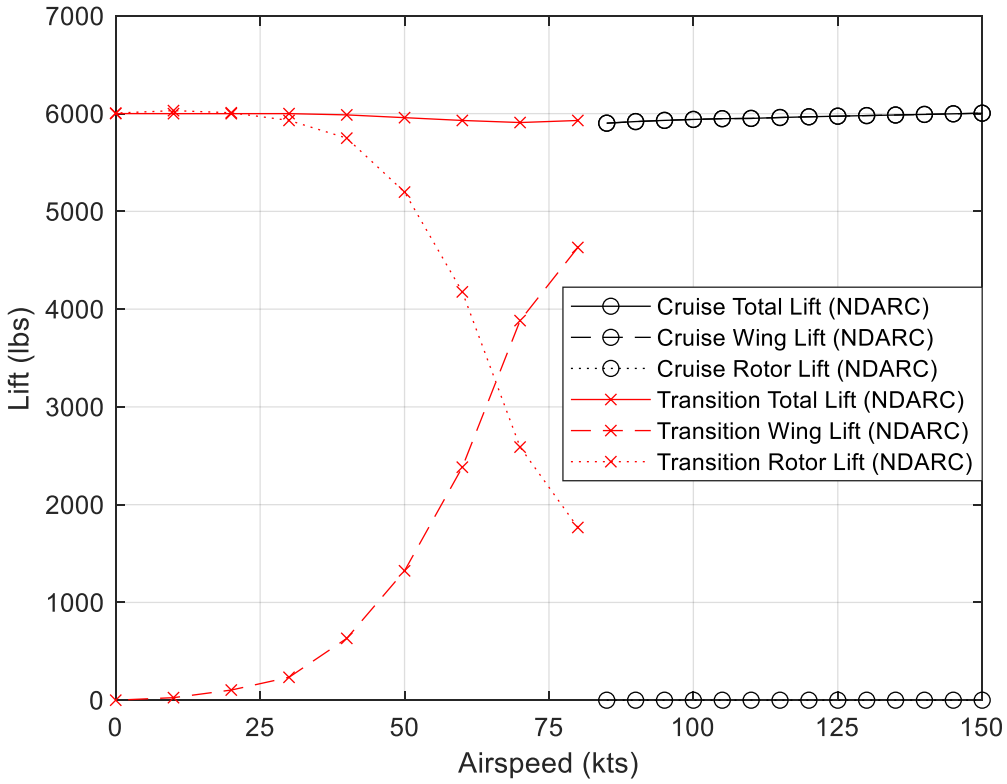

Figure 3.4 Breakdown of lift being generated by the lift rotors and wing, and how they contribute to the total lift of the aircraft.

The last parameters used to understand and judge the performance gap between transition flight and cruise, or airplane mode, relate to the propeller. Both the power required and the collective pitch of the pusher prop, which runs at a constant 2203 RPM, were plotted against airspeed in Figures 3.5-3.6 for both transition mode and cruise/airplane mode.

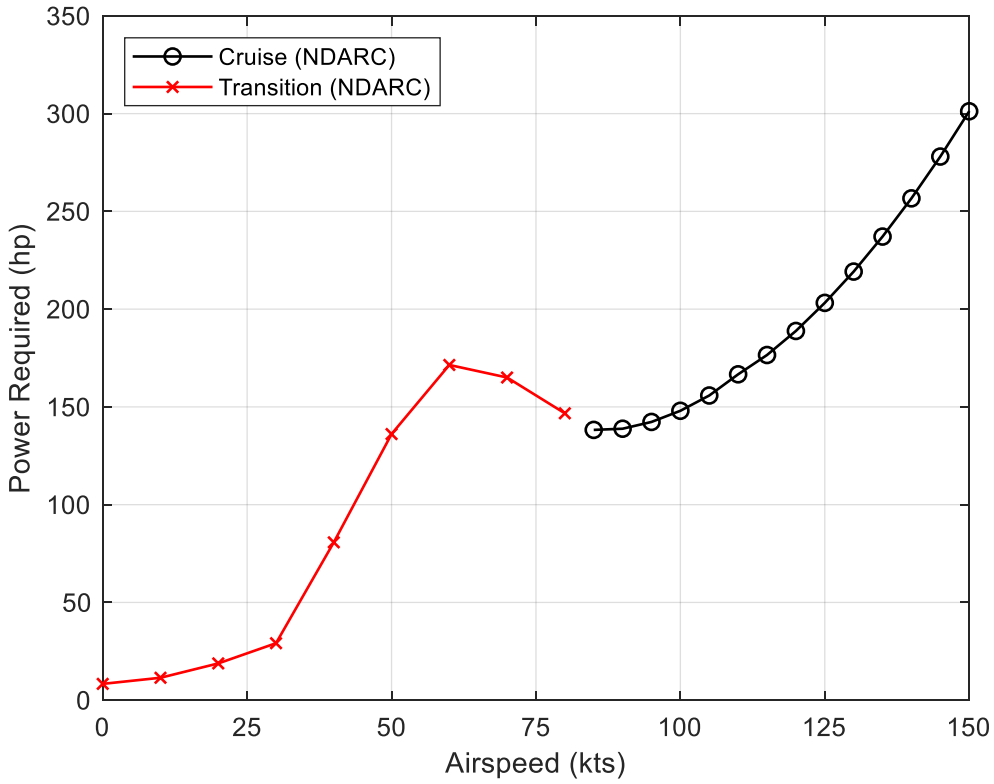

Figure 3.5 Power required for the pusher prop from hover, through transition flight, and through cruising flight.

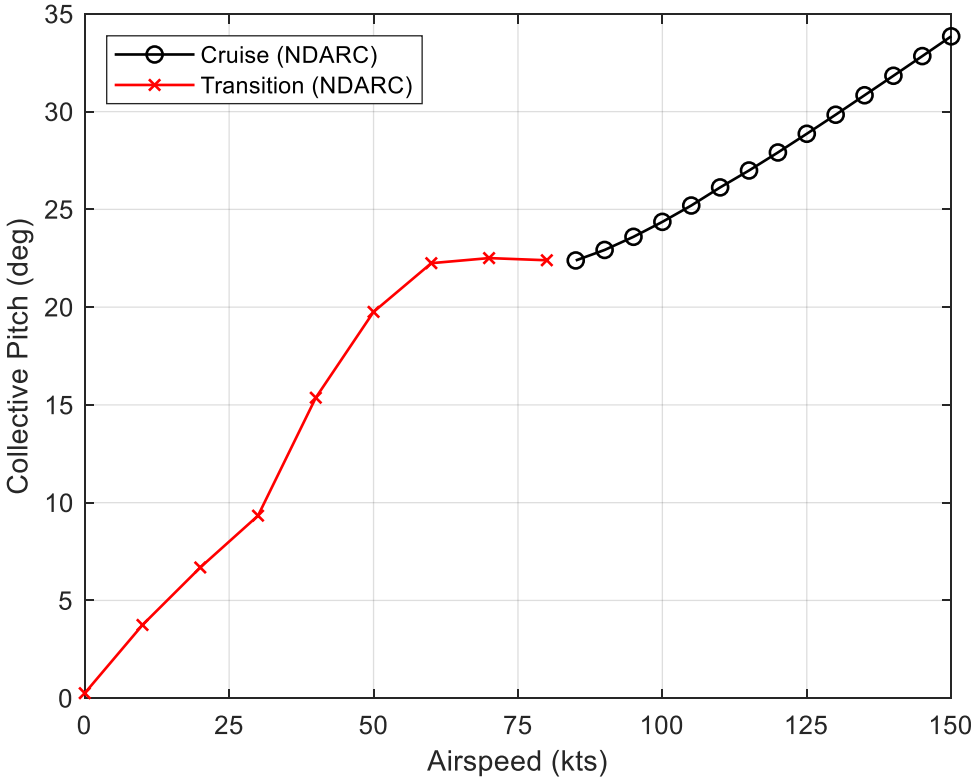

Figure 3.6 Collective pitch angle of the rotor blades for the pusher prop through transition flight and cruising flight (constant 2203 RPM).

By understanding what kind of power or pitch is required by the propellor, it allows the designer to understand if and what changes might need to be made to the component and the plotting of this information served primarily as a check to ensure the propellor was not encountering any unforeseen issues.

As the transition region is the focus of this study, the next step was to gain a better understanding of the performance of the four lift rotors. To do so, the difference in front and rear lift rotor RPM, power required, advance ratio, and blade loading were all plotted in Figures 3.7-3.9. It should be noted that because the NDARC model is set to trim symmetrically, it is only necessary to plot one front rotor and one rear rotor, as the output for each parameter is identical from the left side of the aircraft to the right side.

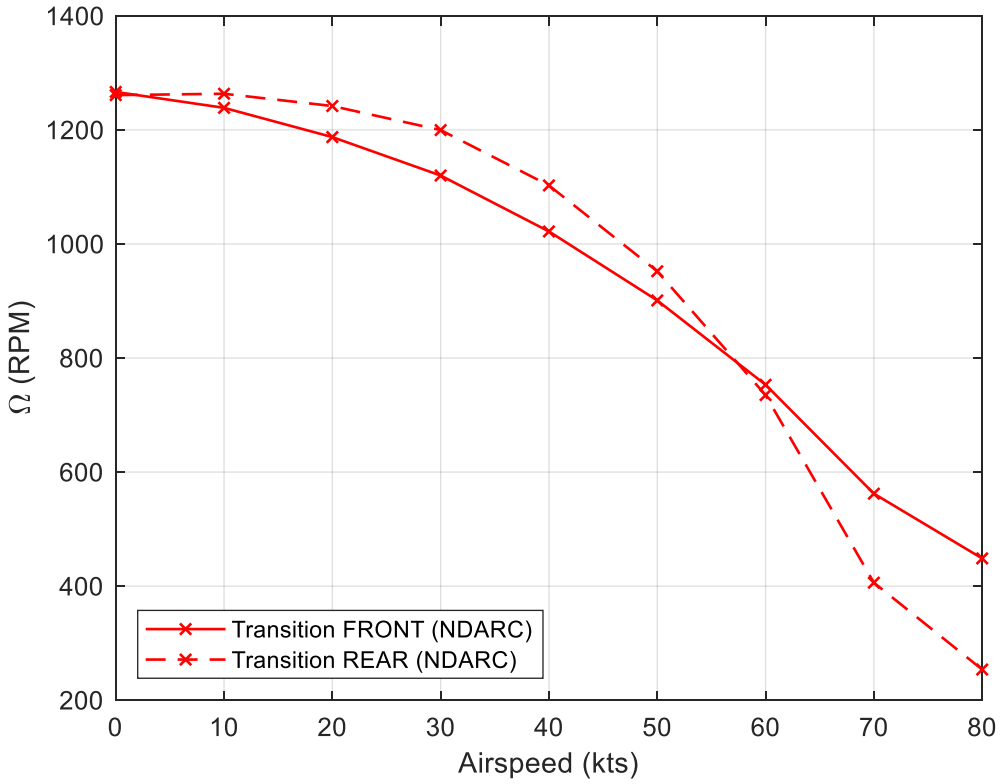

Figure 3.7 Difference in RPM between front and rear rotors for the initial NDARC Alia model.

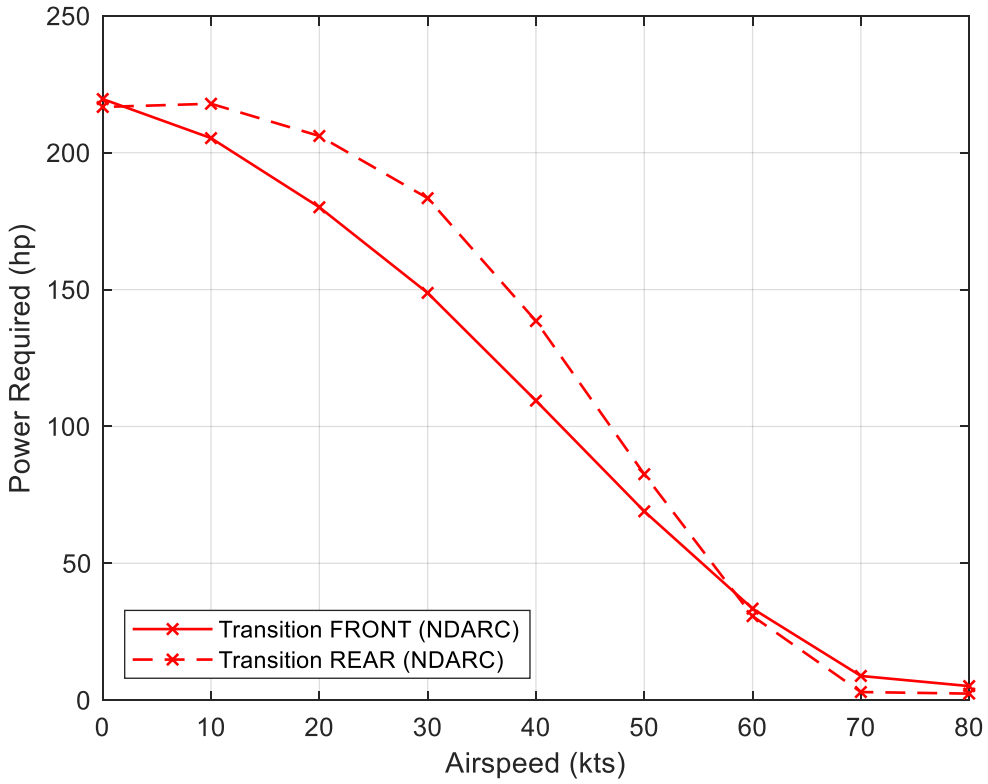

Figure 3.8 Difference between power required for the front and rear rotors of the initial NDARC Alia model.

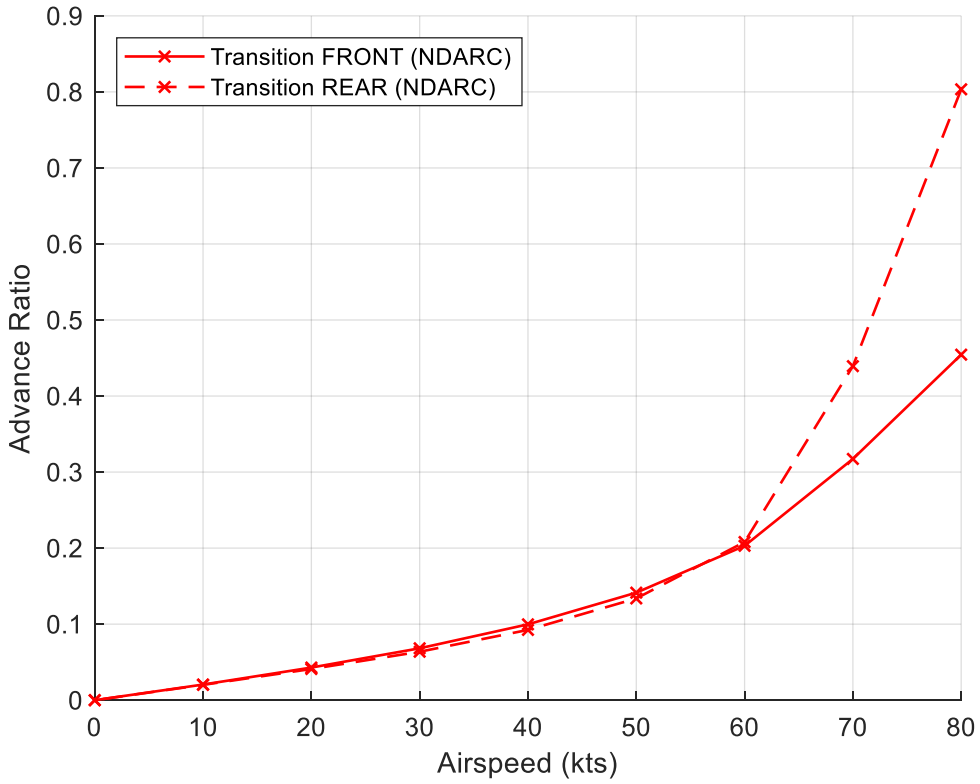
Transition FRONT (NDARC)
Transition REAR (NDARC)
Advance Ratio
Airspeed (kts)
0
0.1
0.2
0.3
0.4
0.5
0.6
0.7
0.8
0.9
0
10
20
30
40
50
60
70
80

(a)

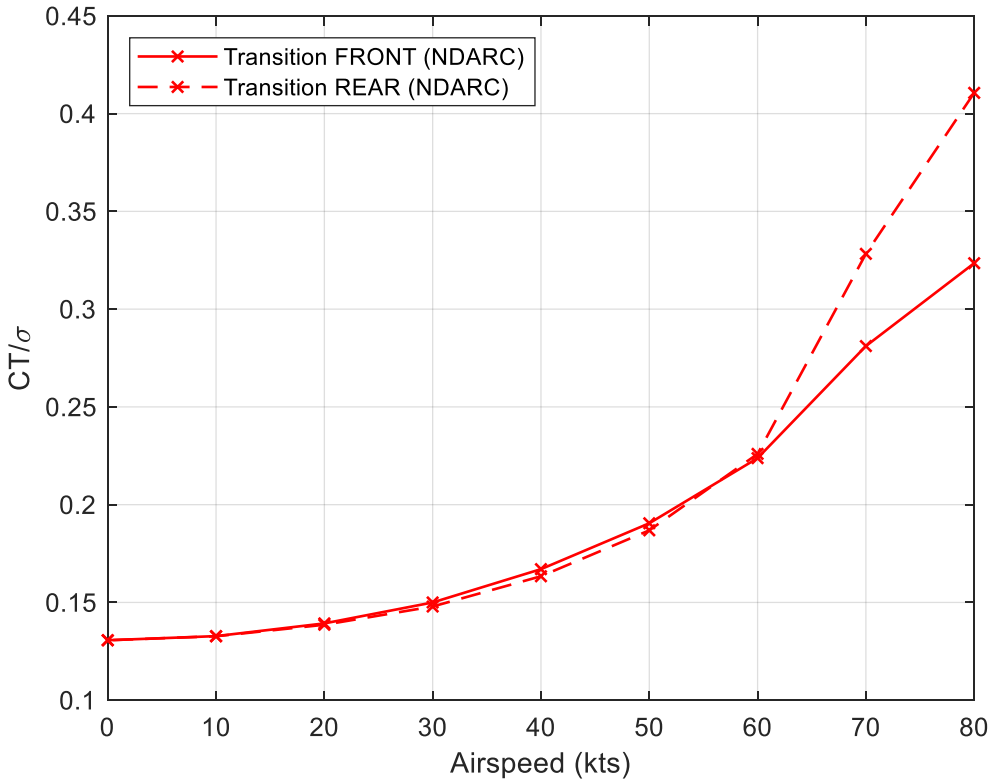

(b)

Figure 3.9 Advance ratio of the front and rear rotors through transition (a) and blade loading of the front and rear rotor blades through transition (b); advance ratio and blade loading of front rotors rises rapidly as airspeed increases and the rotors slow down.

When observing the results for the RPM and power required of the rear and front rotors, it becomes evident that the rear rotors are spinning faster, thus working harder, likely because of aerodynamic interaction affects. Furthermore, it can be seen that the lift rotors quickly begin to experience very high advance ratios and very high levels of blade loading, something that was also observed in Ref. [13] when investigating these new, multirotor aircraft. This is to be expected because as the wing and propeller begin to generate more of the required lift for the Alia with increased airspeed, the lift rotors begin to reduce their RPM, but the edgewise velocity continues to increase. From

here, these results were deemed to be reasonable enough to move forward with the next step of comparing the NDARC model with the DEPSim model.

3.4 High-Fidelity Model Comparison

3.4.1 Initial Comparison

Using the trimmed model discussed in the previous section, the initial comparison between NDARC and DEPSim was made. Note that DEPSim was initially run at five different airspeeds until the DEPSim model was fully developed; the software has issues with trimming the aircraft at exactly 0 knots, therefore 1 knot was used instead. Also, the final NDARC simulation was changed to run at sea-level standard atmosphere rather than the altitude of 2000 feet and ambient temperature of 70 degrees Fahrenheit used previously as DEPSim currently only runs with standard atmosphere and does not feature temperature offset effects. DEPSim's results serve as the benchmark for NDARC's simulations in these comparisons and thus some conclusions about the NDARC model can quickly be drawn. Firstly, when examining the pitch attitude of the Alia in Figure 3.10, DEPSim was able to trim the aircraft at much lower pitch attitudes that would likely suit a pilot's desires better than the pitch schedule of NDARC, so NDARC would need to be adjusted to match. Additionally, DEPSim trimmed the Alia at a significantly lower pitch attitude compared to NDARC when in "airplane mode" (110 knots) which exposed a mistake in the DEPSim model regarding the wing incidence.

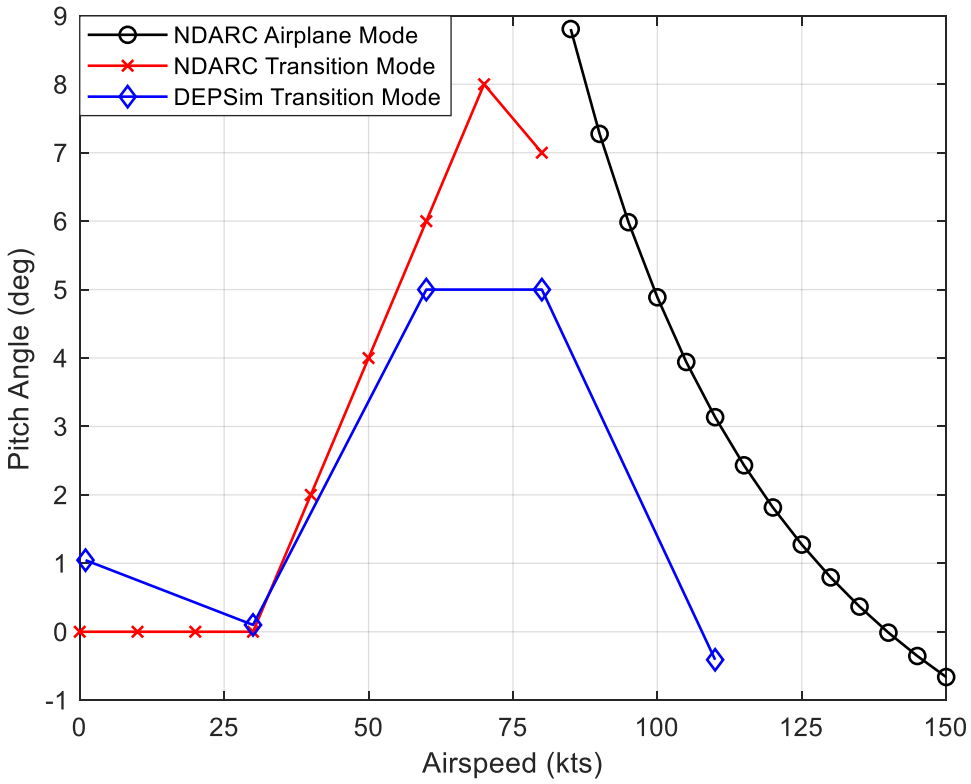

Figure 3.10 Initial comparison of DEPSim and NDARC pitch attitude; pitch scheduled from hover to 80 knots.

Then, when observing the power required for the Alia Figure 3.11, it is seen that DEPSim produces a notably large spike at 30 knots, due to the exceedingly high RPM required by the rear rotors that created a very high Mach number, that is not replicated by NDARC in any capacity. Meanwhile, the power required in hover conditions produced by both programs is different enough to prompt some tuning in NDARC.

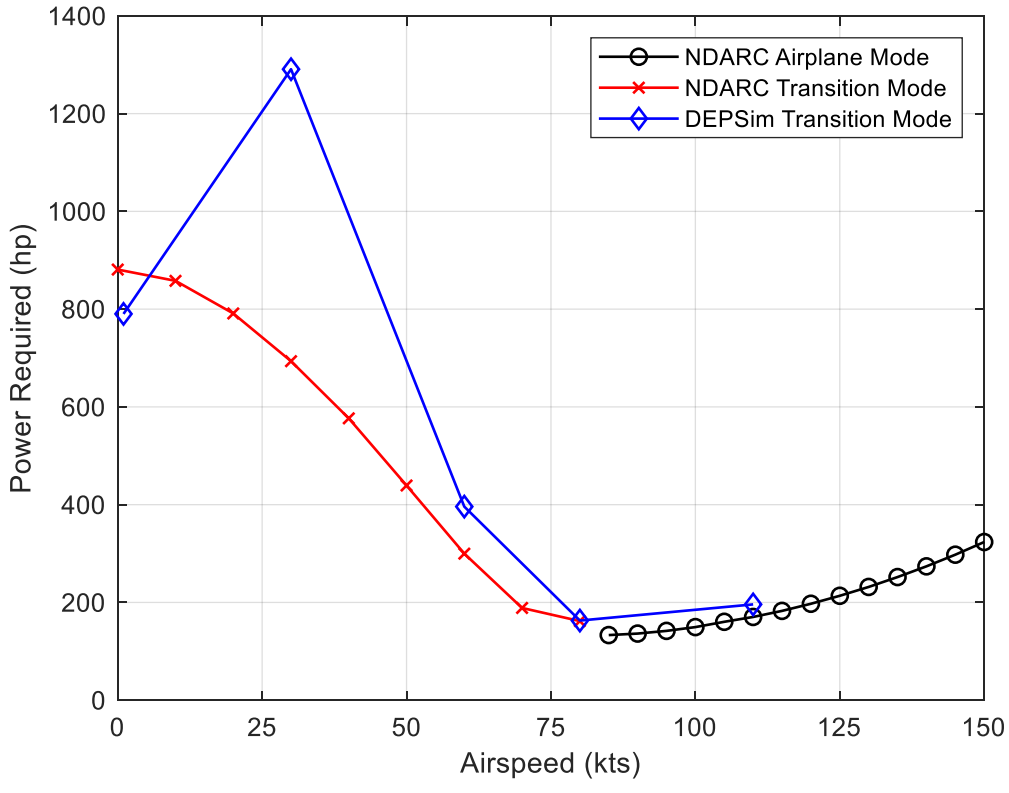

Figure 3.11 Initial comparison of total power required for the Alia as determined by NDARC and DEPSim, which demonstrates NDARC is underestimating power required in low-speed transition.

However, despite this difference in power required for hover, the RPM and the thrust produced for each rotor in hover conditions are quite similar, as seen in Figure 3.12. An obvious difference between the simulations, seen in the aforementioned figures, is that DEPSim is producing a larger difference in RPM and thrust from the front and rear rotors. This is due in part because the interference inputs in NDARC are initially set to default values that essentially eliminate interference effects. Determining where the differential in DEPSim comes from is paramount before tuning the NDARC model and the interference models.

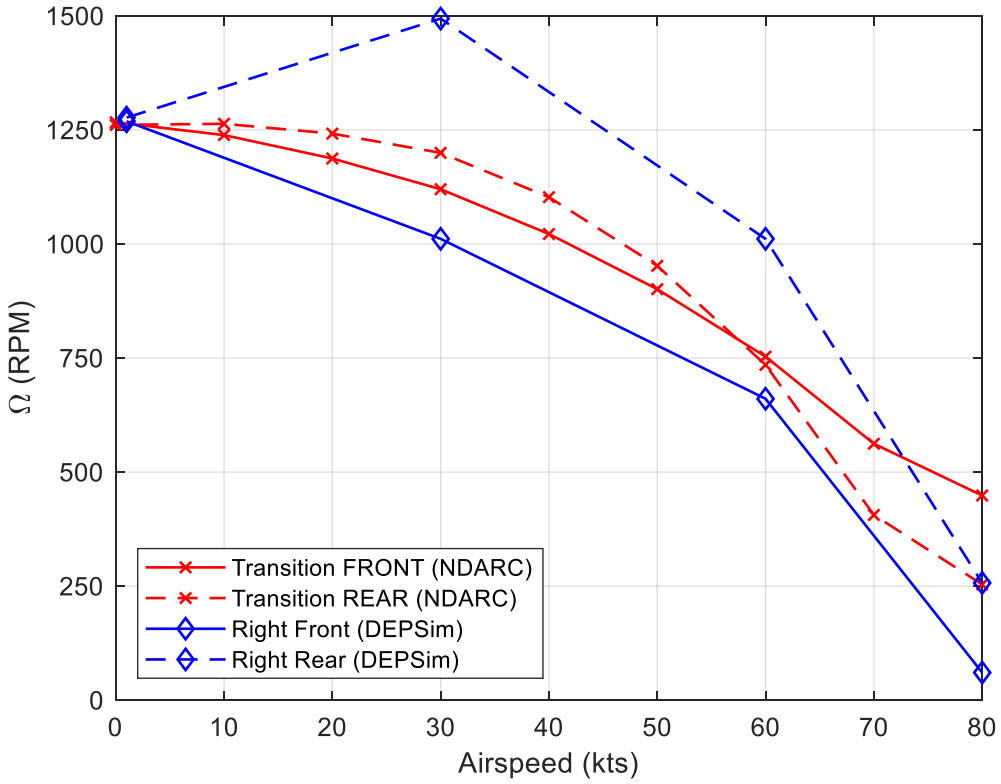
1500
1250
1000
750
500
250
0
Ω (RPM)
0
10
20
30
40
50
60
70
80
Airspeed (kts)
Transition FRONT (NDARC)
Transition REAR (NDARC)
Right Front (DEPSim)
Right Rear (DEPSim)

(a)

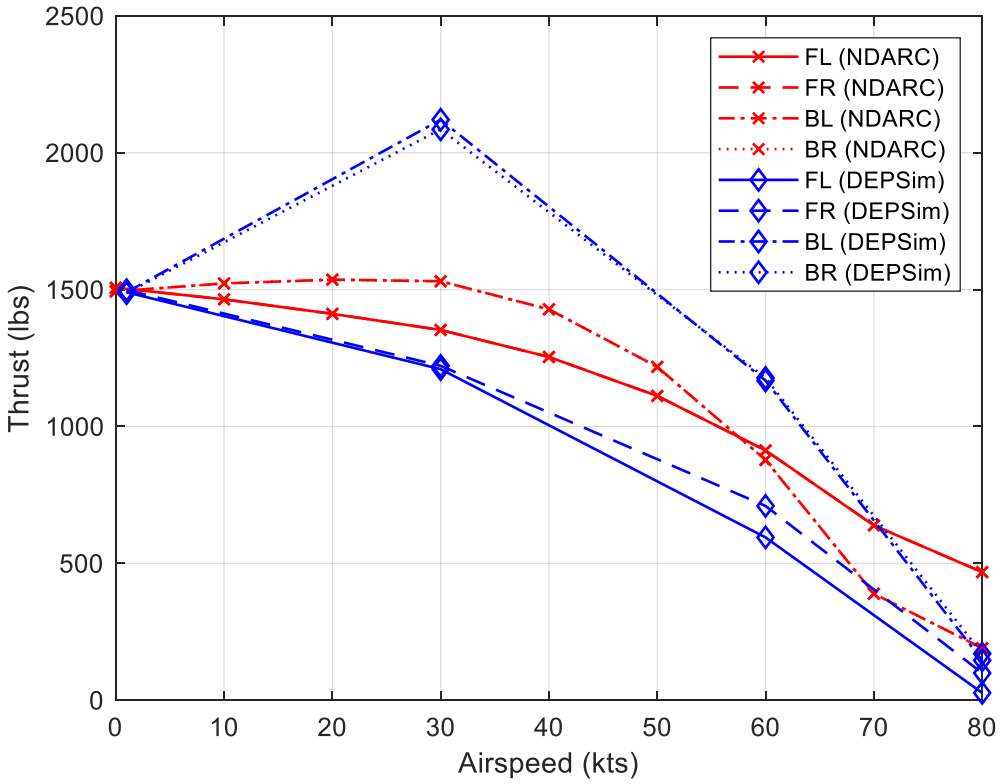

(b)

Figure 3.12 Comparison of the difference in RPM (a) and thrust (b) for the front and rear rotors of the Alia in NDARC and DEPSim.

While comparing the lift production of the four lift rotors is important, it is also important to compare the production of the lifting surfaces of the Alia as it is a lift+cruise aircraft. Specifically, the wing and horizontal tail are of significant interest. To see the lift of the wing and the tails, refer to Figure 3.13.

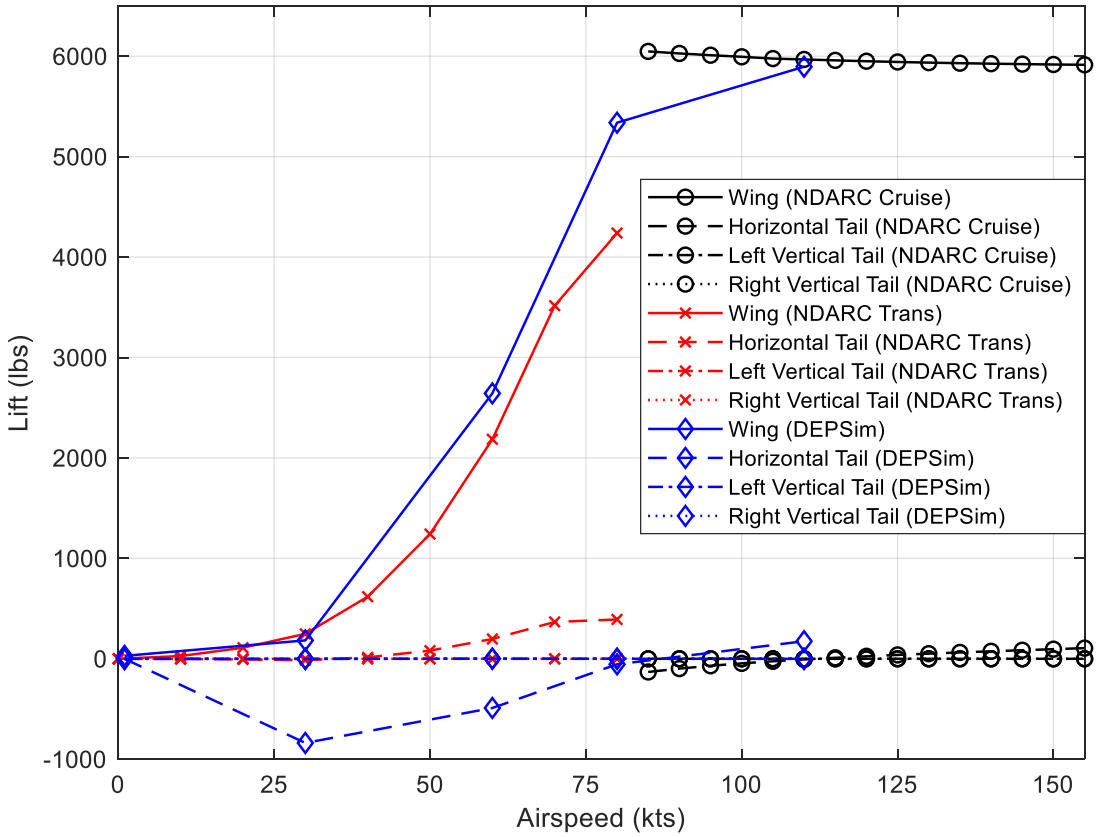

Figure 3.13 Breakdown of lift contribution by aerodynamic component for Alia as determined by NDARC and DEPSim.

It is evident that both NDARC and DEPSim are generating similar levels of lift for the wing, despite different pitch attitudes at 60, 80, and 110 knots. More critically, it is clearly shown that, in DEPSim, the horizontal tail is experiencing a substantial amount of download which in turn generates a significant pitching moment for the aircraft that must be accounted for. Furthermore, this download and pitching moment is likely what creates a large amount of the differential in rotor thrust and RPMs for the front and rear lift rotors, as differential RPM control must be used to overcome the pitching moment. Figure 3.14 provides a direct comparison of how NDARC and DEPSim are generating the required forces to trim the Alia in these conditions, and it can be seen

that the download on the horizontal tail in DEPSim is almost wholly responsible for the difference between the front and rear rotors. To see this difference, refer to Figure 3.15.

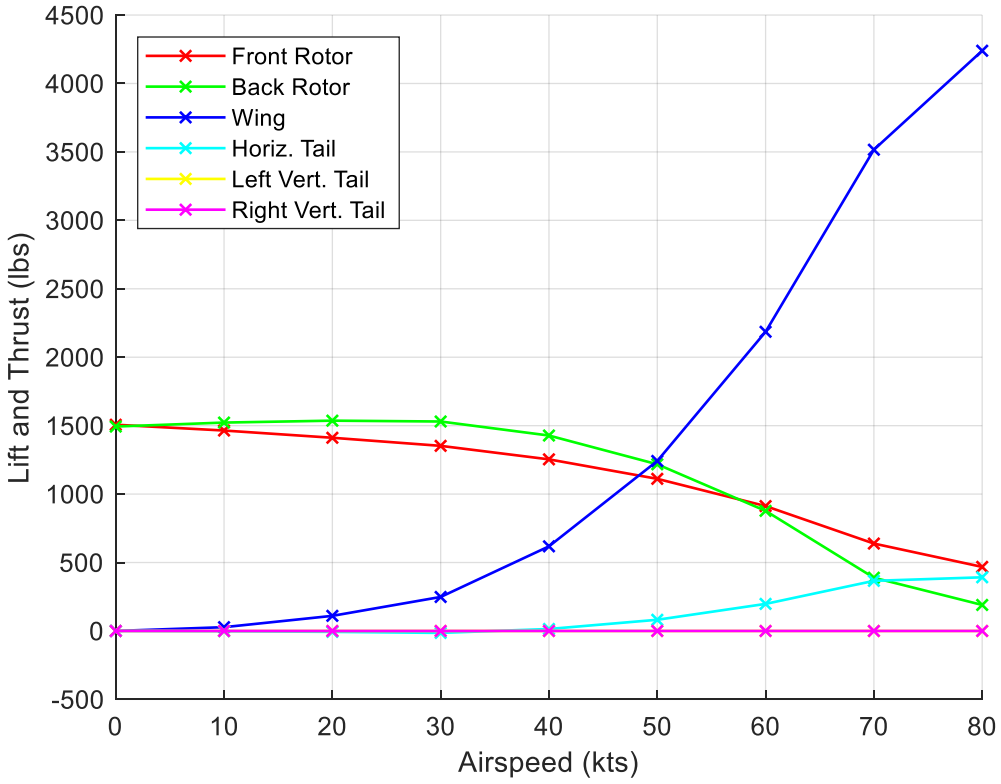

(a)

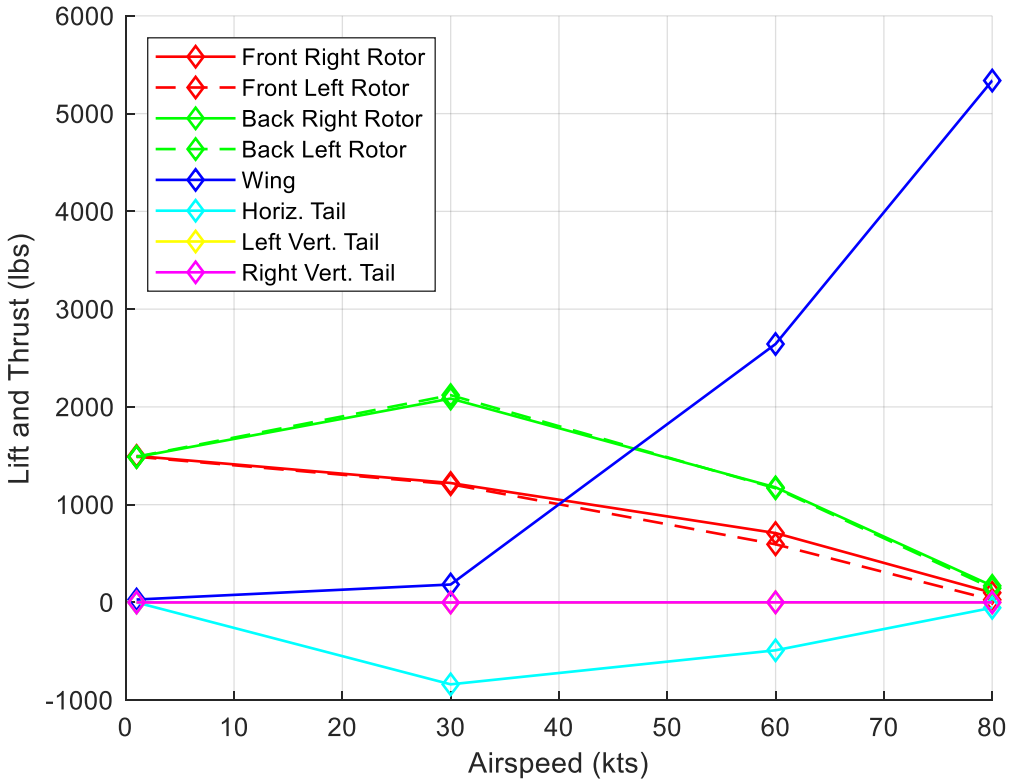

(b)

Figure 3.14 Comparing the lift contribution of each component for NDARC (a) and DEPSim (b).

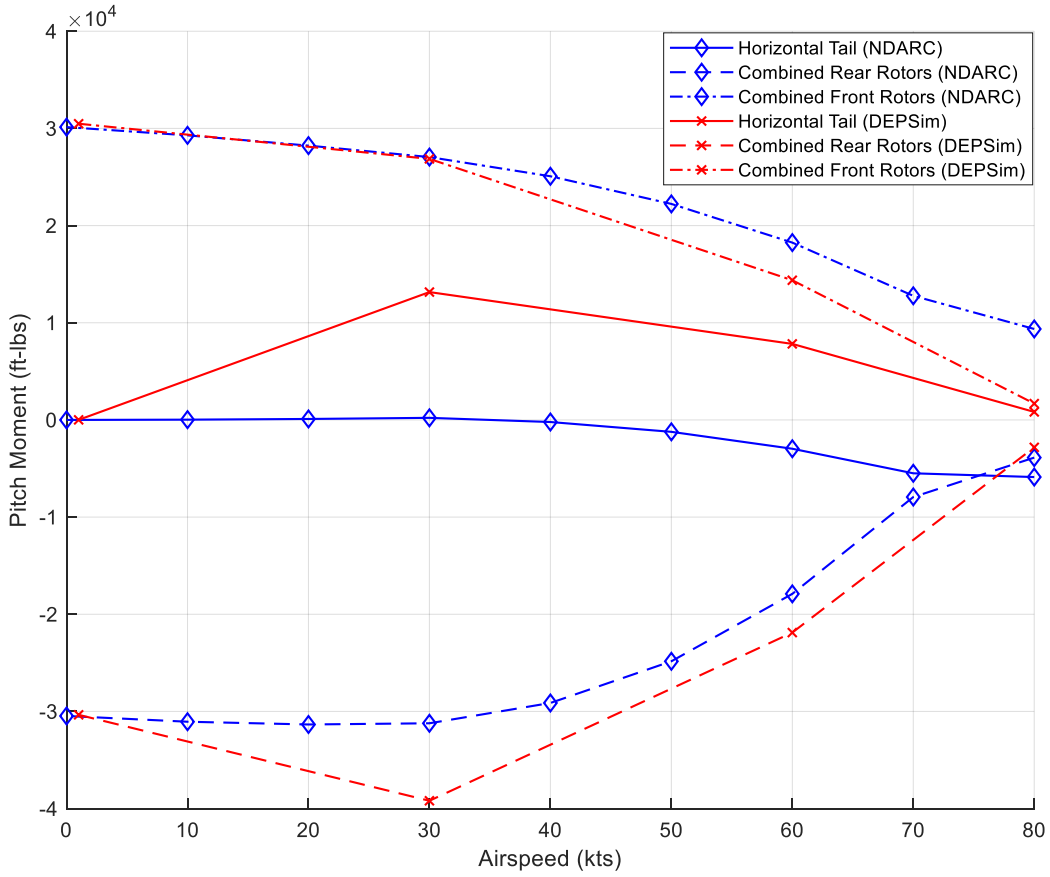

Figure 3.15 Comparison of the difference in pitch moments from NDARC and DEPSim for the combined front rotors, combined rear rotors, and horizontal tail.

Then, in Figure 3.16, a visualization from CHARM demonstrates how much downwash the horizontal tail is experiencing at 30 knots in DEPSim.

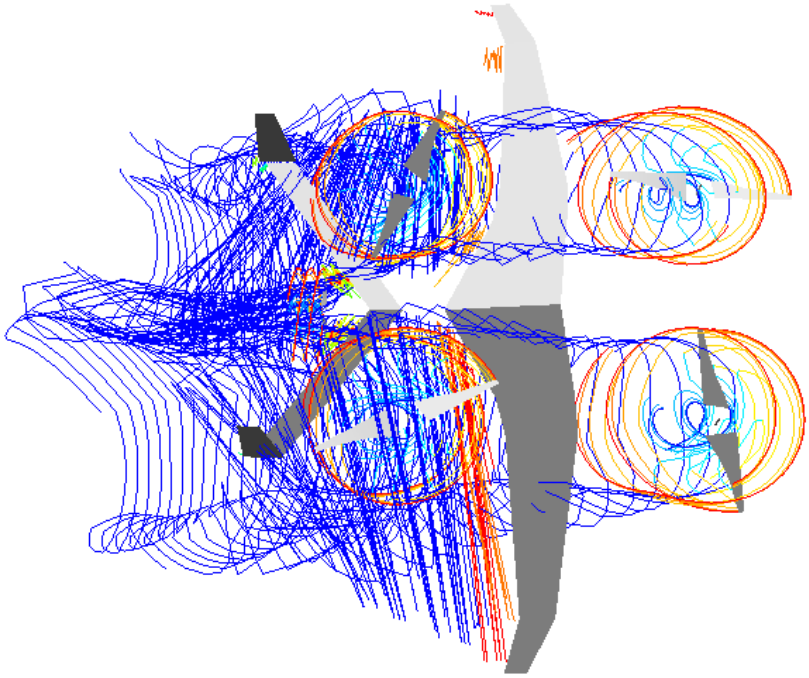

(a)

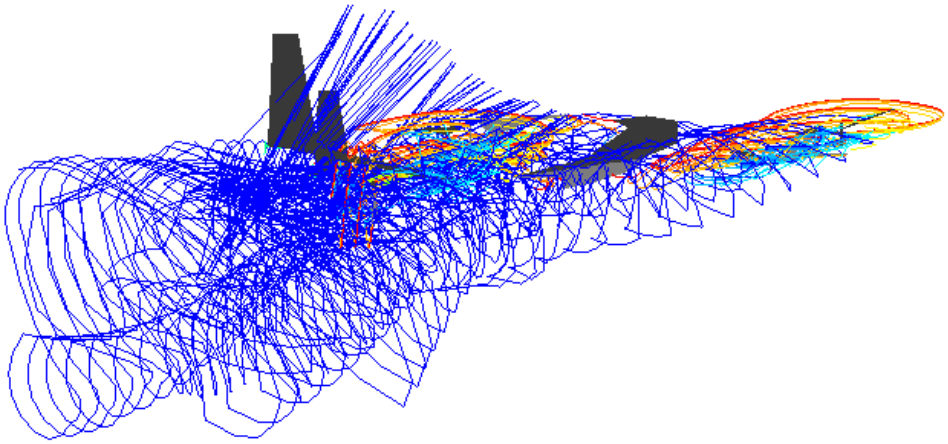

(b)

Figure 3.16 Top view (a) and side view (b) of wake simulation of BETA Alia at 30 knots.

In Figure 3.16, the colored lines show the wake contours near the rotors and lifting surfaces as computed by the CHARM model. Meanwhile, the blue lines show the far wake downstream from the rotors and lifting surfaces. This is the rotor wake contour rolled into a single trailing vortex. If the lifting surface is immersed in a large number of trailing vortices, as the horizontal tail is at this airspeed, then it can be inferred that the surface is experiencing a large amount of downwash

Based upon initial tests using DEPSim to model the Alia in trimmed forward flight, it quickly became evident that the NDARC model needed some adjustments to various inputs to reflect necessary changes required by DEPSim to allow the model to trim. More specifically, the propeller of the Alia required some adjustments. The CHARM simulations in DEPSim revealed that the pusher-propeller was experiencing low levels of efficiency (approximately 50% efficiency) and it was determined that the rotor blades were lacking enough twist and blade area. In turn, the twist (θ_{tw}, *twistL*) was increased in magnitude from 15° to 25° and the chord was effectively doubled from 3 inches to 6 inches by doubling the solidity input in NDARC (σ, *sigma*), which mirrors the changes made in DEPSim. The image shown in Figure 3.17 provides the best look at the propeller for the Alia, and by knowing the radius to be 3.25 feet, it is estimated that the radius is between 6 and 7 inches at 75% blade radius.

Figure 3.17 Close up image of BETA Alia pusher propeller from Ref. [26].

Furthermore, through the use of DEPSim, it was seen that the lift rotors were also having issues. Specifically, the rotors blades were experiencing drag divergence due to the high rotational speeds required given the initial geometry of the blades. To best resolve this issue, the solidity of the lift rotors was increased 50% in both DEPSim and NDARC by increasing the chord dimensions of the rotor blades 50% in DEPSim and decreasing C_W/σ (*CWs*, blade loading) by 50% for NDARC. However, to make this change in NDARC requires some adjustments to the nominal rotor speed (V_{tip}, *Vtip_ref*) and the collective (θ, *coll*), which is measured at 75% blade radius, for these fixed-pitch rotors. Thus, the reference tip speed was reduced from 780 fps to 700 fps and the blade pitch was reduced from 15 degrees to 7.25 degrees. To further understand why these changes are necessary, refer to Figure 3.18. In this figure, the drag coefficient for the NACA 0012 airfoil is plotted as a function of Mach number for angles of attack from 0 to 8 degrees. The NACA 0012

airfoil is what was selected for the rotors NDARC and DEPSim models; the true airfoil(s) used for all five of the rotors of the BETA Alia are unknown After the blade reaches speeds beyond a Mach number of 0.75, Mach divergence quickly becomes an issue, and the black, vertical lines on the plot represent the thresholds for the original reference tip speed for the lift rotors in NDARC. Based upon this plot, it is clear that if the tip speed can be lowered a reasonable amount, then Mach divergence can be better avoided. To address this, solidity of the rotor blade must be increased, which decreases the required RPM of the rotor and, in turn, tip speed.

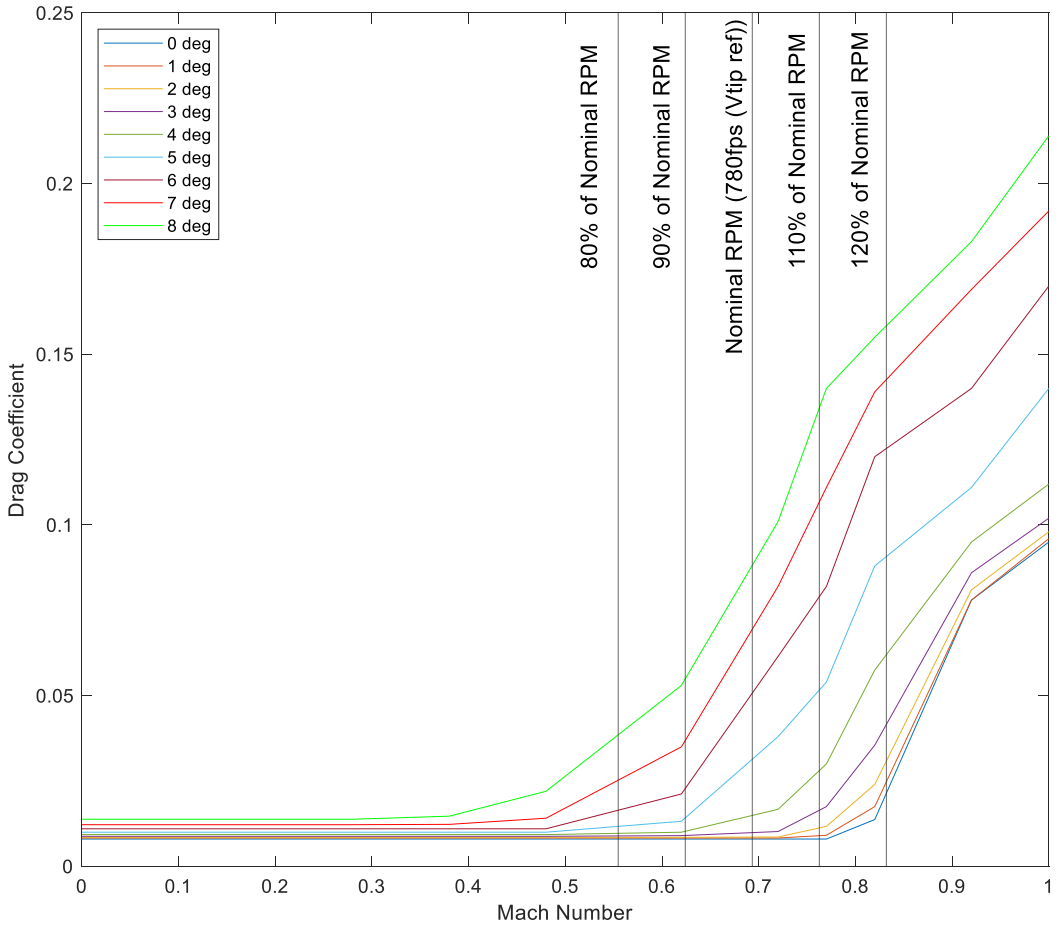

Figure 3.18 Drag coefficient of the NACA 0012 airfoil used for the Alia rotor blades at different angles of attack as a function of Mach number to demonstrate drag divergence at different RPM thresholds.

Changes were also made to the wing and horizontal tail of the original model within DEPSim to create a more accurate representation of the aircraft in terms of geometry and wake influence. Originally, the DEPSim model was experiencing a doubled incidence angle for the wings as it was being input twice and was creating increased lift values for the wing. For the tail, because the extreme amount of download was not anticipated, the original DEPSim model featured simplified geometry. To rectify this, the sweep was decreased to 35 degrees from 45 degrees and

the “reverse taper” that increases the chord along the span of the tail was added based upon available Alia images. Lastly, the wing and the tail dynamics models were changed so that CHARM would switch from using Lifting Surface Vortex Lattice Method and look-up tables to using Lifting Line Theory and 2D look-up tables for lift, drag, and moment at angles of attack greater than or less than ±12 degrees.

3.4.2 Final Results

After these initial changes were made within DEPSim and NDARC, the results of each program were directly compared with one another again. This time, both NDARC and DEPSim have the same pitch schedules through transition mode, which was made possible through the increased solidity, reduced tip speed, and reduced collective for the lift rotors, and is shown in Figure 3.19. Additionally, with a more accurate model in DEPSim, more simulations were run at additional airspeeds to provide a more complete and comparable set of data when evaluating NDARC’s performance. To see a full step-by-step summary of the changes made to the NDARC model, refer to the Appendix.

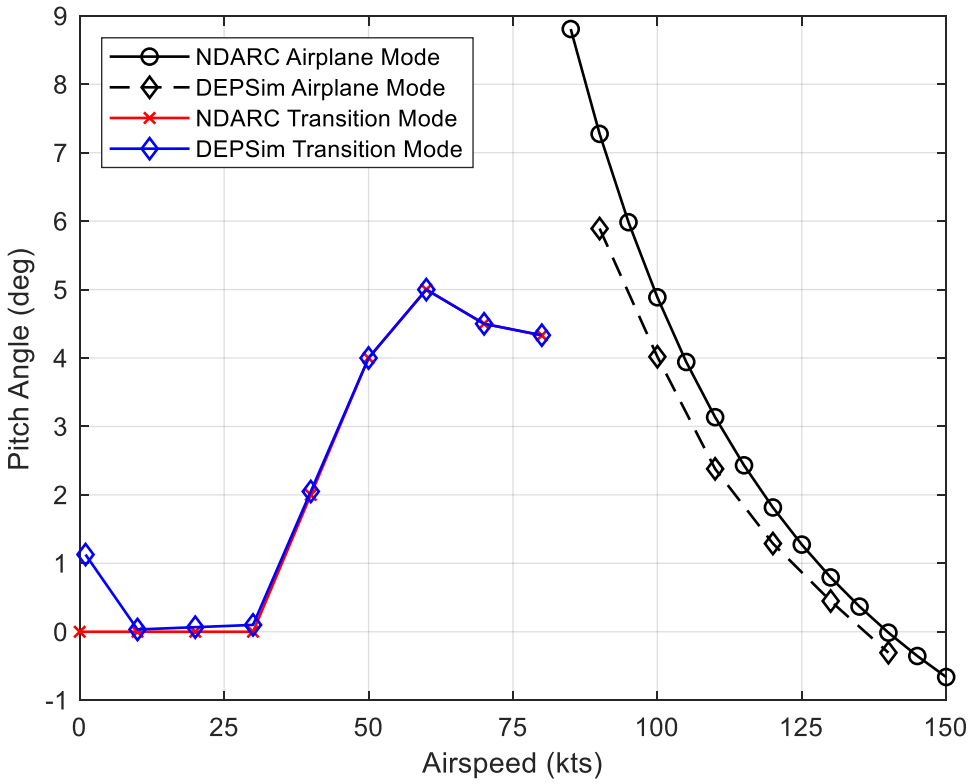

Figure 3.19 Comparison of vehicle pitch attitude of BETA Alia in hover, transition (matching schedule), and cruise (trimmed output) using NDARC and DEPSim.

To tune the NDARC model to match the results from DEPSim, the first step was to have the RPM of the four lift rotors match in hover conditions. To achieve this required adjusting the collective of the fixed-pitch blades. In DEPSim, the collective is set to 21 degrees at the blade root with a linear twist of -15 degrees along the blade radius to the tip. In NDARC, the collective for the rotor blade is set in the rotor component at 75% blade radius, thus the collective input is set to 10.5 degrees. In Figure 3.20, it is shown that the two different models share similar outputs for the rotor RPM in hover using these values.

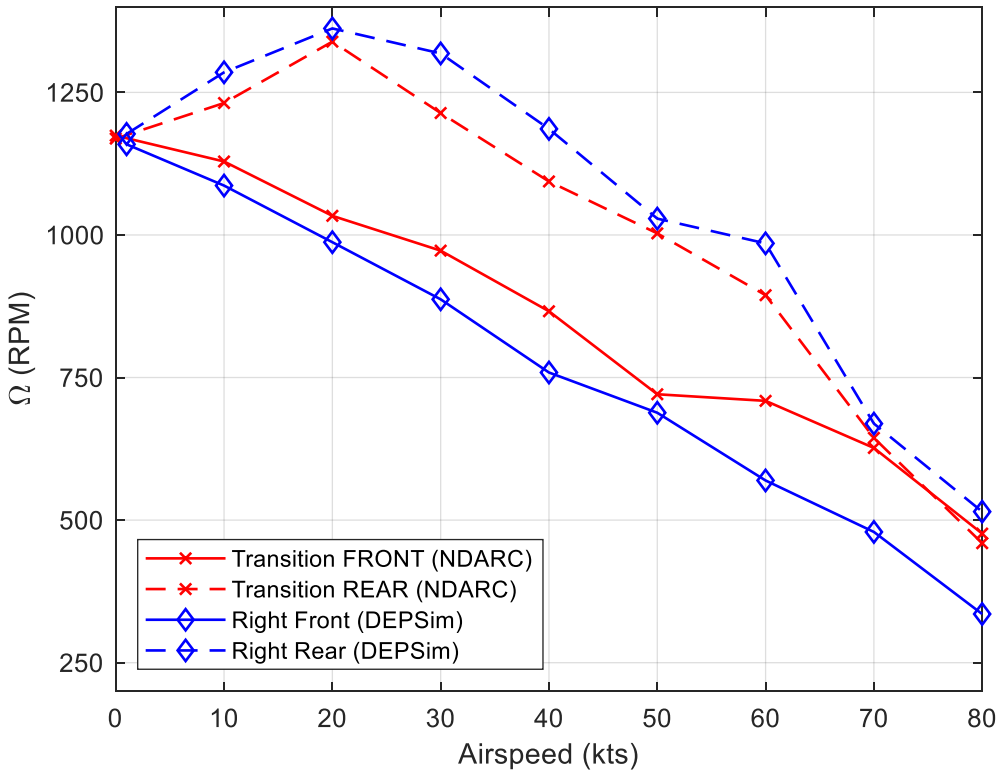

Figure 3.20 Improved matching of RPM for front and rear lift rotors of Alia as determined by NDARC and DEPSim following changes to NDARC model.

Moreover, it is also illustrated that the NDARC model now reflects an increased differentiation of RPM for the front and rear rotors that more closely resembles the output generated by DEPSim. How this was achieved will be discussed later in this section.

Once the RPM in hover for the lift rotors matched, the next step to tune the NDARC model was to obtain power required values that agreed with the DEPSim results through transition. As previously mentioned for the smaller quadcopter models, adjusting the induced power of the rotor via the ratio to momentum theory induced velocity, κ_{hover} (*Ki_hover*), allows the power required to be tuned to an accurate level. The total power required for the Alia in transition and cruise is shown in Figure 3.21.

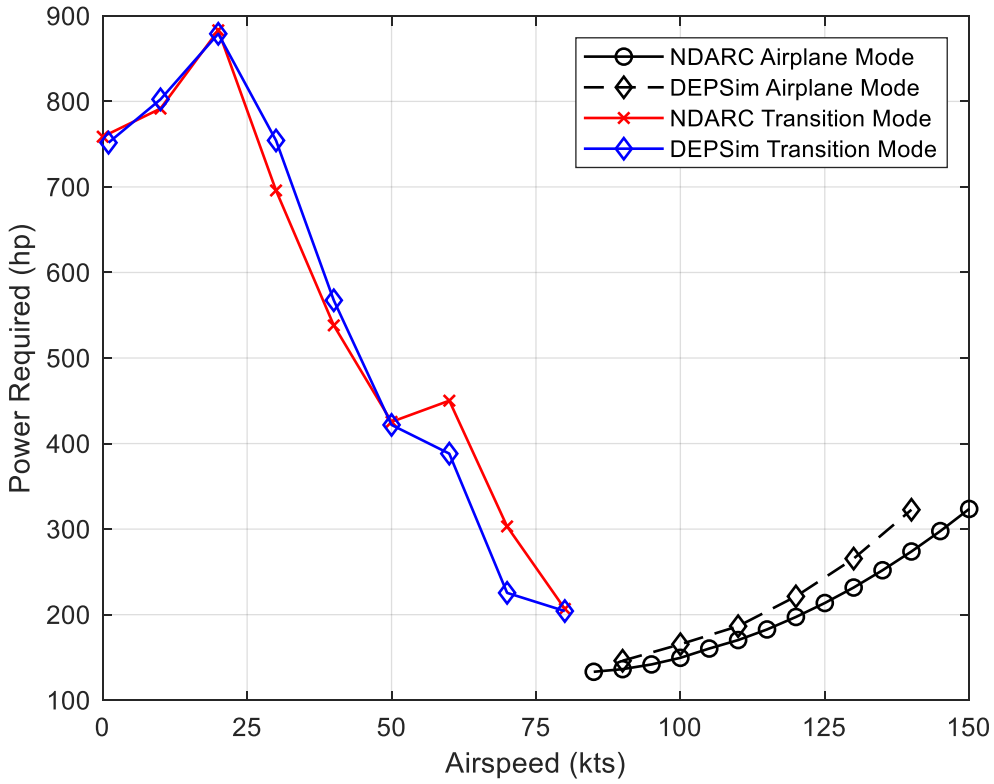

Figure 3.21 Improved matching of total power required for the Alia as determined by NDARC and DEPSim following changes to NDARC model.

This input was originally set to 1.2 when the NDARC model was provided by the CD&A group, but has a default value of 1.12 and was adjusted to 1.1 which allowed NDARC to produce power required results that matched DEPSim's output at critical points including hover and a spike at 20 knots. Additionally, this adjustment produced a similar trend in NDARC through transition that included the deviation in trend at 60 knots.

With the changes to the collective and the pitch schedule in NDARC, the thrust for the rotors also began to resemble the values produced by DEPSim, as shown in Figure 3.22.

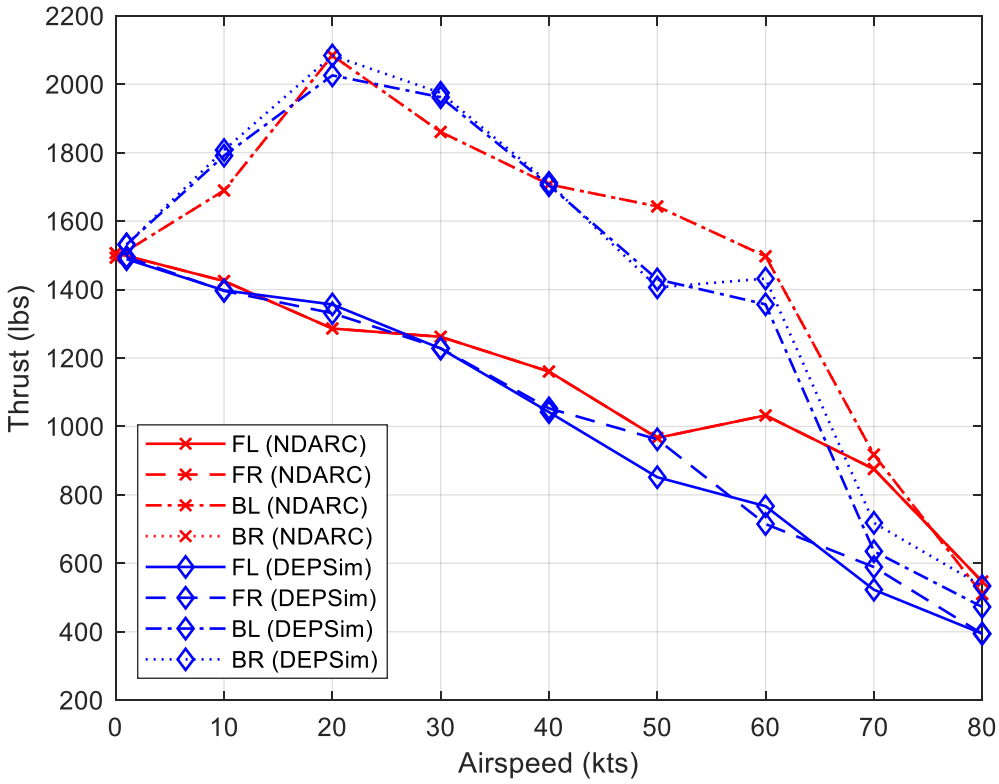

Figure 3.22 Improved matching of thrust for front and rear lift rotors of Alia as determined by NDARC and DEPSim following changes to NDARC model.

However, what truly allows the thrust and the RPM of the lift rotors in NDARC to more closely resemble the rotor thrust and RPM produced by DEPSim is shown in Figure 3.23 where the production of each lifting surface is plotted for both models.

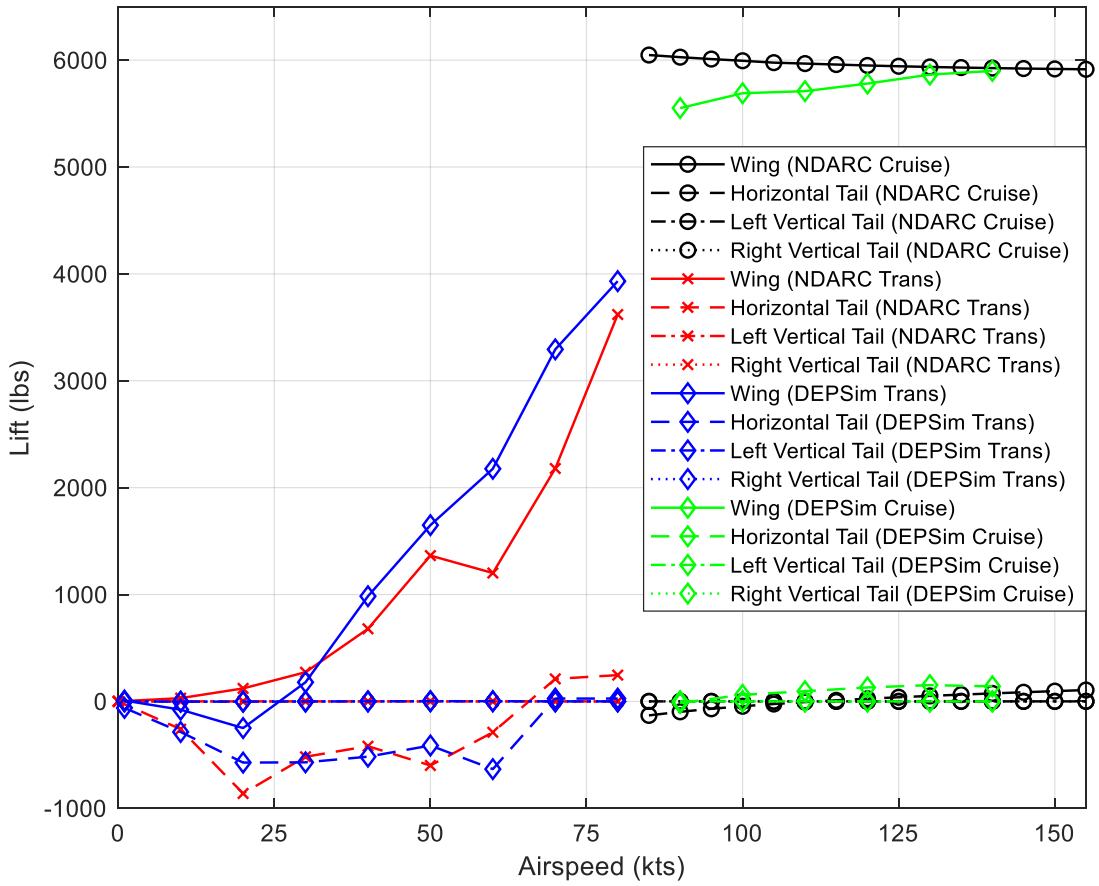

Figure 3.23 Improved matching of lift for aerodynamic surfaces of the Alia in transition and cruise as determined by NDARC and DEPSim following changes to NDARC model.

It was previously observed in DEPSim that the horizontal tail of the Alia was experiencing high levels of download that created a large pitching moment, but accurate changes could not be made in NDARC until this effect was better understood in DEPSim. After the geometry of the horizontal tail was more accurately modeled in DEPSim (previously discussed in §3.4.2), the appropriate changes could be applied in NDARC. To replicate this effect with the NDARC model, changes were made to the horizontal tail component. More specifically, tuning of both the vertical (*CDV*) and horizontal drag (*CD*) components of the drag coefficient, C_D. In the original NDARC model, these values were both initially set to 0.02. Due to the limited capabilities of the wake

model in the software, the best way to account for the download on the horizontal tail was to increase the horizontal drag component to 0.1, and the vertical component to 1.75. To start the tuning, the vertical drag component was set to 2.0 based upon the drag of a flat plate and was tuned, along with the horizontal component, until the tail download was similar to the download seen in DEPSim. Also, in the rotor component, the interference model (*MODEL_int*) was set to "transition" with transition defined as airspeeds from 1 knot (*Vint_low*) to 80 knots (*Vint_high*).

In addition to these changes with the drag coefficient, the location of the horizontal tail needed to be shifted. When observing Figure 3.24 and comparing both plots, the need for this change is seen by the increase in download from hover to 20 knots.

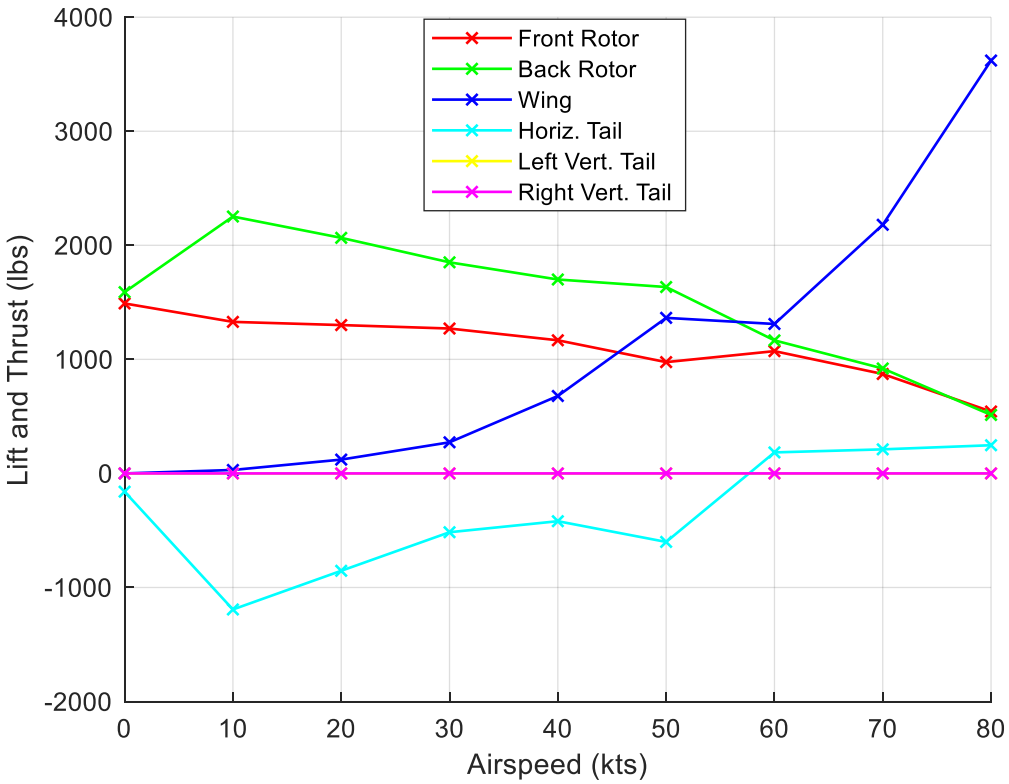

(a)

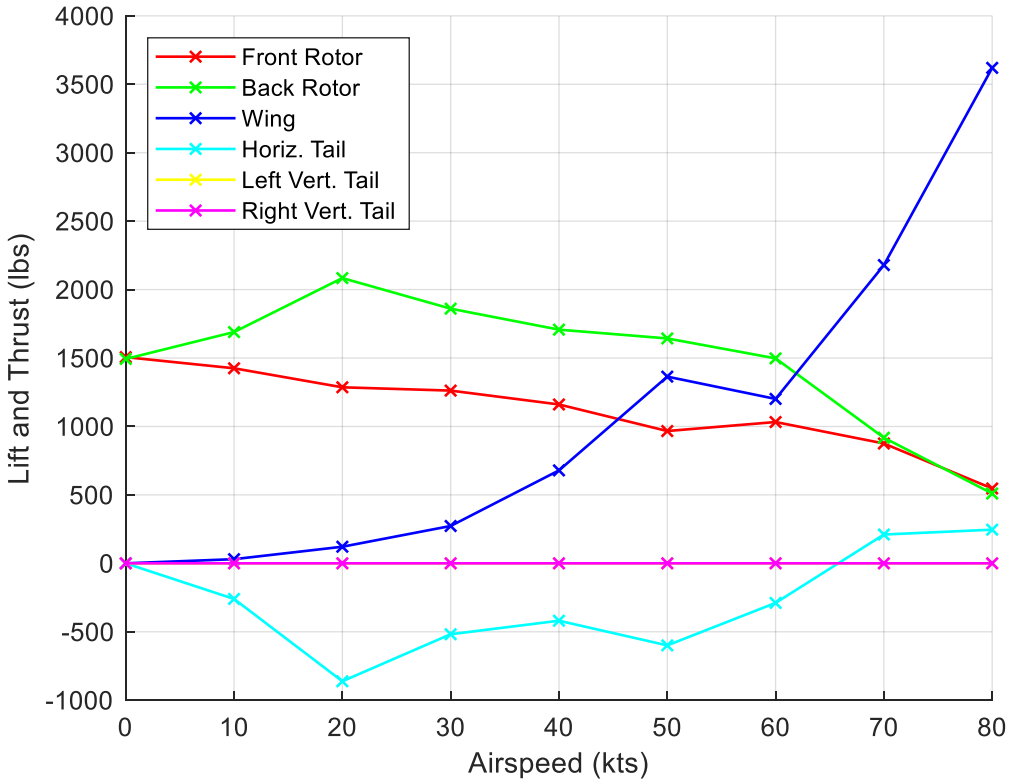

(b)

Figure 3.24 Comparison of the lift and thrust of the various Alia components before (a) and after (b) moving the stationline of the horizontal tail further back in NDARC.

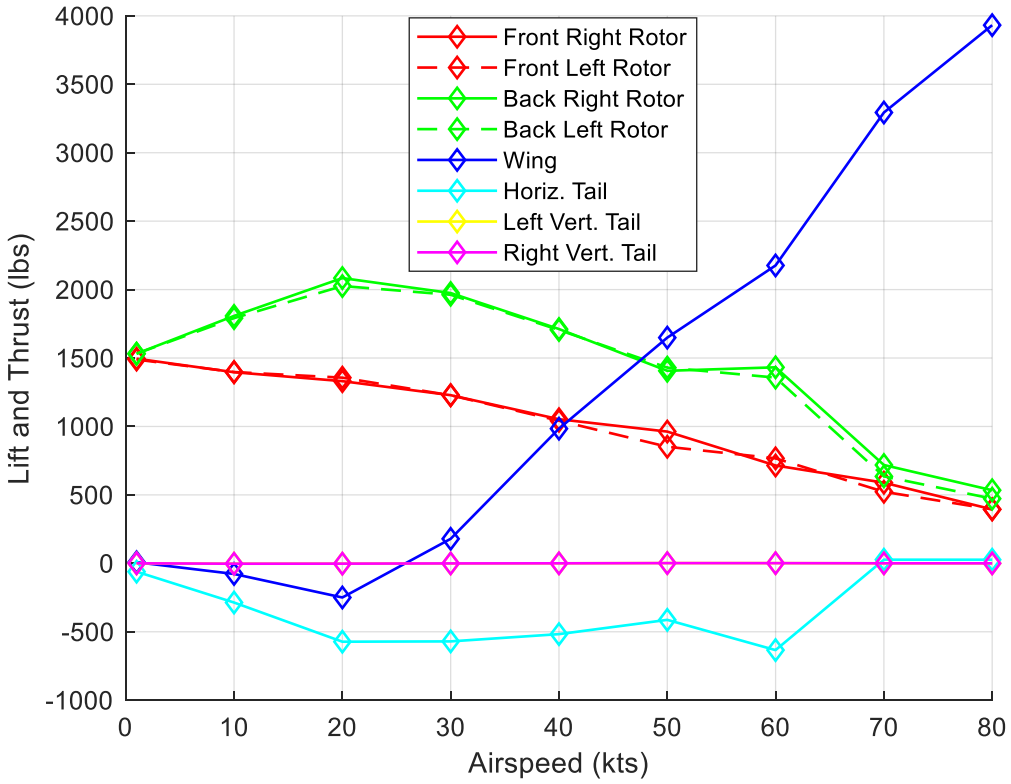

Figure 3.25 The lift and thrust of the various Alia components determined by DEPSim.

By moving the stationline of the horizontal tail further aft by 0.65 feet and thus moving the collocation point of the wake model, NDARC can replicate this trend from hover to 20 knots despite the limited geometry modeling available for tails in the software. This shift in NDARC is a viable adjustment given that the aerodynamic center for the horizontal tail is calculated to be 0.808 feet from the leading edge based on available images of the Alia. The changes to the tail are paramount for matching NDARC to DEPSim as Figure 3.25 clearly demonstrates how the forces of the tail directly impact the production of the rear rotors with the lines for the rear rotors and the horizontal tail being almost perfect mirrors of one another.

An important detail about the BETA Alia model and how it achieves the differences in front and rear rotor performance is that the model does not currently use the rotor-to-rotor interference inputs previously used for the DJI Phantom and SUI Endurance. These interference

factors were the primary inputs that allowed NDARC to match the wind tunnel data. While a majority of the influence on the front and rear rotor performance differential is due to the geometry and location of the horizontal tail and its subsequent download, it is believed that there is still rotor-to-rotor interference for the Alia that needs to be accounted for, just as it was for the quadcopters, and that this would further improve the correlation between NDARC and DEPSim. Unfortunately, the current NDARC model has issues that prevent these interference factors from having any impact on the results that requires more in-depth investigating. Despite the difference in rotor interference models between the Alia and the quadcopters, the use of multirotor thrust factors, x_h and x_f, in the rotor components is not mutually exclusive from the transition interference model used for the Alia.

Chapter 4: Conclusions and Future Work

4.1 Conclusions

Through the work conducted, some valuable conclusions can be drawn. First and foremost, NDARC has proven to be a valuable design tool for small UAS vehicles with multiple rotors. More specifically, the NDARC model was able to be tuned to match both wind tunnel data and high-fidelity models through physically reasonable adjustments to a small number of modelling inputs. Further proving this point is that the two quadcopters tested, the DJI Phantom and the SUI Endurance, possessed varying dimensions and gross weights. By finding the relevant NDARC inputs to tune the quadcopter models and detailing what said inputs adjust, the groundwork for tuning future designs in NDARC has been established. Importantly, the use of both the Phantom and the Endurance showed that models of this configuration can use the rotor-to-rotor interference values in NDARC established here ($x_f \approx 1.2$ for each rotor, $x_f \approx 0.6$ for front rotors in rear rotor components) as a starting point for future models. Additionally, some potentially worthwhile design changes were considered that could improve the performance of the UAS quadcopters for certain missions. Namely, shifting the center of gravity for the aircraft so that the thrust of the front and rear rotors was balanced in forward flight could prove useful considering that a majority of the mission, whatever the desired mission may be, will likely take place in forward flight rather than hover.

Secondly, the work done with NDARC and the quadcopters was expanded upon by attempting to determine if the software could work well for piloted lift+cruise aircraft configurations. The BETA Alia was chosen specifically due to interest from sponsoring parties and, because of the lack of publicly available test data, was compared to higher fidelity results from DEPSim. From this endeavor, it was determined that NDARC is a viable tool for these

complicated and novel aircraft configurations, including a configuration representative of the BETA Alia. Not only did the NDARC results match the DEPSim results well, but it also illuminated some areas for potential design improvement. From this study, the following was found:

1. The original rotor blades for the four lift rotors would be susceptible to drag divergence during transition flight.
2. Said drag divergence was due in part to low rotor solidity.
3. The drag divergence was also due to the download present on the horizontal tail creating a pitching moment that the rear rotors were compensating for by spinning faster.
4. The tail download maintained a significant factor through transitional airspeeds up to 70 knots with the largest impact from 20-60 knots.
5. Increasing the solidity of the lift rotors by 50% allowed for a reduction of tip speed and collective for the rotor blades, thus allowing drag divergence to be largely avoided.

BETA's latest image of a newer version of the Alia, shown in Figure 4.1, supports the increase in rotor solidity as it can be seen that they are using blades that feature much wider chords closer to the blade root.

Figure 4.1 Latest BETA Alia aircraft with larger rotor blades for the lift rotors (downloaded from beta.team).

Additionally, by using NDARC, it was evident that the tail of the Alia could create some performance issues in transition due to the rotor downwash creating high levels of download on the horizontal tail. Something that could alleviate some or all of this issue would be to move the tail to a higher position so that it is no longer in the wake of the wing or, more importantly, the rotors. This valuable information demonstrates NDARC's ability to provide designers with relevant information for complicated and unique lift+cruise configurations that impacts the design of the aircraft.

To further summarize the findings of this thesis, the most critical tuning parameters in NDARC for multi-rotor aircraft are listed:

1. Rotor-to-rotor interference from front rotors to rear rotors.
2. Rotor-to-aerodynamic surface interference effects.
3. Location of center of gravity.

4. Location of aerodynamic center for lifting surfaces.
5. Vertical distance of lift rotors from center of gravity.
6. Collective pitch angle for fixed pitch rotors.

Perhaps the most important of these listed parameters are the first two that involve the interactions of various components on the aircraft, and the last which is the blade pitch for the fixed pitch lift rotors. It is critical to accurately model the aerodynamic interference effects for these aircraft with complex geometries as it was seen that the rotor-to-rotor interaction greatly impacted the performance of the UAVs, and the download on the horizontal tail of the Alia caused by the wake of the rotors severely impacted the rotor performance for the aircraft. These effects created large pitch moments that had to be compensated for through the performance of the rear rotors which can lead to important design improvements in terms of batteries, motors, blade geometry, and tail location.

4.2 Future Work

A primary goal for future work is to determine why the rotor-to-rotor interference inputs used with the quadrotor UAVs have no impact on the results for the BETA Alia. These inputs were paramount in tuning the NDARC model to match the wind tunnel, specifically in terms of aircraft pitching moment. Based upon NDARC documentation, the multirotor thrust factors should allow an NDARC use to further tune the Alia model. It is also recommended that future work include generating more in NDARC using various maneuvers that could reveal further issues with the Alia while also providing important information for pilots when it comes to fully transitioning away from “transition mode” and to solely using the wing and pusher prop. These future tests could lead to the conclusion that the aircraft could require flapped wing or collective control for the lift rotors.

References

[1] Johnson, W. R., "NDARC NASA Design and Analysis of Rotorcraft," NASA/TP-2015-218751, NASA, Moffett Field, CA, 2015.

[2] Johnson, W., "NDARC – NASA Design and Analysis of Rotorcraft Validation and Demonstration," American Helicopter society Aeromechanics Specialists' Conference, San Francisco, CA, January 20-22, 2010.

[3] Russell, C., Willink, G., Theodore, C., Jung, J., and Glasner, B., "Wind Tunnel and Hover Performance Test Results for Multicopter UAS Vehicles," NASA TM—2018—219758, 2018.

[4] Russell, C., Theodore, C., and Sekula, M., "Incorporating Test data for Small UAS at the Conceptual Design Level," AHS International Technical Conference on Aeromechanics Design for Transformative Vertical Flight, San Francisco, CA, January 16-18, 2018.

[5] Russell, C. and Sekula, M., "Comprehensive Analysis Modeling of Small-Scale UAS Rotors," AHS International 73rd Annual Forum, Fort Worth, TX, May 9-11, 2017.

[6] Brandt, J. B. and Selig, M. S., "Propeller Performance Data at Low Reynolds Numbers," 49th AIAA Aerospace Sciences Meeting including the New Horizons Forum and Aerospace Exposition, Orlando, FL, January 4-7, 2011.

[7] Nowicki, N., "Measurement and Modeling of Multicopter UAS Rotor Blade Deflections in Hover," NASA/CR—2017-219428, NASA Ames Research Center, Moffett Field, CA, June, 2017.

[8] Diaz, P. V. and Yoon, S., "High-Fidelity Computational Aerodynamics of Multi-Rotor Unmanned Aerial Vehicles," AIAA SciTech Forum, Kissimmee, FL, 2018.

[9] Govindarajan, B. and Sridharan, A., "Evaluation of UAV Configurations for Package Delivery Missions through Conceptual Design," European Rotorcraft Forum, September, 2019.

[10] Scott, M., "Military Mission Suitability Assessment of eVTOL Aircraft Configurations," VFS International 77th Virtual Annual Forum & Technology Display, Virtual, May 10-14, 2021.

[11] Johnson, W., Silva, C., and Solis, E., "Concept Vehicles for VTOL Air Taxi Operations," AHS Specialists' Conference on Aeromechanics Design for Transformative Vertical Flight, San Francisco, CA, 2018.

[12] Cole, J. A., Rajauski, L., Loughran, A., Karpowicz, A., and Salinger, S., "Configuration Study of Electric Helicopters for Urban Air Mobility," *Aerospace* 2021, 8, 54. https://doi.org/10.3390/aerospace8020054

[13] Silva, C., Johnson, W., Antcliff K.R., and Patterson, M.D., "VTOL Urban Air Mobility Concept Vehicles for Technology Development," 2018 Aviation Technology, Integration, and Operations Conference, AIAA Aviation Forum, AIAA 2018-3847, Dallas, TX, June 2018.

[14] Patterson, M. D., Antcliff, K. R., and Kohlman, L. W., "A Proposed Approach to Studying Urban Air Mobility Missions Including an Initial Exploration of Mission Requirements," AHS International 74th Annual Forum & Technology Display, Phoenix, AZ, May 14-17, 2018.

[15] Malpica, C., and Withrow-Maser, S., "Handling Qualities Analysis of Blade Pitch and Rotor Speed Controlled eVTOL Quadrotor concepts for Urban Air Mobility," VFS International Powered Lift Conference 2020, San Jose, CA, January 21-23, 2020.

[16] Withrow-Maser, S., Malpica, C., and Nagami, K., "Multirotor Configuration Trades Informed by Handling Qualities for Urban Air Mobility Application," VFS 76th Annual Forum & Technology Display, Virginia Beach, VA, October 6-8, 2020.

[17] Diaz, P. V. and Yoon, S., "Computational Study of NASA's Quadrotor Urban Air Taxi Concept," AIAA SciTech Forum, Orlando, FL, 2020.
[18] Staruk, W., Butt, L., Hennig, G., Bonny, E., Gray, C., Represa, D., and Toner, R., "Wind Tunnel Testing and Analysis of a Rigid, Variable Speed Rotor for eVTOL Applications," VFS 76th Annual Forum, Virtual, October 6-8, 2020.
[19] Johnson, W. "NDARC — NASA Design and Analysis of Rotorcraft. Theoretical Basis and Architecture," American Helicopter Society Specialists' Conference on Aeromechanics, San Francisco, CA, January 2010.
[20] Sinsay, J., Hadka, D., and Lego, S., "An Integrated Design Environment for NDARC," AHS Technical Meeting on Aeromechanics for Vertical Lift, 2016.
[21] Vegh, J. M., Botero, E., Clark, M., Smart, J., and Alonso, J. J., "Current Capabilities and challenges of NDARC and SUAVE for eVTOL Aircraft Design and Analysis," AIAA Propulsion and Energy Forum, Indianapolis, IN, August 19-22, 2019.
[22] Theron, J.-P., Horn, J. F., and Wachspress, D. A., "An Integrated Simulation Tool for e-VTOL Aeromechanics and Flight Control Analysis," VFS Aeromechanics for Advance Vertical Flight Technical Meeting, San Jose, CA, January 21-23, 2020.
[23] Theron J.-P., Horn, J. F., Wachspress, D. A., and Enciu, J., "Nonlinear Dynamic Inversion Control for Urban Air Mobility Aircraft with Distributed Electric Propulsion," VFS International 76th Forum & Technology Display, Virginia Beach, VA, Oct 6-8, 2020.
[24] Johnson. W., "NASA Design and Analysis of Rotorcraft – Input and Data Structures," NASA Ames Research Center, Moffett Field, CA, April, 2019.
[25] Warwick, G., "Beta Technologies Keeps it Simple in Certifying its EVTOL," *Aviation Week,* September 9, 2021. https://aviationweek.com/aerospace/urban-unmanned-aviation/beta-technologies-keeps-it-simple-certifying-its-evtol
[26] "Aircraft – BETA," https://www.beta.team/aircraft/, accessed July 7, 2021.

Appendix

DJI Phantom Tuning Instructions

Step Number	Variable	NDARC Input Mnemonic	Initial Value	Final Value	Details
1	*N/A*	*STATE_trim*	symm	none	Model is being compared to untrimmed wind tunnel data
2	*N/A*	*SET_lift*	2	1	Using a fixed drag model
3	$d(L/q)d\alpha$	*dLoQda*	0.0	0.266	Value calculated using wind tunnel data
4	*N/A*	*FIX_drag*	3	3	Aircraft component
	k	*kDrag*	10.9	10.9	Aircraft component
5	*N/A*	*SET_drag*	1	1	Fuselage component
	$(D/q)_0$	*DoQ*	N/A	0.0	Drag of fuselage is essentially constant
	C_D	*CD*	0.005	0.006	Value determined by wind tunnel data
	K_d	*Kdrag*	N/A	0.0	Fuselage component
6	*N/A*	*SET_moment*	2	1	Switched from scaled model to fixed model for fuselage
7	$(M/q)_0$	*MoQ0*	-0.0375	-0.0358	Average of wind tunnel data from -30° to -5° angle of attack

					as trimmed pitch attitude is in this range
	$d(M/q)/d\alpha$	*dMoQda*	0.0341	0.0	Keep fuselage pitch moment constant
8	*N/A*	*KIND_control*	3	4	Change rotor control from pitch and tip path plane to pitch and no flapping plane to include flapping in model and tune power required
9	d_{0prop}	*d0_prop*	0.04732	0.125	Increased to help drag
	d_{0hel}	*d0_hel*	0.04732	0.125	Increased to help drag
10	κ_{ftwin}	*Kf_twin*	1.18	1.0	Reduced to 1.0 to simplify tuning of x_f
11	x_f	*xf_multi(#)*	1	1.25	This value is applied to all rotors to tune pitch moment and power required
	x_f	*xf_multi(front)*	0	0.6	This value is applied in both rear rotors to account for reduced thrust caused by rotor-to-rotor interference
12	*N/A*	*Loc_rotor(#)% Zol*	0.500	0.125	This value further tunes pitching moment of aircraft

Table A.1 Step-by-step changes to DJI Phantom NDARC model.

SUI Endurance Tuning Instructions

Step Number	Variable	NDARC Input Mnemonic	Initial Value	Final Value	Details
1	*N/A*	*STATE_trim*	none	none	Model is being compared to untrimmed wind tunnel data
2	*N/A*	*SET_lift*	1	1	Using fixed model like Phantom
3	$d(L/q)d\alpha$	*dLoQda*	0.266	0.75	Calculated using Endurance wind tunnel data
4	*N/A*	*FIX_drag*	3	0	Aircraft component, turning off drag model for this component to use fuselage drag model
	k	*kDrag*	10.9	2.5	Aircraft component, default
5	*N/A*	*SET_drag*	1	1	Fuselage component
	N/A	*MODEL_drag*	1	2	Quadratic model
	α_{Dmin}	*AoA_Dmin*	0.0	0.0	Drag minimum occurs at 0° angle of attack
	$(D/q)_0$	*DoQ*	0.0	0.30212	Value calculated using wind tunnel data
	C_D	*CD*	0.006	0.006	Value calculated using wind tunnel data
	K_d	*Kdrag*	0.0	2.5	Fuselage component

6	*N/A*	*SET_moment*	1	1	Continue to use fixed model from Phantom
7	$(M/q)_0$	*MoQ0*	-0.0358	-0.03333	Value determined by average of wind tunnel data from -20° to 10° to provide best matching
	$d(M/q)/d\alpha$	*dMoQda*	0.0	0.0	Kept constant to provide best matching with full aircraft
8	θ	*coll*	17.0	13.25	Rotor blades of Endurance have lower pitch
9	κ_{hover}	*Ki_hover*	1.15	1.15	Value carried from Phantom
10	*N/A*	*KIND_control*	4	4	Carried over from Phantom to include blade flapping
11	d_{0prop}	*d0_prop*	0.125	0.05	Adjusted for drag model
	d_{0hel}	*d0_hel*	0.125	0.05	Adjusted for drag model
12	κ_{ftwin}	*Kf_twin*	1.0	1.0	Kept at 1.0 to simplify tuning of multirotor thrust factor
13	x_f	*xf_multi(#)*	1.25	1.2	Initially used Phantom values, but tuned to match wind tunnel data; applied to all four rotors
	x_f	*xf_multi(front)*	0.6	0.5	Applied to only rear rotors
14	*N/A*	*Loc_rotor(#)% Zol*	0.500	0.050	Reduced to improve total pitching moment of Endurance

Table A.2 Step-by-step changes to SUI Endurance NDARC model.

Alia Tuning Instructions

Step Number	Variable	NDARC Input Mnemonic	Initial Value	Final Value	Details
1	*N/A*	*MODEL_int*	0	2	Set to scale with transition
2	*N/A*	*Vint_low*	0	1	Can be set higher, but transition for Alia is assumed to start at 1 kt
	N/A	*Vint_high*	0	80	Set to 80 kts based upon NDARC's ability to trim up to this airspeed
3	θ	*coll*	15	10.5	Lowered from 15° as a result of increase in rotor solidity and to match hover RPM between models
4	κ_{hover}	*Ki_hover*	1.2	1.1	Reduced because NDARC was over-predicting hover power req.
5	$C_{D,horizontal}$	*CD*	0.02	0.1	Hand tuned
	$C_{D,vertical}$	*CDV*	0.02	1.75	Hand tuned after being set to 2.0 based on flat plate drag coefficient
6	*Stationline*	*loc_tail(1)%SL*	30.85	31.5	Increased due to NDARC's limited wake model (aero center 0.808 feet behind leading edge of tail)
7	x_f	*xf_mutli*	1	N/A	Current model does not use this input, theoretically can improve matching with DEPSim

Table A.3 Step-by-step changes to Alia NDARC model.